National Library of Canada

Acquisitions and Bibliographic Services Branch

395 Wellington Street
Ottawa, Ontario
K1A 0N4

Bibliothèque nationale du Canada

Direction des acquisitions et des services bibliographiques

395, rue Wellington
Ottawa (Ontario)
K1A 0N4

Your file Votre référence

Our file Notre référence

NOTICE

The quality of this microform is heavily dependent upon the quality of the original thesis submitted for microfilming. Every effort has been made to ensure the highest quality of reproduction possible.

If pages are missing, contact the university which granted the degree.

Some pages may have indistinct print especially if the original pages were typed with a poor typewriter ribbon or if the university sent us an inferior photocopy.

AVIS

La qualité de cette microforme dépend grandement de la qualité de la thèse soumise au microfilmage. Nous avons tout fait pour assurer une qualité supérieure de reproduction.

S'il manque des pages, veuillez communiquer avec l'université qui a conféré le grade.

La qualité d'impression de certaines pages peut laisser à désirer, surtout si les pages originales ont été dactylographiées à l'aide d'un ruban usé ou si l'université nous a fait parvenir une photocopie de qualité inférieure.

Canada

CHONDROGENESIS AND LAMPRIN EXPRESSION IN DEVELOPMENTAL STAGES OF THE SEA LAMPREY, *PETROMYZON MARINUS*

A Thesis

Submitted to the Graduate Faculty

in Partial Fulfilment of the Requirements

for the Degree of

Masters of Science

in the Department of Anatomy and Physiology

Faculty of Veterinary Medicine

University of Prince Edward Island

Kim M. McBurney

Charlottetown, P.E.I.

May, 1995

ISBN 0-315-99742-7

CONDITION OF USE

SIGNATURE PAGES

ii-iii

REMOVED

ABSTRACT

Ultrastructural and molecular aspects of chondrogenesis in the sea lamprey, *Petromyzon marinus* were examined. An *in situ* hybridization (ISH) protocol was developed and used to analyze the spatial and temporal distribution of lamprin, a structural protein unique to lamprey cartilage, in metamorphic and prolarval stages. This investigation is the first to use ISH on lamprey connective tissues. Optimal fixation was achieved with 30 minute immersion in 4% paraformaldehyde. Hybridization was achieved using an ^{35}S-labelled 156 base pair riboprobe for 16-22 hours at 45^{0}C. Pre-hybridization with a cold competitor, produced using vector sequences and cold S-UTP, reduced the background. This protocol enabled the detection of lamprin expression in all lamprey cartilages, with the exception of branchial and pericardial cartilage. The absence of lamprin transcripts in branchial and pericardial cartilage may indicate differential expression of the two known lamprin genes. Chondrogenesis of the trabecular cartilage in prolarval stages was examined by ISH, light and electron microscopy. Similar to cartilages in metamorphic lamprey and higher vertebrates, chondrogenesis of trabecular cartilages in prolarva commenced with the formation of mesenchymal condensations. Epithelio-mesenchymal interactions appeared to perform a role in induction of chondrogenesis. Bilateral condensations first appeared by day 17 post-fertilization (pf), ventromedial to the eyes in a band of tightly packed, yolk-laden mesenchymal cells which may represent a neural crest derived tissue. Cartilage differentiation occurred by day 19pf and was indicated by the first ultrastructural appearance of lamprin and detection of lamprin mRNA by *in situ* hybridization. Unlike collagen type II in higher vertebrates, lamprin mRNA was not detected prior to cartilage differentiation. Like collagenous-based cartilages, non-lamprin extracellular matrix (ECM) components appeared ultrastructurally within a 24-48 hour margin of the first detection of lamprin. Following the initial expression of lamprin mRNA, hybridization signals became progressively more intense, paralleling matrix accumulation and suggesting a transcriptional control of the lamprin gene expression. Lengthening of the trabecular cartilage was primarily by appositional growth at its rostral end. A gradient of differentiation occurred along the longitudinal axis of the cartilage. The most developmentally advanced aspects were located ventral to the eye. Lamprin was initially deposited in the ECM as discrete, scattered 15-40nm globules. Subsequently, the lamprin fibrils aggregated into branching and densely packed parallel arrays, arranged into pericellular, territorial and interterritorial zones similar to those described for cartilage of adult lampreys. The temporal developmental pattern of trabecular cartilages in prolarval stages likely reflects the functional importance of these structures for protecting the brain as the animal assumes burrowing behaviour. It is concluded that certain aspects of chondrogenesis are critical to the normal development of a functional cartilaginous structure and are therefore conserved throughout the vertebrate taxa.

ACKNOWLEDGEMENTS

I would like to extend my gratitude and appreciation to Dr. Glenda Wright for her patience, supervision and continual support throughout this project. I also thank Dr. Cathy Chan, Dr. Bill Ireland and Dr. Brian Hall for their guidance. Much appreciation is extended to Dr. Fred Kibenge and Dr. Fred Keeley for the use of their laboratory facilities and direction in the areas of molecular biology and lamprin biochemistry respectively.

I am deeply indebted to many people for help in the collection, maintenance and raising the lamprey: Annie Ferraro, Robbie Wilson, Paul Lyon, and Lee Dawson, Julie Heinig, and John Guchardi. A special thanks is extended to Dr. John Youson for allowing me to visit and examine his laboratory facilities. In addition, I extend my thanks to Eric Jefferson and staff of the Department of Fisheries and Oceans for assistance in obtaining upstream migr t spawners.

For their helpful advice concer g technical aspects of the molecular biology work I gratefully acknowledge, Paul Robson, Patricia McKenna and Clair Colbert. I would like to recognise Glenda Clem nts-Smith's role in preparing the final version of the artwork included in this thesis. extend my appreciation to Dave Groman and Shelly Ebbett for their assistance wi e light micrographs. A heartfelt thanks goes to Susan Plourde for taking time f her own busy schedule to translate French manuscripts. A special thanks Evelyn Daley, Ramona Taylor and Dianne O'Connell for their advice conc aspects of processing and staining for light microscopy, and their "wonderf d" humour which made months of embedding fun!

Finally I thank Dr. Glen ght and Dr. Fred Keeley for financial support supplied through their NSER ants and the Department of Anatomy and Physiology for partial funding graduate student stipend.

To Scott, Shilo and Tessa for their patience, and to my father for encouraging a love of science in a young daughter.

LIST OF FIGURES

LIST OF TABLES

TABLE OF ABBREVIATIONS

A	-	Type A cell
B	-	Type B cell
BE	-	Buccal epithelium
bp	-	base pair(s)
Br	-	Brain
C	-	Type C cell
C^0	-	Centigrade
CA	-	Carotid artery
Cc	-	Core condensation cell
Ce	-	Centriole
Ch	-	Chondrocyte
CMP	-	Cartilage matrix protein
Cn	-	Condensing cell
Co	-	Collagen
D	-	Type D cell
DEPC	-	Diethylpyrocarbonate
DTT	-	Dithiothreitol
E	-	Type E cell
ECM	-	Extracellular matrix
EDTA	-	Ethylenediaminetetraacetic acid
EM	-	Electron microscopy
Ey	-	Eye
En	-	Endothelial cell
G	-	Golgi apparatus
H	-	Hyaline cartilage
I	-	Intercellular space
ISH	-	*In situ* hybridization
IZ	-	Interterritorial zone
L	-	Lipid droplet
LM	-	Light microscopy
Mc	-	Mitochondria
Me	-	Mesenchymal cell
Mi	-	Mitotic figure
MS-222	-	0.05% tricaine methanesulphate
N	-	Notochord
No	-	Nucleolus
Nu	-	Nucleus
O	-	Otic capsule
P	-	Pigment cell
PAS	-	Periodic-acid Schiff's reagent
PBS	-	Phosphate-buffered saline

Pc	-	Perichondrial cell
Pe	-	Pericellular area
pf	-	Post-fertilization
PFA	-	Buffered paraformaldehyde
pGEM	-	Promega ™Gemini plasmid vector
RER	-	Rough endoplasmic reticulum
SSC	-	Saline sodium citrate
S-UTP	-	Uridine 5'-[α-thio]triphosphate (non-radioactive)
^{35}S-UTP	-	Uridine 5'-[α-thio]triphosphate (radioactive)
T	-	Trabecular cartilage
T-Blue	-	1% Toluidine blue
TA	-	Trabecular arc
TE	-	Tris/EDTA buffer
TEA	-	Triethanolamine
Tu	-	Microtubules
TZ	-	Territorial zone
V	-	Autophagic vacuole
y	-	Yolk globule

TABLE OF CONTENTS

1. GENERAL INTRODUCTION

1.1. PHYLOGENY OF LAMPREY

The agnathans (jawless fish) are the most primitive group of vertebrates. They include five fossil groups, Heterostraci, Osteostraci, Galeaspida, Anaspida, and Thelodonta, and two extant groups, Myxinoidea (hagfish) and Petromyzontia (lampreys) (Blieck, 1992; Forey and Janvier, 1993). Taxonomic features which define the class Agnatha include the absence of both jaws and paired fins. Because hagfish and lampreys further share the characteristics of an eel-shaped body, absence of bone, specialized mouthparts, single median hypophyseal opening and pouch-like gills, they have been classically grouped together into Subclass Cyclostomata (Kent, 1969). However, recent paleontological evidence and cladistic analyses have determined that these commonalities result from convergent evolution and that hagfish and lampreys are less closely related to each other than lampreys are to the first jawed vertebrates, the gnathostomes (Janvier, 1981; Forey and Janvier, 1993). Furthermore, hagfish are no longer considered vertebrates because they lack arcual elements and instead are included in the broader classification of Craniata (Janvier, 1981). This recent reclassification has accredited lampreys with being the sole representatives of the most ancient, extant vertebrates. However, lampreys are not believed to be the stem vertebrate group (Romer and Parsons, 1977). Studies on lampreys provide

researchers with opportunity to examine vertebrate systems and mechanisms extant for 450 million years.

1.2. LAMPREY LIFE CYCLE AND ECONOMIC IMPACT

Ten of the 39 species of lampreys are anadromous (i.e., migrate from the sea to freshwater to spawn) parasites as adults and feed upon blood, fluid and to a lesser degree, tissues, of many species of fish (Hardisty, 1979). Four parasitic species are landlocked forms confined to lake systems. When given a suitable environment, parasitic lamprey species that have become landlocked are capable of inflicting severe damage on fish populations (Smith, 1971). This is demonstrated historically by the case of the sea lamprey, *Petromyzon marinus,* which brought about collapse of the Great Lakes Fishery in less than 30 years from the time of its introduction. In addition to its severe impact on species important to the fishing industry, *P. marinus* caused a series of biological changes within the Great Lakes ecosystem (Smith, 1971).

Parasitic species such as *P. marinus* have a complex life cycle. Early developmental stages of the sea lamprey have been described by Piavis (1961, 1971). Ten to 13 days post-fertilization (pf) the embryo hatches as a prolarva. The prolarva progresses through three developmental stages, Pigmentation (13-16 days pf), Gill-cleft (15-17 days pf) and Burrowing (17-33 days pf), before reaching the larval stage when most non-genital systems are fully differentiated. During the last prolarval stage, sea lampreys burrow into the substrate of the stream bed (Piavis, 1961, 1971) and assume a microphagous mode which continues for the four to five-year duration

of the larval stage (Hardisty and Potter, 1971). During transformation from larva into parasitic adult, the sea lamprey advances through seven metamorphic stages over approximately three to four months (from mid-July to October), when profound external and internal changes occur in its morphology and physiology (Potter *et al.*, 1978; Youson and Potter, 1979; Youson, 1980). The ensuing adult of anadromous *P. marinus* migrates to the sea where it remains for several years before returning to freshwater streams to spawn (Beamish, 1980).

Effective control of lamprey populations by application of lampricides in the Great Lakes has resulted in reestablishment of a fishing industry worth two to four billion dollars annually (Great Lakes Fisheries Commission, 1992 written communication). However, use of toxic chemicals to control pest species conflicts with the philosophy of recent environmental trends. In 1992 the Great Lakes Fishery Commission appealed to the scientific community to find new control techniques as alternatives to lampricides.

The lamprey is especially sensitive to factors causing mortality during the metamorphic stages (Damas, 1935; Hardisty and Potter, 1971). Little information is available on the embryonic and prolarval stages, but it is assumed that lamprey would be more vulnerable during this time period (Hardisty and Potter, 1971). Research on mechanisms such as chondrogenesis during early developmental and metamorphic stages may reveal alternative methods of controlling lamprey populations. For example, the problem of lamprey parasitism would be eliminated if metamorphosis of the larval into the adult skeleton could be prevented.

1.3. THE VERTEBRATE SKELETON

Elements of the vertebrate skeleton are classified by criteria of position, structure, function, ontogeny and phylogeny. Romer and Parsons (1977) divide the skeleton into two major subdivisions; the dermal skeleton and the endoskeleton. In Osteichthyes (bony fish) the dermal skeleton is composed of bones and cartilages which shield the head, and support the gills, operculum and teeth (Hildebrand, 1974). In higher vertebrates the dermal skeleton is much reduced and persists as the clavicle, and elements of the skull and jaw. (Hildebrand, 1974; Webster and Webster, 1974). Ancient agnathans (such as ostracoderms) demonstrated a extensive armour consisting of dermal bones. The dermal skeleton is nonexistent in lampreys.

The second division of the skeleton, the endoskeleton, can be further subdivided into the axial skeleton including the skull, notochord, vertebrae, ribs and sternum and the appendicular skeleton comprised of pectoral and pelvic girdles, limbs and fins (Kent, 1969; Evans and Christensen, 1979). The appendicular skeleton is completely lacking in agnathans (Hardisty, 1981) and snakes (Kent, 1969). The skull, notochord and vertebral rudiments are the only aspects of the axial skeleton present in lampreys (Hardisty, 1981; Janvier, 1993).

1.3.1. The skull

The skull (ie. braincase and upper jaw) is considered to be the oldest and most complex component of the skeleton (DeBeer, 1971; Romer and Parsons, 1977), and

has its own terminology reflecting function and/or embryonic origin of its elements. The elements of the skull are grouped into the neurocranium (or chondrocranium in the absence of bone), splanchnocranium (viscerocranium) and dermatocranium (DeBeer, 1971; Hildebrand, 1974; Webster and Webster, 1974). The neurocranium surrounds and supports the brain and sense organs and can be subdivided into basicranium and lateral braincase walls (Rieppel, 1993). Principal elements of the neurocranium include the trabeculae, parachordals, basal plate, cranial vertebrae or neural arches (later occipital arches in advanced vertebrates), and nasal and auditory capsules (Hildebrand, 1974). The splanchnocranium (viscerocranium), surrounds the oral cavity, pharynx and upper respiratory region. In fish and some amphibians the splanchnocranium consists of the jaws and branchial cartilages which support the gills. In embryos of amniotes, the splanchnocranium combines the branchial arches, which later develop into structures such as the jaws, inner ear ossicles, and hyoid in the adult. The final component of the skull, the dermatocranium, is represented in higher vertebrates by the nasals, vomers and maxillae. In addition, bones of the dorsal and lateral aspects of the braincase form as a result of fusion of dermatocranial with neurocranial or splanchnocranial elements. The extent of the contribution by the dermatocranium in the formation of these bones varies between classes.

1.3.2. The lamprey cranial skeleton

The neurocranium and splanchnocranium collectively compose the cranial skeleton or "head skeleton" in lampreys. The head skeleton, notochord and vertebral rudiments represent the entire skeleton of the lamprey (Hardisty, 1981). Due to the absence of an extensive dermal skeleton and jaws, the lamprey head skeleton differs from the higher vertebrate skull in that there is very clear definition between neurocranium and splanchnocranium (Romer and Parsons, 1977). The high proportion of splanchnocranial elements in the lamprey skeleton is seen only during the embryo stage in higher vertebrates. Because of these characteristics, the lamprey skeleton was once considered to be a primitive form of the vertebrate skeleton and an illustration of how "ontogeny recapitulates phylogeny". However, today it is recognized that certain components of both larval and adult lamprey skeletons are highly specialized structures (Romer and Parsons, 1977; Hardisty, 1981). The adult skeleton in particular demonstrates a number of skeletal elements which have no homologous counterparts in other vertebrates (Hildebrand, 1974; Hardisty, 1981).

Classical morphological descriptions of the lamprey head skeleton have been given by Damas (1935, 1944) and Johnels (1948). More recent descriptions have been made by DeBeer (1971) and Hardisty (1981). The complexity of the lamprey head skeleton increases with each successive developmental stage. During prolarval stages, cartilaginous components of the neurocranium include the trabeculae and their caudal extensions, the parachordals, and the basitrabecular processes (Figure

1.1). By the larval stage the lamprey neurocranium has expanded to include the otic and nasal capsules and trabecular commissure.

The trabeculae are thin rods of cartilage which support the brain ventrally. They are round to oval in cross-section and extend cranially from a point just behind the rostral tip of the notochord and between the otic capsules, to the rostral end of the infundibulum. Caudally the trabeculae run parallel to each other along the lateral aspects of the notochord which they juxtapose. They deviate laterally from one another just caudal to the tip of the notochord and continue ventrolaterally to the brain. At the infundibulum they bend inwards and are united by a trabecular commissure (Figure 1.2).

The parachordals appear histologically as caudal extensions of the trabeculae. They are tightly flattened against the lateral edges of the notochord and caudally unite with the branchial arches of the splanchnocranium. Anatomically, the parachordals are separated from the trabeculae by the presence of lateral extensions of cartilage, the basitrabecular processes, and by their ontogenic origin are considered to be splanchnocranial elements (DeBeer, 1971; Hardisty, 1981).

During metamorphosis the lamprey skeleton undergoes developmental changes that result in a slightly more complex and rigid skeleton in the adult (Hardisty, 1981). In the neurocranium, the lateral aspects chondrify, an intertrabecular plate forms between rostral portions of the trabeculae, and a sub-ocular arch extends between the trabecular commissure and the otic capsules. However, the most dorsal aspect of the neurocranium remains membranous. The branchial "basket" becomes more

Figure 1.1. The skeleton of the lamprey in the A) prolarval, B) larval, and C) adult stage. The neurocranial cartilages are listed on the right side of the key and splanchnocranial cartilages on the left. The solid grey represents additional adult neurocranial cartilages not listed in key. Diagrams based upon Sewertzoff (1916, 1917), Johnels (1948) and Hardisty (1981).

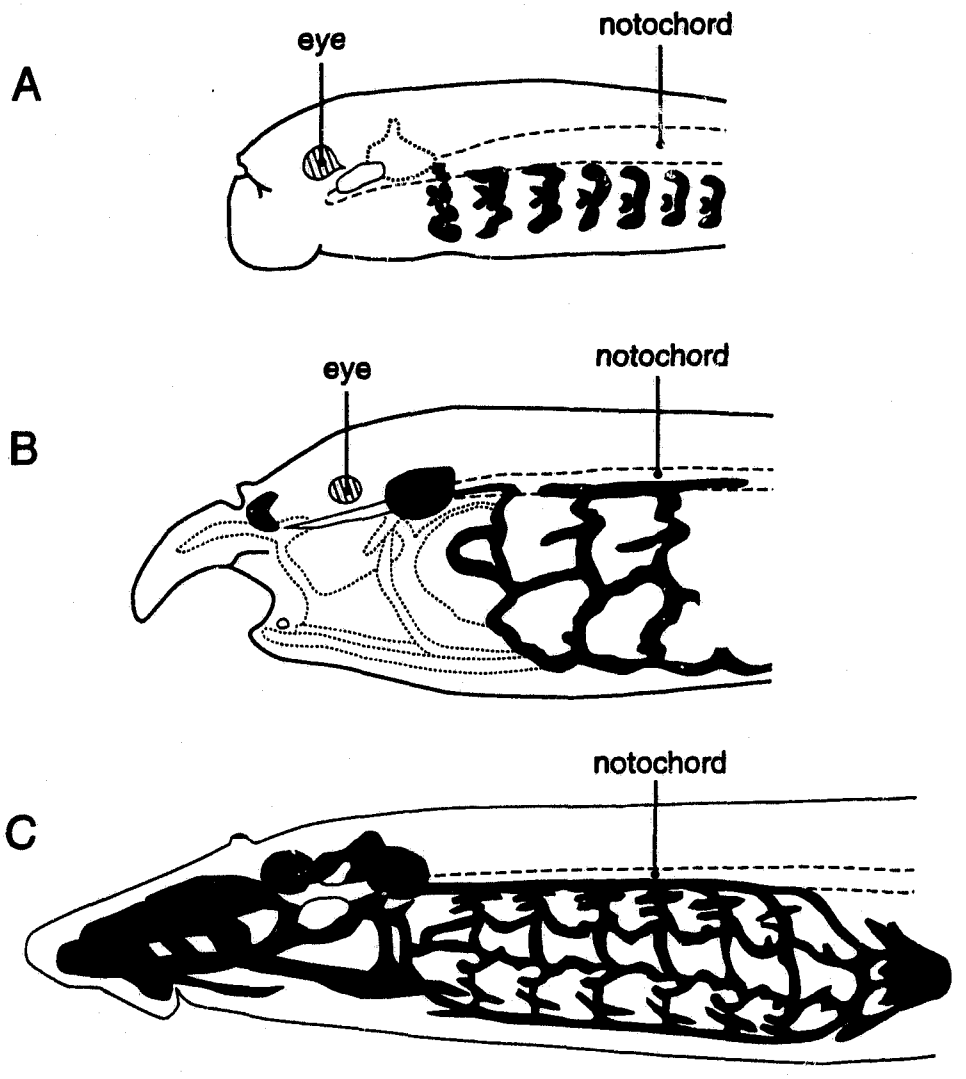
A
eye
notochord
B
eye
notochord
C
notochord
trabecular
otic capsule
non-cartilagenous otic capsule
nasal
parachordal
pericardial
branchial basket
annular

Figure 1.2. Ventral view of the larval lamprey neurocranium. Notochord is stippled. Membranous floor of braincase is shaded grey. Based upon Hardisty (1981).

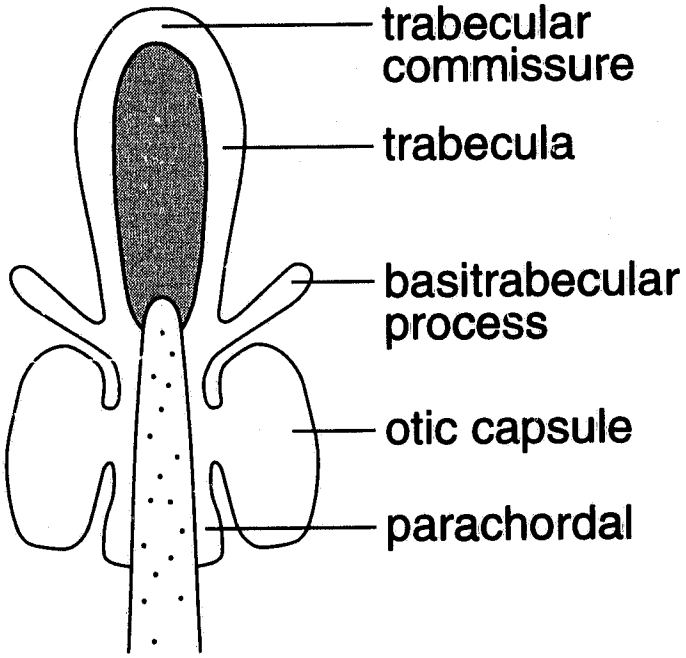
trabecular commissure
trabecula
basitrabecular process
otic capsule
parachordal

elaborate than that of earlier stages and by the adult stage is secured to the neurocranium. The splanchnocranium extends caudally to form the pericardial cartilage which surrounds the heart in the adult. It continues cranially to develop the tongue (piston cartilage) and the cartilages that both support the buccal funnel and serve as an anchorage site for muscles controlling its movements.

Morphological differences between skeletons of each lamprey stage are necessary adaptations to different diets, habitats and behaviours (Hardisty, 1981). In the larval stage the lamprey is a burrowing animal that filter feeds and requires a flexible skeleton. In the adult stage, however, *P. marinus* is free-swimming and feeds parasitically upon blood and tissues of fish. Metamorphic development of a rigid cartilaginous skeleton equips the lamprey with an oral sucker and necessary support (annular cartilage) for sucking and attaching to the host. New feeding structures, including a rasping tongue, also develop.

1.3.3. Ontogeny of the vertebrate skeleton

The majority of vertebrate skeletal elements originate from mesoderm while the remainder are neural crest derivatives (Hall, 1977, 1978; Urist, 1983; Carlson, 1988; Hall and Horstadius, 1988). Appendicular skeletal elements; vertebrae, and ribs of the axial; jaws; and the basal plate, parachordals, otics, and orbital cartilages of the skull are of mesodermal origin (Webster and Webster, 1974; Hall, 1978; Carlson, 1988). During embryogenesis mesoderm on either side of the notochord segments into distinct blocks of cells or somites, and becomes organized as an epithelium

surrounding a central core (Hall, 1977; Carlson, 1988). Upon induction by the neural tube and notochord, the axial skeleton progenitor cells located in the ventromedial aspect of the somite (the sclerotome), become mesenchymal and migrate into a position surrounding the notochord and ventral neural tube (Carlson, 1988). The extracellular matrix (ECM) products of these latter structures further induce sclerotomal cells to differentiate into chondrogenic cells of the vertebrae and ribs (Olson and Low, 1971; Hall, 1977). The remaining mesoderm becomes reorganized into several layers of cells which extend subectodermally from the somites along the lateral aspects of the embryo. The outer most layer of this lateral plate mesoderm interacts with ectoderm and eventually differentiates into the appendages (Hall, 1978; Solursh, 1983; Kosher, 1983)..

The dermal skeleton and elements of the viscerocranium are derived from neural crest cells (Carlson, 1988; Hall and Horstadius, 1988; LeDouarin *et al.*, 1993; Stemple and Anderson, 1993). Neural crest cells are migratory in nature and while the temporal pattern of neural crest emigration varies depending on species and craniocaudal location within the animal, crest cells begin to stream out from between neural and nonneural ectoderm about the time of closure of the neural tube (Horstadius, 1950; LeDouarin and Teillet, 1974; Noden, 1975; Tosney, 1982; Tan and Morriss-Kay, 1986; Osumi-Yamashita and Eto, 1990; Serbedzija *et al.*, 1992; Erickson and Perris, 1993). There are four distinct populations of neural crest cells along the craniocaudal axis; cranial, vagal, trunk and lumbosacral (Noden, 1975; Tan and Morriss-Kay, 1986; Hunt *et al.*, 1991; Erickson and Perris, 1993; Eisen and Weston,

1993; Bronner-Fraser, 1994). Neural crest cells may migrate along several pathways including beneath the dorsal ectoderm, through the rostral portion of the somites, or they may remain close to their original location (Carlson, 1988; Bronner-Fraser, 1994). The phenotypic fate of neural crest cells results from complex interactions of craniocaudal origin of neural crest cell, migration route taken, and environmental stimuli received along this route (Carlson, 1988; Hall and Horstadius, 1988; Bronner-Fraser, 1994). For example, cranial and trunk neural crest cells that migrate beneath the dorsal ectoderm differentiate into pigment cells while those that remain close to the original site along side the neural tube develop into ganglia. Cranial neural crest cells differ from trunk neural crest cells in that they contribute to connective tissue such as those of muscles, blood vessels, meninges and thyroid gland. They are also able to differentiate into connective tissue and craniofacial skeletal elements including branchial arches, ear ossicles, larynx, hyoid, jaws, trabeculae, and facial bones (LeLievre and Le Douarin, 1975; Hall, 1978; LeLievre, 1978; Noden, 1988; Thorogood, 1988; Carlson, 1988; Bronner-Fraser, 1994). Trunk neural crest cells lack the potential to develop into skeletal elements (Noden, 1988).

Mesodermal or ectodermal germ layers destined to become part of the skeleton differentiate into mesenchyme which transforms directly into bone by the process of intramembranous ossification, or into cartilage, which may later be replaced by bone) by a process of endochondral ossification (Junqueira *et al.*, 1986; Bloom and Fawcett, 1994). In intramembranous bone formation, mesenchyme differentiates into fibroblasts and osteoblasts. Fibroblasts produce a meshwork of collagen and reticular

fibres on top of which apatite minerals are deposited by osteoblasts (Webster and Webster, 1974). Flat bones in the skull and the limb girdles are formed by this process.

Bones of limbs, appendages, vertebral column, ribs, sternum, and braincase develop by endochondral ossification. Except for the cervical vertebral column (Olson and Low, 1971), the first step in endochondral bone formation in the embryo is organization of mesenchyme into condensations of cells (membranous skeleton). This organization of the mesenchyme occurs as a result of inductive interactions on the part of epithelia such as that of the notochord or neural tube (Hall, 1978; Ede, 1983; Hall, 1983a,b; Kosher, 1983; Solursh, 1983; Saunders, 1988; Hall and Miyake, 1992). Condensations are structures distinct from blastemas and anlages (Hall and Miyake, 1992). Cells of a prechondrogenic condensation lose their mesenchymal characteristics and exhibit a high nucleo-cytoplasmic ratio, large nucleoli, small mitochondria, plentiful free ribosomes and a poorly developed endoplasmic reticulum (Gould *et al.*, 1972; Searls *et al.*, 1972; Thorogood and Hinchcliffe, 1975; Hall, 1978; Ede, 1983; Hall and Miyake, 1992). Differentiation of cells of the mesenchymal condensation into chondroblasts is marked by production of cartilage matrix molecules which result in the formation of the cartilaginous model of the skeletal element (Ede, 1983). During endochondral ossification, bone is deposited directly in the cartilaginous model and the cartilage is eventually removed (Junqueira *et al.*, 1986; Bloom and Fawcett, 1994). In nonossified skeletal tissues, such as those of the lamprey, tracheal and laryngeal cartilages, the cartilage persists in the adult.

1.4. SKELETAL TISSUES

Principal skeletal tissues include cellular bone, chordoidal, chondroidal (cartilage-like), calcified cartilage, true cartilage, mucocartilage, aspidin (acellular bone), and notochordal tissue (Schaffer, 1930; Moss and Moss-Salentijn, 1983; Beresford, 1993). The latter two tissue types will not be considered. Bone is a very rigid tissue as a result of deposition of calcified material in its matrix, which contains type I collagen (Hall, 1978). The rigidity required to provide support for an organism is closely related to the size of the organism and the medium of its environment. Nonaquatic species require support of an ossified skeleton. Bone is found in all vertebrates higher in the evolutionary hierarchy than Chondricthyes; sharks and cyclostomes have lost bone secondarily through regression (Webster and Webster, 1974; Hall, 1978). However, sharks have developed calcified cartilage for additional support (Webster and Webster, 1974).

In taxa lower than reptiles on the evolutionary scale, including some invertebrates (Moss and Moss-Salentijn, 1983), there are several morphologically distinct skeletal tissues. These highly cellular tissues include chordoidal tissue, which is found in primitive fish such as the Chimera (Moss and Moss-Salentijn, 1983) and chondroidal tissue, found in epiglottal cartilages of some rodents and the Achilles tendon of frogs. Chondroidal tissue is more organized than chordoidal tissue and exhibits large, ovoid chondrocytes in a sparse matrix (Moss and Moss-Salentijn, 1983). Mucocartilage of the larval lamprey neurocranium is a specialized form of loose connective tissue unique to lampreys (Wright and Youson, 1982). It retains

embryonic qualities and is able to dedifferentiate into cartilage during metamorphosis Armstrong *et al.*, 1987).

1.4.1. Vertebrate cartilage

True cartilage, like bone, is a connective tissue that consists of cells lying in a self-synthesized matrix. The matrix imparts functional properties. It is the matrix rather than the chondrocytic phenotype that characterizes the cartilage cell. The matrix is composed of a fibrillar component, which provides structural integrity and framework for the attachment of the ground substance. Ground substance consists predominately of a tertiary complex of large proteoglycans (aggrecan), link proteins and hyaluronic acid. Anchorin, chondronectin, type VI collagen and cartilage matrix protein (CMP) are involved in attachment of chondrocytes to the matrix.

Three vertebrate cartilages are classically described based upon the composition of their fibrillar component: 1) hyaline cartilage of the nose, larynx, trachea and bronchi, ventral end of the ribs, articular surface of the joints, epiphyseal plate of long bones and cartilaginous model of the embryo, which contains predominantly type II collagen (Bloom and Fawcett, 1994); 2) elastic cartilage of the ear auricle, eustachian tubes and epiglottis, which has a predominance of elastic fibers composed of amorphous elastin and microfibrils in addition to type II collagen (Mayne and von der Mark, 1983; Kostovic-Knezevic *et al.*, 1986); and 3) fibrocartilage found in intervertebral discs and attachments of some ligaments to bone, which contains mostly type I collagen (Stockwell, 1979; Benjamin and Evans, 1990). Hyaline cartilage

matrix is by far the most studied and best understood of the three cartilages. For this reason the following description of composition and structural organization will be based upon this cartilage type.

Fibrillar collagen is responsible for the tensile strength of cartilage and is the major structural protein of matrix, comprising 40-50% (Mayne and von der Mark, 1983; Upholt and Olsen, 1991). Collagen fibrils in vertebrate tissue are polymerized forms of tropocollagen, a soluble monomeric form of the collagen protein (Serafini-Fracassini and Smith, 1974). Tropocollagen in turn is composed of three polypeptide chains intertwined in a helix. These are stabilized by covalent cross-linkages and hydrogen bonding between the chains (Stockwell, 1979; Mayne and van der Mark, 1983; Linsenmayer, 1991). Type II collagen is composed of three α1(II) chains while type I collagen is composed of one α2 and two α1(I) chains. Of the fifteen different collagens known (Linsenmayer, 1991), nine (I, II, III, V, VI, IX, X, XI, XIII) have been reported to be present in hyaline cartilage, depending on the cartilaginous structure and stage of differentiation (Sandberg, 1991; Bruckner and van der Rest, 1994).

It has been established that Type II is the characteristic collagen of cartilage matrix. However, recent examinations have demonstrated that a number of other minor collagens also contribute to the composition of cartilage fibrils. Aggregations of collagen type II around a core of collagen type XI are stabilized by cross-links with a nonfibrillar collagen, type IX, on the surface of the fibril (van der Rest and Mayne, 1988; Bruckner and van der Rest, 1994). Cartilage matrix protein is believed to

further assist organization of the collagen fibril by binding to adjacent ends of surface-located, collagen type II molecules (Winterbottom *et al.*, 1992). It is worth noting that while in cartilage collagen type IX is thought to play an important role in stabilizing the type II collagen molecules, type II is also found without type IX in basement membranes in early avian embryos and the notochord. It is therefore suspected that type II may play multifunctional roles independent of interactions with type IX (Kosher and Solursh, 1989).

Cartilage matrix contains five proteoglycans: aggrecan, decorin, biglycan, fibromodulin, and collagen type IX (for reviews of structure and function see Takagi, 1990; Yanagishita, 1993; Hardingham *et al.*, 1994; Roughley and Lee, 1994). The most abundant proteoglycan in cartilage, aggrecan, is composed of a large number of glycosaminoglycans, keratin and chondroitin sulphate, covalently bound to a core protein in a "bottlebrush" arrangement. Resiliency of cartilage is attributed to the hydrophilic nature of the large number of negatively charged aggrecan glycosaminoglycans. Monomers of aggrecan attach to long strands of hyaluronic acid to form large aggrecan aggregates which are the second principal component of cartilage. The surface of the cartilage collagen fibril supports the small proteoglycans decorin and fibromodulin, which assist in attaching the fibril to the aggrecan aggregate (Bruckner and van der Rest, 1994; Roughley and Lee, 1994). Decorin also binds to and regulates growth factor TGF-ß. Biglycan is localized in the pericellular matrix and is believed to interact with collagen type IV.

1.4.2. Ultrastructure of cartilage

Ultrastructure of chondrocytes has been described in detail by Searls *et al.* (1972); Thorogood and Hinchliffe (1975); Stockwell (1979); Sheldon (1983); Kosher (1983); Hunziker and Herrmann (1984) and Hunziker and Schenk (1984). Chondrocytes are round to ovoid in shape, with a large nucleus and ruffled cell membrane. The projections of the membrane contain many microfilaments that extend into the surrounding matrix. Small invaginations, caveolae, are characteristic of chondrocyte plasma membranes (Horton, 1993). Glycogen is abundant in chondrocytes, and many of these cells, especially those of elastic tissue, contain large lipid droplets (Anderson, 1964; Junqueira *et al.*, 1986; Sheldon, 1983). Most cells also exhibit microtubules and a cilium. Morphology of cartilage cells varies depending on their state of maturity and position within the cartilage (Olson and Low, 1971). During early differentiation, chondrogenic cells are flattened cells with dense cytoplasm, poorly developed rough endoplasmic reticulum (RER), few Golgi saccules and secretory vesicles. Chondroblasts (cartilage cells that are actively synthesizing cartilage matrix) have numerous mitochondria, active Golgi complexes with associated secretory vesicles and abundant RER. In the final stages of maturity cartilage cells (chondrocytes) exhibit pale cytoplasm, few Golgi and fragments of RER cisternae. The centrally located cells of mature cartilaginous structures generally display these features. Cartilage matrix appears ultrastructurally as a network of collagen type II fibrils (10-20nm in diameter) that do not exhibit a distinct banding pattern. Interdispersed among the fibrillar components are matrix granules (20-30nm in

diameter). In routine electron microscopic preparations, these granules are structural representations of monomers (Hascall, 1980) or groups (Phillips and Pottenger, 1989) of collapsed aggrecan aggregates.

1.4.3. Lamprey skeletal tissues

The entire skeletal system of the lamprey is cartilaginous. Lamprey cartilage resembles mammalian and avian hyaline cartilage at the gross and light-microscopic level (Hardisty, 1981). Both cartilage types are white and translucent, but lamprey cartilage has been found to be ultrastructurally and biochemically distinct from all other known vertebrate cartilages (Wright et al., 1983; Wright and Youson, 1983; Robson *et al.*, 1993). Initially lamprey cartilage was thought to contain elastin or elastin-like substances, since positive histochemical reactions were obtained with stains such as Verhoeff's elastin stain, but biochemical analysis has proven otherwise (Wright *et al.*, 1983). Ultrastructural examination has shown that unlike the randomly distributed type II collagen fibrils that compose 40-50% of the dry weight of a mammalian cartilage (Mayne and von de Mark, 1983), matrix of lamprey cartilage contains a complex network of branched matrix fibrils (15-40 nm in diameter), very little collagen and no observable elastin component (Wright and Youson, 1983; Wright *et al.*, 1988). However, matrix granules similar to those of mammalian hyaline cartilage are present and are believed to be collapsed aggrecan molecules.

Branched matrix fibrils in lamprey cartilage are morphological representations of a structural protein, lamprin, unique to lamprey cartilage called lamprin (Wright

and Youson, 1983). Lamprin has been found to comprise 44-51% of adult annular cartilage (Wright *et al.*, 1983). Recently, much information on the biochemistry of this protein has been accumulated (Robson *et al.*, 1993). Lamprin has been isolated from annular cartilage of adult lamprey and its amino acid sequence determined. Polyclonal antibodies to a soluble component of lamprin have been produced and used to localize lamprin immunocytochemically within tissue sections. Oligonucleotide probes to lamprin mRNA have been synthesized and used to probe Northern blots of total RNA isolated from annular cartilage. A cDNA library has been produced for this same cartilage. This information has provided new avenues for research on lamprey cartilage and chondrogenic mechanisms.

In recent decades much information has become available on genetic, biochemical and ultrastructural aspects of chondrogenesis in higher vertebrates. This information has contributed to our understanding of skeletogenesis. It has illuminated ontogenic origins, processes of migration and differentiation, skeletal patterning, induction mechanisms, gene regulation, and matrix formation and biochemistry. In contrast our knowledge of chondrogenic mechanisms in the lamprey is limited. In addition to the classical histological examinations by Damas (1944) and Johnels (1948), and biochemical studies by Wright *et al.* (1983) and Robson *et al.* (1993), chondrogenesis in the metamorphic lamprey has been examined ultrastructurally and immunocytochemically in a series of studies by Wright and Youson (1982) and Armstrong *et al.* (1987). However, studies on chondrogenic mechanisms during embryonic and prolarval stages are limited to the aforementioned

classical histological examinations and recent extirpation experiments by Newth (1956) and Langille and Hall (1986, 1988a,b). Biochemical analysis of the lamprey skeleton has demonstrated existence of a previously unknown noncollagenous-based vertebrate cartilage. Continued research on the molecular biology and biochemical aspects of mechanisms such as chondrogenesis, that are in place during early developmental and metamorphic stages, may provide alternative methods of controlling lamprey populations. Before such research is undertaken, however, there must be a clear understanding of the basic morphology and developmental patterns of these mechanisms.

The purpose of this study is to describe the morphology and molecular biology of chondrogenesis in prolarval and metamorphic stages of *Petromyzon marinus*. This information will contribute to understanding of relationships between the chondrogenic processes in primitive noncollagenous-based cartilages and those in the collagenous-based cartilages of higher vertebrates.

1.5. RESEARCH OBJECTIVES

1. To complete a light microscopic morphological study of spatial and temporal development of trabecular cartilage during prolarval stages of the sea lamprey, *Petromyzon marinus*, and compare the findings with those of classical investigations. The information gained from this study will be used to correlate chronological age with stage of development of the trabecular cartilage and serve as a guideline for ultrastructural and molecular analyses.

2. To describe ultrastructural changes that occur during chondrogenesis in prolarval stages of the sea lamprey. Comparisons will be made with the fine structure of cartilage development in metamorphic lampreys, and embryos of avian and mammalian vertebrates.

3. To develop and use *in situ* hybridization techniques in determining temporal and spatial expression patterns of lamprin mRNA during early developmental and metamorphic stages of the sea lamprey.

2. CHONDROGENESIS OF THE TRABECULAR CARTILAGE OF THE SEA LAMPREY, *PETROMYZON MARINUS*: A LIGHT MICROSCOPIC AND ULTRASTRUCTURAL EXAMINATION

2.1. INTRODUCTION

The skeleton remains completely cartilaginous throughout the entire life of the lamprey. It is composed of two distinct elements; the neurocranium, which is ventral support for the brain, and the splanchnocranium, including the branchial baskets (Hardisty, 1981). Studies of chondrogenesis in early developmental stages of the lamprey are limited to a series of classical morphological examinations at the light microscopic level (Sewertzoff, 1916, 1917; Damas, 1935, 1944; Johnels, 1948). More recently, Newth (1956) and Langille and Hall (1986, 1988a,b) evaluated the role of the neural crest in formation of the lamprey skeleton, using extirpation studies. While the information obtained from classical studies is heavily relied upon today, there are a number of inherent problems. The most critical of the difficulty in comparing earlier staging criteria of number of somites, body length and age to currently used staging criteria defined by Piavis (1961, 1971). This problem is compounded by lack of controlled conditions for rearing lampreys, and by the long intervals, with respect to cartilage development between sampling times.

Much information has accumulated regarding biochemical and molecular processes of chondrogenesis in higher vertebrates. It is now known that chondrogenesis is a series of well-defined and orderly events that commences with formation of a distinct structure, the mesenchymal condensation (Fell, 1925; Fell and Canti, 1934; Gould *et al.*, 1972; Searls *et al.*, 1972; Thorogood and Hinchcliffe, 1975; Ede, 1983; Hall and Miyake, 1992). The formation of a condensation initiates a series of chain reactions which eventually cause differentiation of mesenchymal cells into chondrocytes capable of synthesizing the collagens and proteoglycans characteristic of cartilage matrix (Solursh, 1983; Hunter and Caplan, 1983; Coelho and Kosher, 1991; Hall and Miyake, 1992). In contrast to our extensive knowledge of chondrogenic events and processes in higher vertebrates, the information we possess today regarding development of skeletal elements in early embryonic/prolarval stages of the lamprey remains limited.

Our laboratory has been involved in a comprehensive investigation of lamprey cartilage at the molecular, biochemical, and ultrastructural levels. It is now known that, while lamprey cartilage grossly resembles hyaline cartilage found in higher vertebrates, it is unique in a number of aspects (Wright and Youson, 1983; Wright *et al.*, 1983; Robson *et al.*, 1993). Trabecular, nasal and branchial cartilages of larval, young juvenile, and upstream-migrant adults, and the annular, piston and pericardial cartilage of the latter two stages has been described at the ultrastructural level (Wright and Youson, 1983; Wright *et al.*, 1988). The only ultrastructural study of developing lamprey cartilage has addressed the transformation of a region of

mucocartilage in larva into the adult piston (tongue) cartilage during metamorphosis (Armstrong *et al.*, 1987). To date, there has been no ultrastructural examination of chondrogenic events in early embryonic or prolarval stages of the lamprey.

Because of technical limitations in classical studies, the great expansion of knowledge concerning chondrogenic mechanisms in higher vertebrates, and new appreciation of the uniqueness of lamprey cartilage, re-evaluation of chondrogenesis in the lamprey is warranted. The purpose of this study is 1) to examine temporal and spatial patterns of development of neurocranial trabeculae in early developmental stages of the sea lamprey, *Petromyzon marinus*, using modern techniques and 2) to provide descriptions of ultrastructural changes associated with prolarval chondrogenic events. Findings of this study will provide a frame of reference for future examinations of chondrogenic events in this ancient vertebrate.

2.2. METHODS AND MATERIALS

2.2.1. Artificial fertilization and raising of embryos

Adult lamprey were captured during upstream spring migration in May at a fish ladder (operated by the Department of Fisheries and Oceans Canada) on the LeHave River in New Germany, Nova Scotia. They were transported to the laboratory where they were maintained in a 1000L fibreglass raceway with continuous flow-through, fresh, 11-15^{0}C ground water. Lighting conditions alternated between 12 hours of dark and 12 hours of green filtered light as a means of keeping the lamprey quiet and subdued.

A minimum of four females and four males were transferred to 200 L fibreglass tanks containing fresh 18.4^{0}C groundwater and maintained until they reached sexual maturity. Sexual maturity was determined by external criteria (Piavis, 1961). Females develop a swollen, purplish ridge caudal to the cloacal region and demonstrate a soft, distended ventral surface. Sexually mature males display a prominent mid-dorsal ridge and a whitish papilla protruding through the cloaca.

Eggs and sperm were extracted manually from ripe, unanesthetized lamprey. Sperm were collected in 50ml beakers and stored on ice for a maximum of 30 minutes. Viability of sperm was determined by examining for motility under a light microscope. Following sperm collection, eggs were collected in monolayers in glass bowls with base diameter of eight cm. Viewed with a dissecting microscope viable eggs appeared as taupish-colored, evenly-shaped spheres. Several drops of undiluted sperm were applied to the eggs with a Pasteur pipette. The mixture was gently stirred with a clean pipette bulb, covered and allowed to sit for five minutes. Eggs and resultant zygotes were never exposed to light for intervals exceeding 10 minutes. The mixture was flooded with fresh 18.4^{0}C groundwater and left undisturbed at room temperature for 1 hour. Following this period, water was siphoned off the eggs and replaced with fresh water before the bowls were placed in 18.4^{0}C incubators. In this manner fresh water was applied to the embryos at 4 hours post-fertilization (pf) and thereafter every 12 hours. After 24 hours unfertilized eggs, dead embryos and contaminating material were carefully removed from the viable embryos to prevent fungal infection. Embryos were staged using criteria of external appearance

described by Piavis (1961, 1971) (Appendix A). Post-gastrulation embryos (days 4-5pf) were transferred to Heath trays in a continuous running-water system.

2.2.2. Light microscopy

Three to 10 prolarvae were collected daily between day 15 (stage 15:pigmentation) and day 33 (stage 18:larval), anesthetized in 0.05% tricaine methanesulfonate (MS-222) and fixed at room temperature *in toto* for 10-24 hours in Bouin's fixative in preparation for light microscopy (LM). Samples were dehydrated through an ascending series of graded alcohols, cleared in xylene and embedded in Tissue Prep II paraffin (Allied Corporation, Fisher Scientific, Fair Lawn, NJ, USA). Six micrometer thick sections were cut using an A.O. Spencer 820 rotary microtome and mounted on glass slides. Tissues were stained with 1) alcian blue, pH 1 or 2.5 with and without 0.1% nuclear fast red (Kernechtrot) counterstain (Luna, 1960); 2) Verhoeff's elastic stain (Humason, 1972); 3) periodic acid-Schiff's reagent (PAS) with alcian blue, pH 2.5 or light green counter stain (Humason, 1972); or 4) hematoxylin and eosin (Luna, 1960).

2.2.3. Electron microscopy

For electron microscopic examination, four to six prolarvae were collected daily between days 16-20pf and on days 22, 25, 26, 27, 28 and 31pf. Prolarvae were anesthetized in 0.05% tricaine methanesulfonate (MS-222) and fixed *in toto two* hours at 4^0C in 2.5% glutaraldehyde in 0.1 M Sorenson's phosphate buffer pH 7.3 (Dykstra,

1993). They were then postfixed one hour at room temperature in similarly buffered 1% osmium tetroxide. Samples were rinsed in buffer, dehydrated through a series of graded ethanols, and embedded in a mixture of Epon/Araldite via propylene oxide. Sequential thick sections (0.5μm) were taken at random intervals between the anterior tip of the notochord, through the central region of the eye, caudally, to the anterior end of the otic capsule. Sections were stained with 1% toluidine blue (T-blue) in a 1% sodium borate aqueous solution and photographed with a Zeiss Photoscope III. Ultrathin sections of 90 nm thickness were cut and mounted on Super-200 copper grids (J.B. EM, Dorval, Quebec, Canada). They were stained for 30 minutes with saturated uranyl acetate in 50% ethanol, followed by Sato's lead stain for two minutes (Sato, 1968). Ultrathin sections were examined and photographed using a Hitachi H-600 electron microscope operated at 75kV.

Cell numbers per area were estimated using low magnification electron micrographs (X3,750 to X12,500) of prolarval stages 15-18 days pf. Cells from three to four prolarvae of each stage were counted. One to three counts were made per animal. Actual counts of cells, including cell fragments, were made within the ventral medial aspects of the trabecular arc region (see section 2.3.1 for definition) for days 15pf and day 16pf, and within the condensations of later developmental stages. To estimate area, the length and width of regions counted were converted to micrometers and multiplied by each other. For consistency all counts were made using cross-sections that included the rudimentary eye. Ranges given represent highest and lowest counts obtained per stage.

Measurements of dimensions of cellular inclusions and organelles were made using micrographs of magnifications of X15,000 or higher. Matrix components and diameter and lengths of all fibrils and filaments were measured on electron micrographs magnified X100,000. For structures with magnified dimensions less than 1cm, a Bausch and Lomb Measuring Magnifier (Ladd Research Industries, Inc., Burlington, Vermont, USA) was used. A minimum of three animals per stage and 6-10 structures per animal was used in all calculations of structural dimensions. Minimum and maximum dimensions obtained are given as ranges.

2.3. RESULTS

Of the stains employed for LM, alcian blue (pH 2.5)/nuclear fast red was found to be the most useful for analysis of temporal and spatial development of condensations and trabecular cartilage in lamprey prolarvae. T-blue, 0.5μm plastic sections, which enable greater resolution of detail, were examined in conjunction with the alcian blue sections to provide gross morphological descriptions.

2.3.1. Gross morphology and pattern of development

By day 33pf (larval stage) the paired trabeculae were thin, curved rods of cartilage, oval in cross-section, which lay ventrolateral to the brain (Figures 1.1; 1.2; 2.1A,B). Caudally, these were closely apposed to lateral aspects of the notochord and merged with the anterior portion of the parachordals. The trabeculae diverged cranially from a point just behind the rostral aspect of the notochord and between

Figure 2.1. A) A light micrograph of a cross-section of a day 33pf larva at the level of the buccal cavity and the eye. T-blue stain. X 100. B) Higher magnification from the same stage embryo showing in cross-section the relationship between the trabecular cartilage (T), eye (Ey), brain (Br), and notochord (N). The buccal epithelium is indicated by arrowheads. Stain is alcian blue (pH 2.5)/nuclear fast red. X 830.

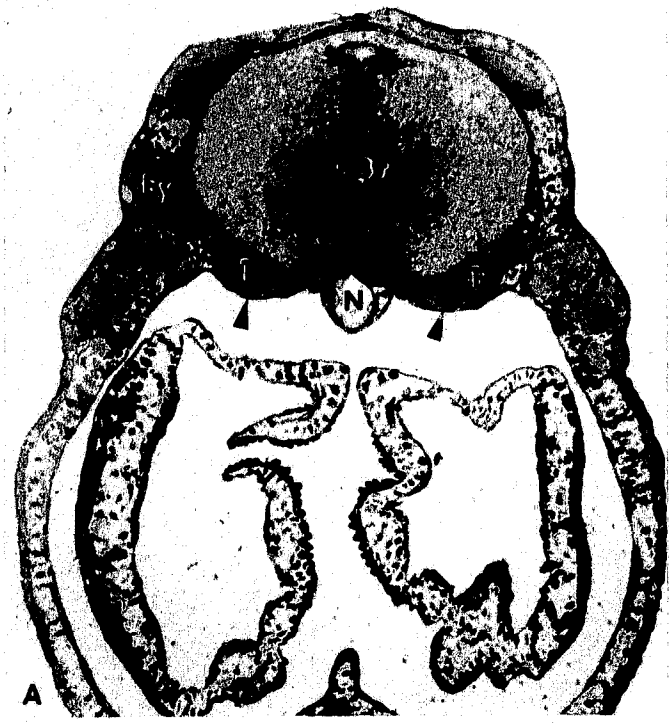
NT
A

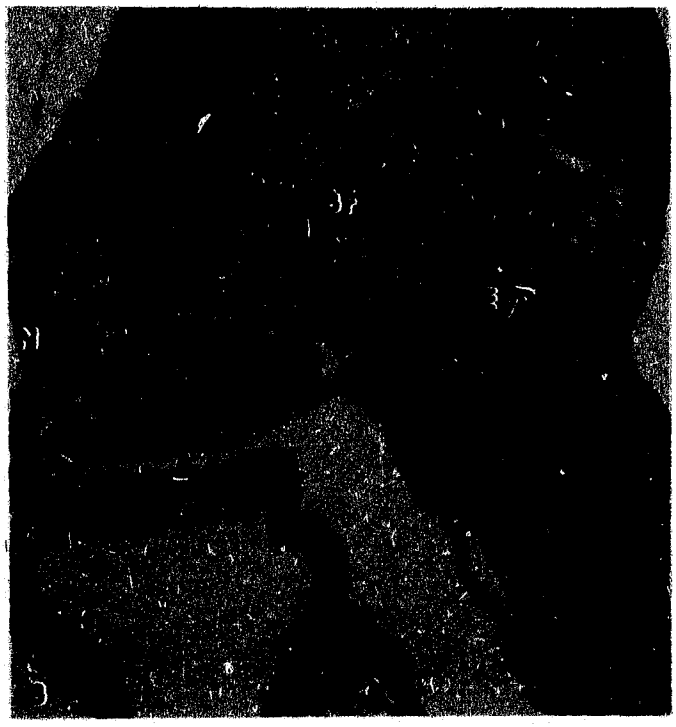

the otic capsules to a point slightly anterior to the eye. While the two cartilage rods were not united via the trabecular commissure at this stage of development, they are reported to join later during early aspects of the larval stage (Damas, 1944; Johnels, 1948; Hardisty, 1981).

The trabecular cartilage developed within a band of cells that were morphologically distinct from other head mesenchymal populations. For simplicity this band will be referred to as the trabecular arc (TA). In cross-sectional views, the TA was noted to extend dorsoventrally from ventral to ventrolateral aspects of the eye and curved medially (Figure 2.2A). The TA extended longitudinally from a point slightly rostral to the eye to end rostral to the otic capsules (Figure 2.2B). The TA was bounded dorsolaterally by the brain, and ventrally by the carotid artery and/or epithelium of the dorsal surface of the buccal cavity. The TA did not extend ventrally into the lateral body wall of the lamprey.

Each trabecular cartilage formed from one condensation. Pretrabecular condensations developed from cells within ventral medial aspects of the TA from the level of the eye to the otic capsule (Figures 2.2A,B; 2.3A,B). These latter two structures lengthened very little prior to the late burrowing stage (days 27-33pf). The condensations were spherical to rod-shaped and lengthened slightly in both cranial and caudal directions prior to overt cartilage differentiation. The ensuing trabecular cartilage buds also lengthened, in both cranial and caudal directions, as a result of an increase in cell number. However, growth in the rostral direction exceeded that in the caudal direction. The trabeculae were of thickest diameter in the cross-sectional

Figure 2.2. Schematic diagram showing the location of the trabecular arc (cross-hatching). Mesenchymal condensations are indicated by solid black shading. A) Cross-section. The buccal cavity is stippled. B) Longitudinal section. Eye (Ey); Notochord (N); Brain (Br); Otic capsule (O).

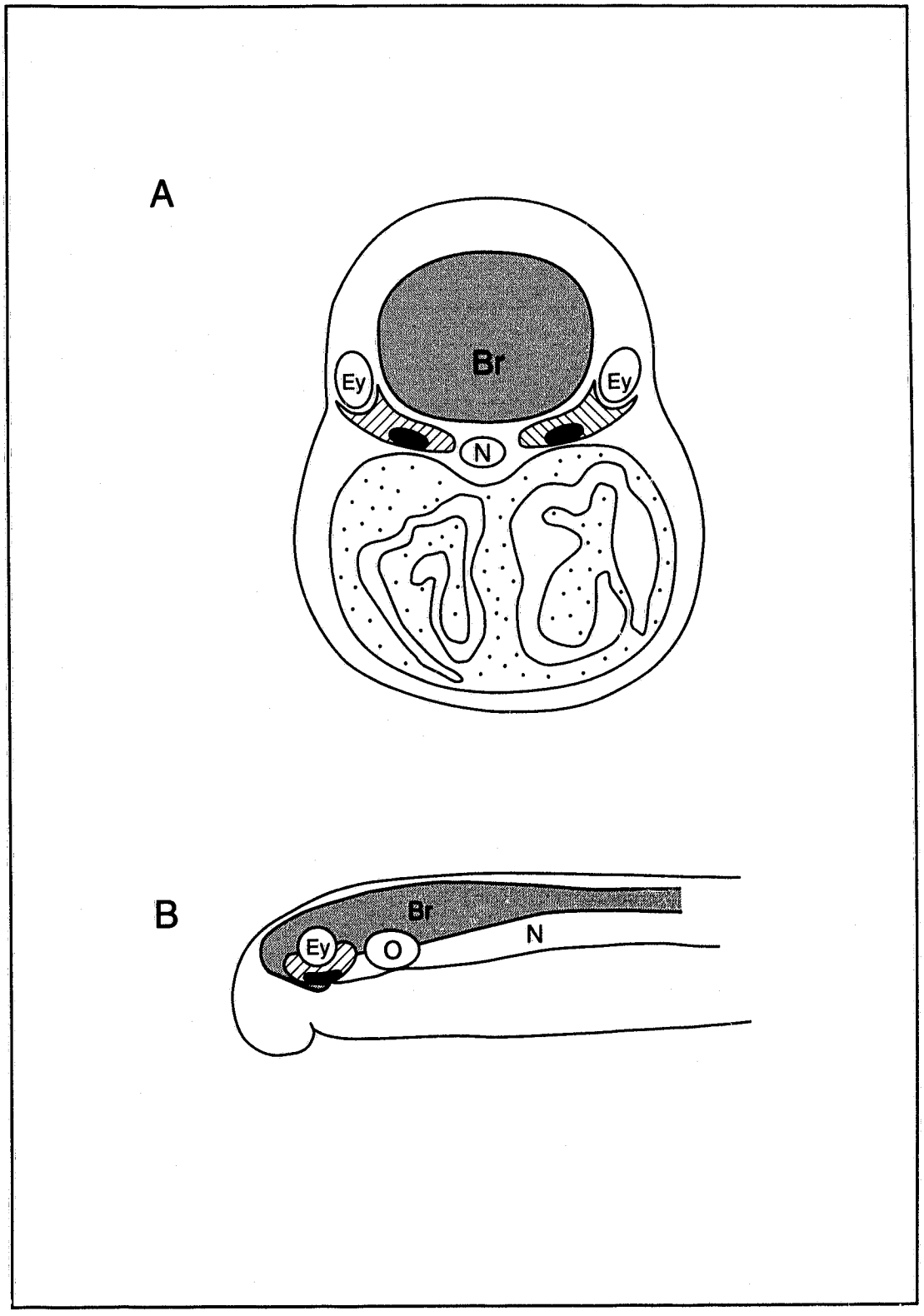
A
Br
Ey
Ey
N
B
Br
Ey
O
N

Figure 2.3. Idealized diagram demonstrating the relationship of the developing head cartilages to the notochord (N), eye (Ey), and otic capsules (O) in prolarval stages of the lamprey. Ventral view. Trabecular condensations are indicated by solid black shading in A (day 17pf) and B (day 18pf). Trabecular cartilage (dark-grey shading) is shown in C (day 20pf), D (day 25pf) and E (day 30pf). Parachordal cartilage (lighter-grey shading) and basitrabecular process (stippling) in D and F.

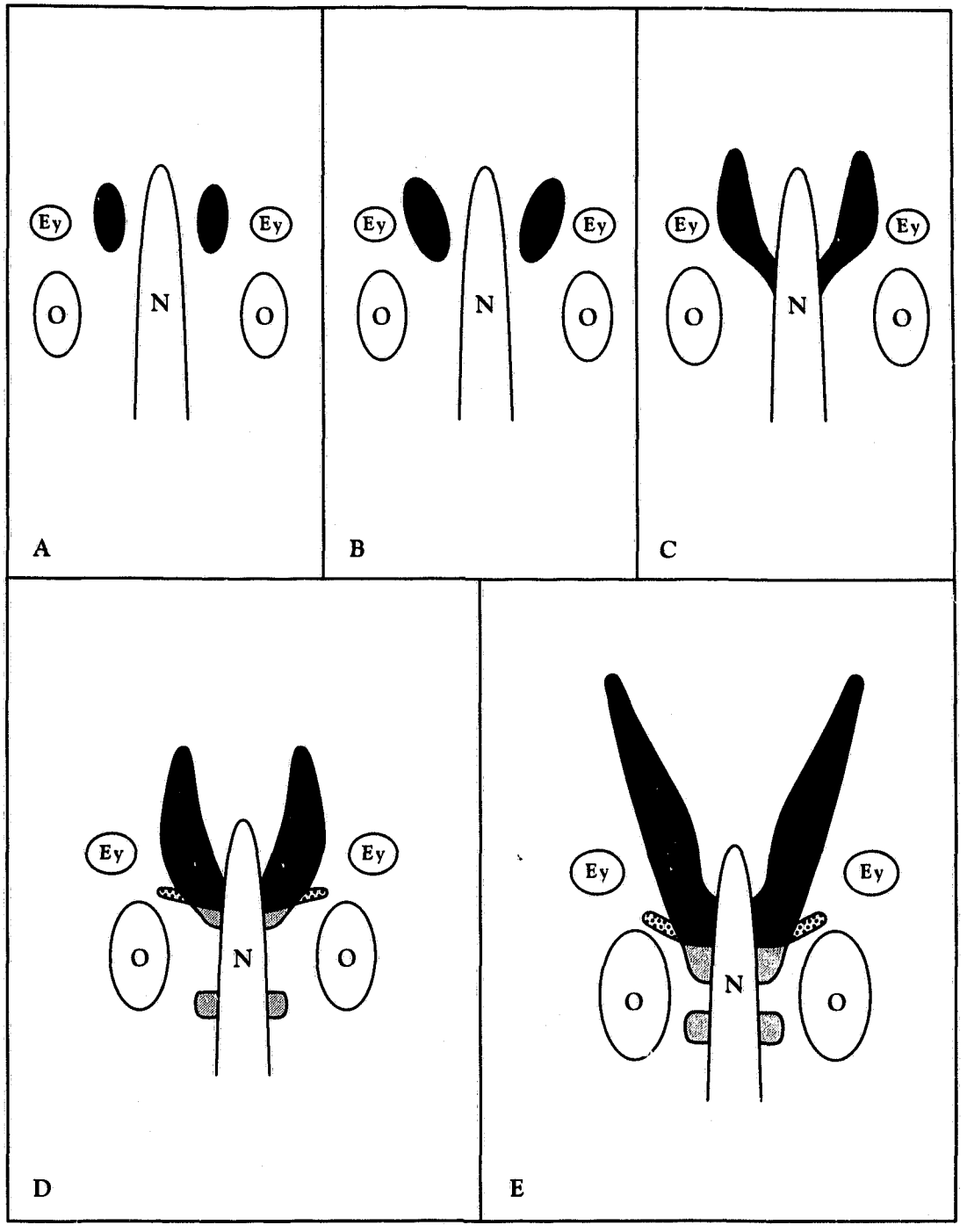
Ey
Ey
O
N
O
A
B
C
D
E

plane containing the eye. This region of the cartilaginous rods was the most developmentally advanced with respect to extent of cellular differentiation and quantity of ECM. As one proceeded in a rostral or caudal direction from the midpoint of the eye, the trabecular cells occurred in progressively earlier stages of differentiation.

Twenty-four to 36 hours after the first appearance of bilateral condensations rostral aspects of developing trabecular cartilages extended beyond the eye and the caudal ends terminated at points behind the rostral tips of the otic capsules (Figure 2.3C). Caudal tips of the trabeculae tightly juxtaposed the notochord (Figure 2.3C,D,E). Growth after day 20pf was predominantly in a rostral direction. The parachordals appeared by day 25pf as two distinct pairs of buds tightly pressed against lateral aspects of the notochord; the first were caudal extensions of the trabeculae while the second were rostral extensions of branchial basket cartilage, which had begun to develop prior to day 15pf. At the junction of the parachordals and trabeculae, lateral extensions of cartilage, the basitrabecular processes, were visible by day 25pf (Figure 2.3D,E). The two developing parachordal buds had not united by day 33pf.

2.3.2. Light and electron microscopy analyses

2.3.2.1. Day 15pf (stage 15:pigmentation to stage 16:gill-cleft)

2.3.2.1.1. Cells

The TA of the day 15pf prolarvae was populated by large, irregularly shaped cells filled with yolk-like material and to a lesser degree, lipid (Figure 2.4A). These cells were packed tightly together (25 cells/1000μm^2) with narrow intercellular spaces and often indiscernible cell membranes. The yolk-like globules within the cytoplasm were oval to football-shaped and ranged between approximately 3 and 5μm in length. Yolk globules were electron-dense and had a predominantly homogeneous appearance (Figure 2.4B). Occasionally, yolk globules displayed a less electron-dense halo around the periphery. The second major cytoplasmic constituent of the day 15 TA cells was lipid droplets of moderate electron density. These droplets ranged between 1-6μm in diameter, although those at the upper limits of the range were less abundant. In some cases vacuoles containing heterogenous material resembling yolk and lipid were observed. Yolk material was observed in other cells including those of the brain, epithelium, and subepithelium but it did not occur to the extent observed within the TA cell population (Figure 2.4A). Lipid had a more extensive distribution and was found intracellularly throughout the animal. At higher magnifications TA cells were observed to have a peripherally located, indented nucleus. Most other organelles were displaced by the large quantities of yolk and lipid although flattened Golgi saccules, ribosomes and fragments of rough endoplasmic reticulum (RER) cisternae were occasionally observed.

Figure 2.4. A) The trabecular arc region (TA) in a day 15pf prolarva extends from the ventral aspects of eye (Ey) to the notochord (N). X 140. B) It consists of tightly packed cells containing large amounts of yolk globules (y) and lipid droplets (L). X 2,350. Buccal epithelium (BE); Brain (Br).

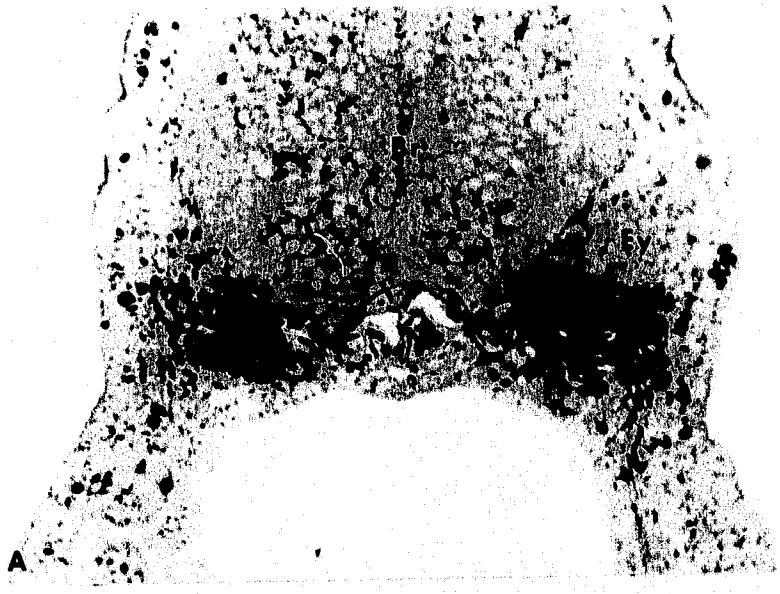
A

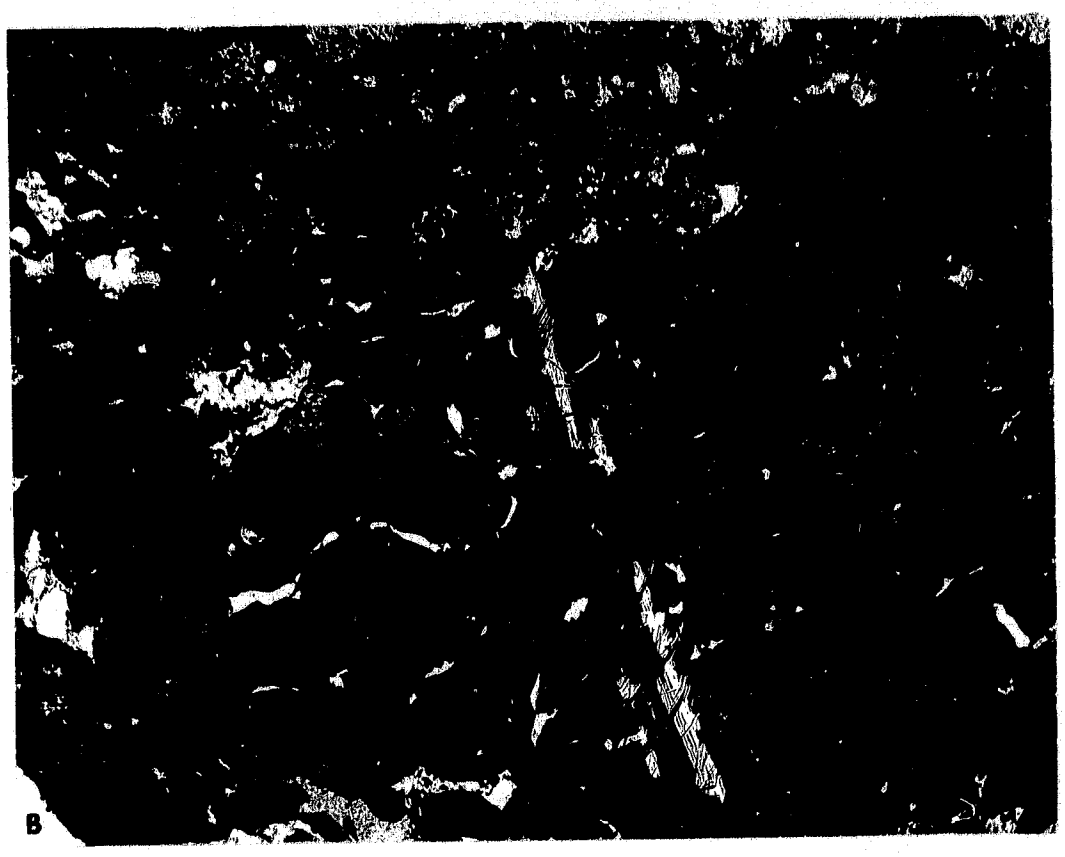
B

2.3.2.1.2. Matrix

Very little material was present in the ECM between TA cells. It consisted of cross and tangential sections of filopodia and scattered groups of 20nm diameter collagen fibrils. These fibrils were usually banded or striated but were without a distinct periodicity. The surface of these fibrils appeared to be coated with a flocculent material. They were most frequently observed in the TA periphery.

2.3.2.2. Day 16pf (stage 16:gill-cleft)

2.3.2.2.1. Cells

The ventral medial population of cells within the TA was apparently smaller in size and had fewer yolk globules than day 15pf cells (Figure 2.5A). Yolk globules of these cells were of less homogenous nature and often appeared in autophagic vacuoles (Figure 2.5B). Most cells had a large lipid component. Large homogeneous yolk globules remained the dominant feature in TA cells adjacent to the eye and in those located in more distal regions. These latter cells resembled those described for day 15pf and will not be discussed further here. Other cell types observed within close proximity to the TA included maturing and developing pigment cells, stellate mesenchymal cells, epithelial cells and endothelial cells (Figure 2.5C).

The TA cells of day 16pf were polygonal and possessed numerous filopodia that could be seen in cross and tangential sections within extracellular spaces. While intercellular spacing was variable, portions of the plasma membranes of these cells

Figure 2.5. A light micrograph (A) and electron micrograph (B) displaying the (TA) in day 16pf lampreys. A mitotic figure (Mi) and yolk-containing autophagic vacuole (V) can be seen in B. C) Other cells in the vicinity of the TA include pigment cells (P) and mesenchymal cell (Me). Brain (Br); Notochord (N); Eye (Ey); Buccal epithelium (BE). A= X 150; B= X 3,800; C= X 3,900.

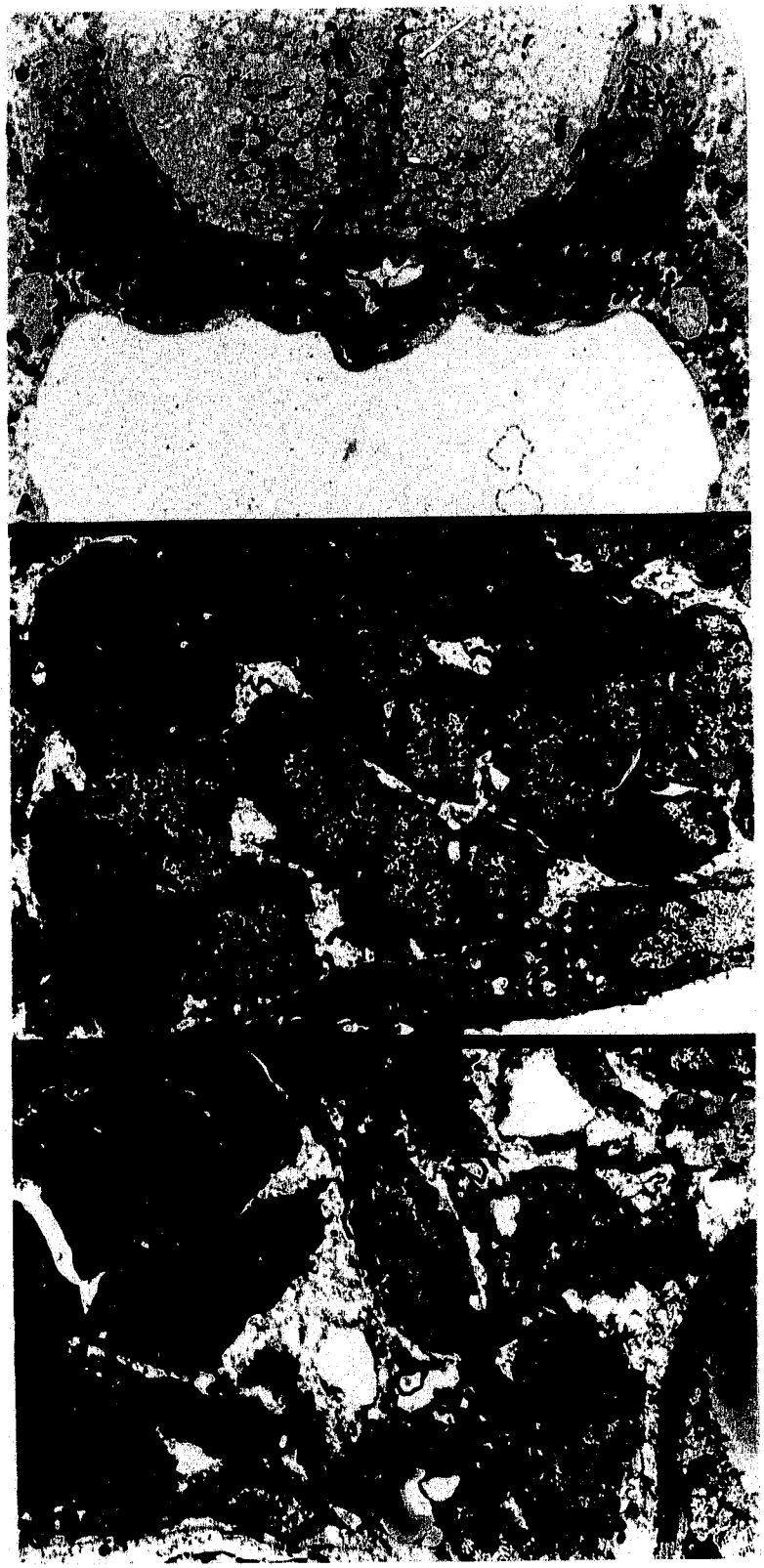

were in close apposition over much of the cell surface. Cell densities ranged between 35-46 cells per 1000μm^2. Occasional intercellular junctions (tight junction and desmosome) were observed. The TA cells most ventrally located were closely apposed to buccal epithelium and carotid artery endothelium. Trabecular arc cells often contacted the basal lamina of these tissues by extended cytoplasmic processes and blebs of their cellular membrane (Figure 2.6A,B).

Cytoplasm of the TA cells was moderately to densely granular and contained abundant free ribosomes and ribosomal clusters (Figure 2.7A). The poorly developed endoplasmic reticulum consisted of very few thin, ribosome-studded cisternae. A small but distinct Golgi apparatus with associated smooth vesicles was present in many cells. Mitochondria were circular to rod-shaped and possessed tubular cristae and dense granules. Dense bodies were also present within the cytoplasm. The large irregularly shaped nuclei often contained granular, well-developed nucleoli. Mitotic figures, centrioles and a single cilium were frequently observed (Figures 2.5B, 2.7A).

2.3.2.2.2. Matrix

The ECM material was similar to that observed on day 15pf and consisted of scattered, individual and groups of banded 20nm collagen fibrils lacking a distinct periodicity. These fibrils were most abundant in the periphery of the TA and often closely associated with the surface of the cells (Figure 2.7B).

Figure 2.6. Epitheliomesenchymal contact between the TA cells of day 16pf prolarva and A) buccal epithelium (BE) and B) carotid artery endothelium (En). The basal lamina of the BE is indicated by arrowheads. A= X 18,000; B= X 45,000.

B

Figure 2.7. A) Electron micrograph demonstrating cellular detail in a mesenchymal cell of the TA region in a day 16pf prolarva. Nucleus (Nu), Lipid (L), Golgi (G), Centriole (Ce), Dense bodies (arrowhead), Filopodia in extracellular space (asterisk). X 31,500. B) The ECM of day 16pf lamprey consisted of 20nm collagen fibrils (asterisk). Developing pigment cell (P). X 19,600.


B

2.3.2.3. Day 17pf (stage 17:burrowing)

2.3.2.3.1. Cells

In general, quantity of yolk within the cells of the TA continued to decrease. However, cells adjacent to the eye continued to demonstrate high yolk content but those more ventrally located contained little or no yolk (Figure 2.8A,B). Ventral cells were situated dorsal to the buccal epithelium, and lateral to the carotid artery. They displayed the first signs of entering the condensation phase of chondrogenesis (Figures 2.8A,B; 2.9A). Often a group of 2-4 cells could be identified as the center of the condensation (Figure 2.9B). Large expanses of the cell membranes of these "core" cells were in close apposition (Figure 2.9B, 2.10A) and focal points, and gap junctions were observed (Figure 2.10B). Cells peripheral in the condensation were separated from core cells by wide extracellular spaces. They were arranged in a whorled or circumferential pattern around the core cells. Cellular densities within the region of the condensation ranged from 15-23 cells per 1000μm^2. Close apposition of cell membranes and contact via desmosomes were observed between peripheral cells.

Cytoplasm of the condensing cells was dense and filled with numerous ribosomes and polyribosomes (Figure 2.10A). The predominant organelle was a large irregularly shaped nucleus that displayed one, or occasionally two, well-developed nucleoli in section. The Golgi apparatus was composed of one to several stacks of 3-5 saccules and numerous small (40-60nm) vesicles. These vesicles contained material of light to moderate electron density. In contrast, the RER was poorly developed. Variably

Figure 2.8. A) Mesenchymal condensations (arrow) first appeared by day 17pf in a ventral medial position to the eye. Yolk-filled cells (arrowhead) still predominated in distal and dorsal regions bordering on the condensation. Eye (Ey), Brain (Br), Notochord (N). X 130. B) Higher magnifications of the same region in A) showing the difference in cellular density of the condensation and yolk-filled cells. Condensing cell (Cn). X 2,350.

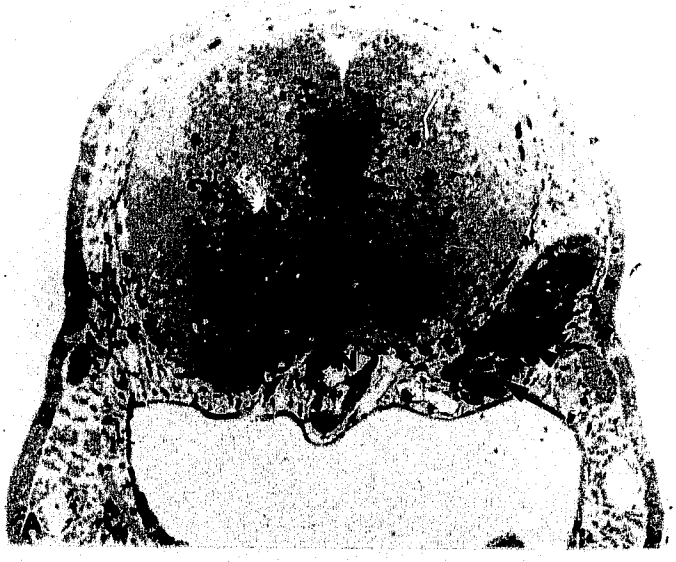

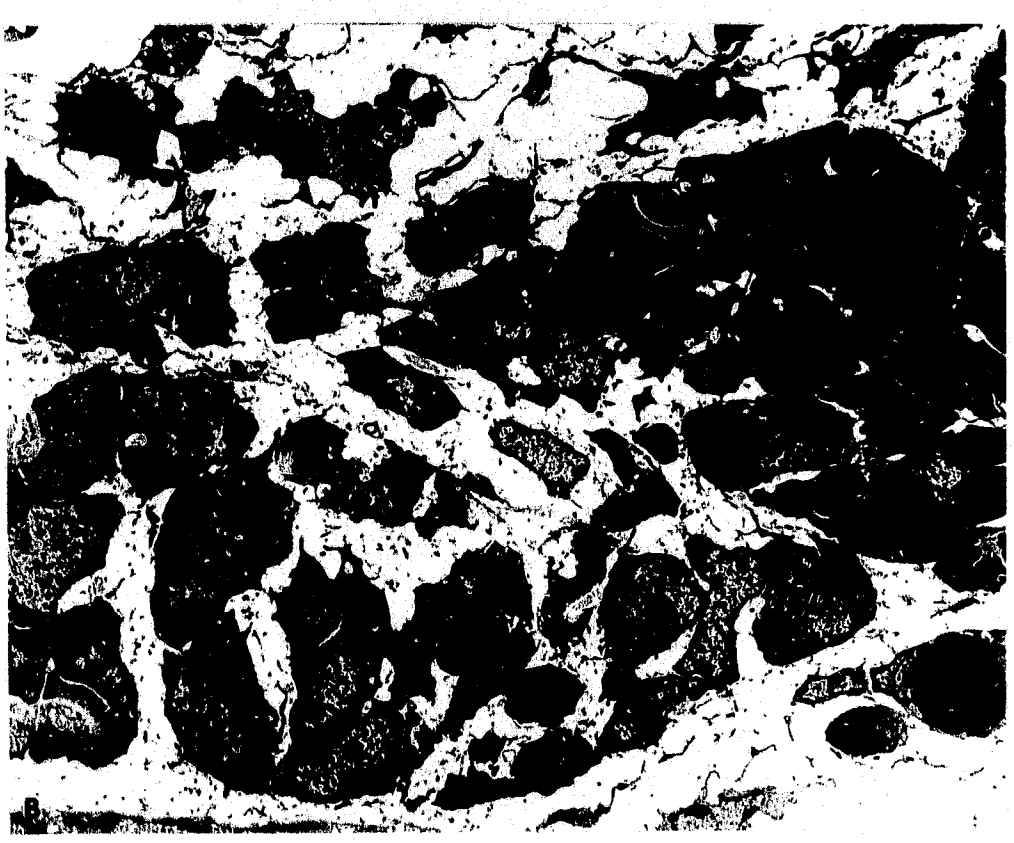

Figure 2.9. Condensations in a day 17pf prolarva. A) Condensations were in close association with the carotid artery (CA) and the buccal epithelium (BE). X 3,750. B) The central core of the condensation was frequently composed of 2-4 closely apposed cells (asterisks) and shortened filopodia (arrow). X 7,350.

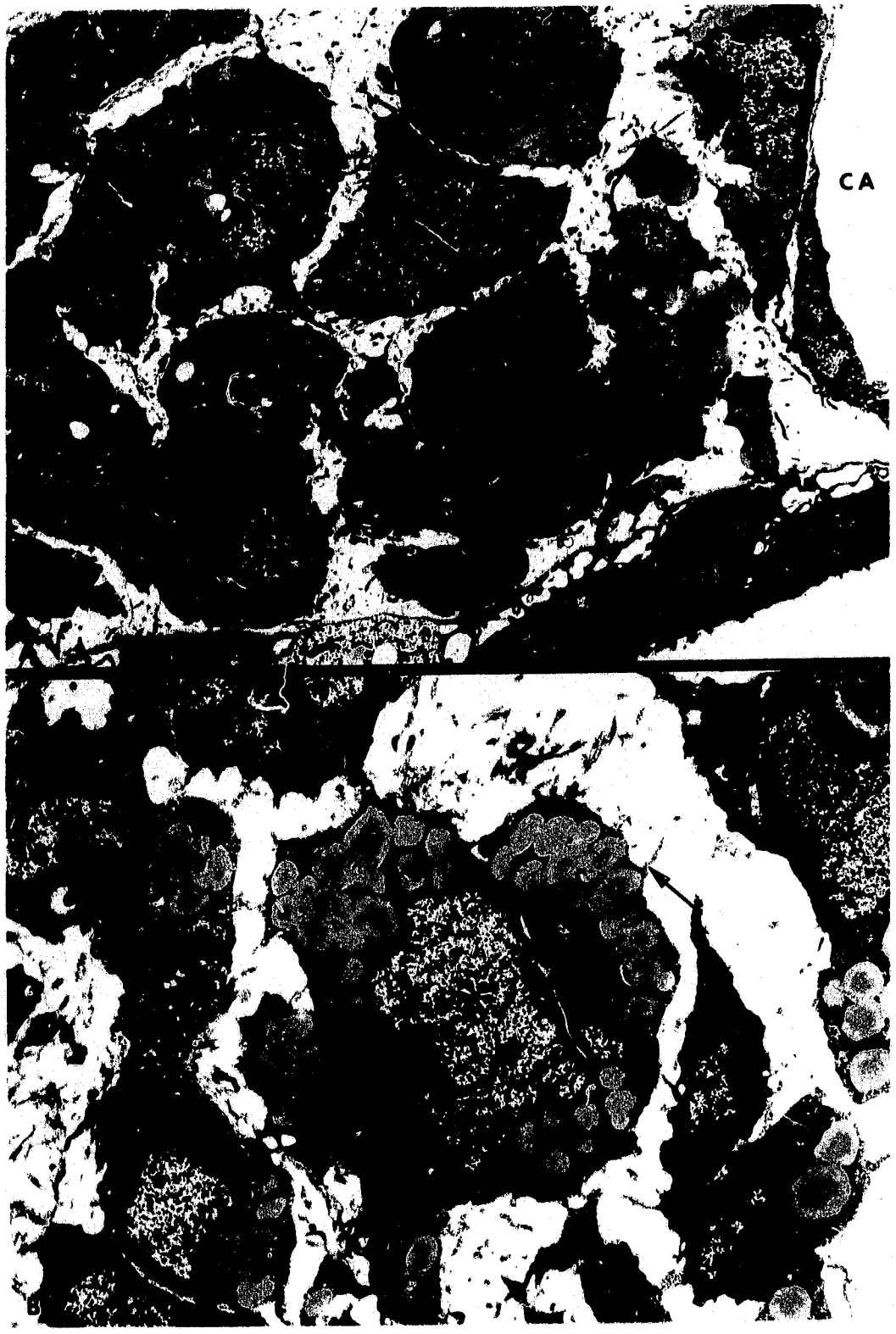
CA
B

Figure 2.10. A) The core condensation cells (Cc) of day 17pf prolarvae were in apposition for large expanses of the cell membranes. X 20,000. B) Focal contacts (arrows) were frequently observed between these cells. X 82,250.

shaped mitochondria were scattered throughout the cytoplasm. Occasional yolk globules, membrane-bound dense bodies, membrane whorls and vacuoles containing dense heterogenous material were observed. A few microtubules were seen lying parallel beneath the cell surfaces. Lipid droplets (0.6-0.8 μm in diameter) appeared less abundant than observed in earlier stages.

2.3.2.3.2. Matrix

The 20nm fibrils observed during day 15pf and day 16pf appeared to be more plentiful by day 17pf and were arranged both in loose meshworks and parallel bundles (Figure 2.11A,B). Fibrils were frequently observed in close association with the cell surface, often being located within extracellular pockets or compartments of the cell membrane. The 20nm matrix fibrils were associated with randomly scattered filaments of 10nm in diameter and flocculent to granular material.

2.3.2.4. Day 18pf (stage 17:burrowing)

3.3.2.4.1. Cells

By day 18pf, condensations of approximately 18-22, tightly packed mesenchymal cells (45-54 cells/1000μm^2) were located adjacent to the epithelium of the buccal cavity in the position of future trabecular cartilage (Figure 2.12A). Cells comprising the condensation had "rounded-up" and either lacked filopodia or possessed a few short processes. Membranes of adjacent cells were in very close contact over much of the cell surface, and cell boundaries were often difficult to discern. Focal contacts

Figure 2.11. A) The composition of the matrix surrounding condensing cells (Cn) of day 17pf contained greater quantities of the 20nm collagen fibrils (asterisk) seen in earlier stages. X 15,200. B) Higher magnification of matrix fibrillar material. Note banding pattern of 20nm collagen fibrils (arrow). Smaller non-striated fibrils (arrowhead). X 80,000.

B

Figure 2.12. A) By day 18pf, condensations were tightly juxtaposed to the buccal epithelium (BE) and consisted of tightly packed, rounded mesenchymal cells with a high nucleo-cytoplasmic ratio. Yolk quantities are greatly reduced. Condensing cell nuclei (Nu), Yolk-containing autophagic vacuole (V), Mitotic figure (Mi). X 4,750. B) Electron micrograph showing close apposition between cellular membranes (arrowheads) of two 18pf prechondrogenic condensed cells. Nucleolus (No), Centriole (Ce), Mitochondria (Mc), Golgi (G), Lipid droplet (L). X 28,500.

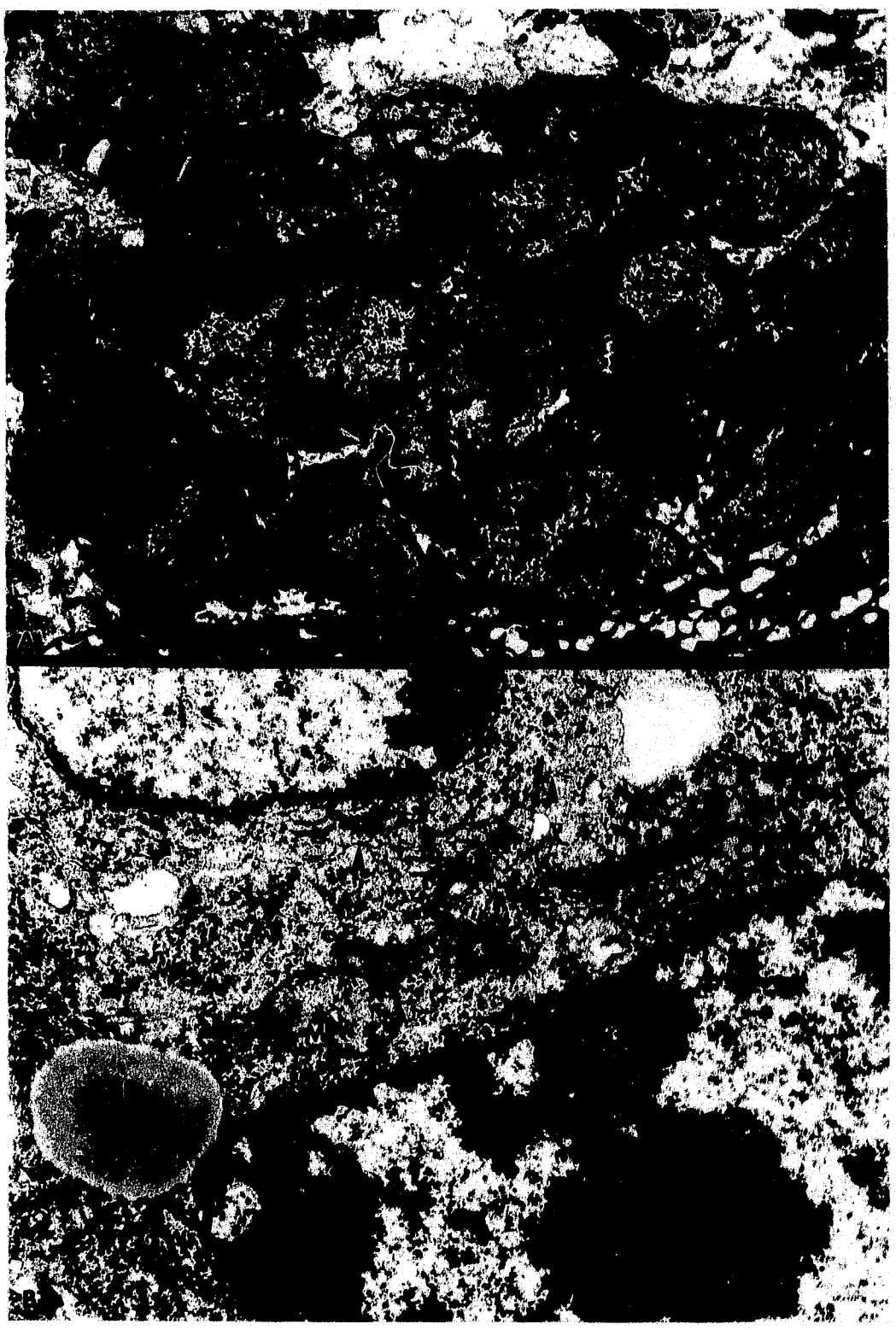

and gap junctions were frequently observed. In areas where their membranes were not closely apposed, cells contacted each other by several short cytoplasmic extensions and blebs.

Day 18pf cells possessed a large oval to cuboidal nucleus that occupied much of the cell volume and contained a prominent nucleolus (Figure 2.12A,B). Mitotic figures were frequently observed and many cells contained centrioles. Spherical to rod-shaped mitochondria were present. Moderate quantities of lipid were observed within the cytoplasm. Intact and degenerating yolk globules appeared less extensively within the cells of the condensation than in more distal localities and in regions ventral and lateral to the eye.

The cytoplasm of cells during day 18pf contained abundant ribosomes that frequently formed polysomal formations. The extensively developed Golgi apparatus was observed as saccules, vesicular, tubular and vacuolar profiles (Figure 2.13A). The ends of the Golgi saccules were dilated and filled with a moderate to electron-dense homogenous material. The large number of Golgi associated vesicles ranged from 46-88nm in size and contained electron-lucent to electron-dense material. Vacuoles, with a maximum diameter of 0.2μm, contained electron-lucent, sometimes flocculent material. Coated vesicles were often observed

close to the cell surface. Smooth tubules approximately 46nm in diameter existed closely associated with the Golgi apparatus. In contrast to the extensive development of the Golgi apparatus, the rough endoplasmic reticulum of most cell of day 18pf prolarvae was similar to that of day 17pf.

Figure 2.13. A) Electron micrograph of the Golgi apparatus (G) of condensing mesenchymal cells in a day 18pf prolarva. Golgi-associated vesicles (arrow) contain a moderate to electron-dense material. Larger vacuoles (V) filled with a flocculent material are seen in association with the cell surface. Mitochondria (Mc), fragments of rough endoplasmic reticulum (RER). X 36,000. B) Twenty nanometer collagen fibrils in cross and tangential section (arrow) are embedded in increased amounts of flocculent material (arrowhead). X 88,000.


V

2.3.2.4.2. Matrix

The extracellular space was minimal within the condensation of day 18pf prolarvae. When it existed, the material observed within the extracellular space was similar in ultrastructural appearance to that of day 17pf prolarvae, but appeared to be more abundant (Figure 2.13B).

2.3.2.5. Day 19pf (stage 18:burrowing)

2.3.2.5.1. Cells

Trabecular cells of day 19pf and older prolarva varied in extent of their differentiation and ultrastructural appearance. For the sake of clarity, a simple classification scheme has been employed in which cells of the trabecular cartilage proper (ie. excluding the perichondrium) that exhibit similar morphological features are grouped together and assigned a letter from A-D. Position of these cell types along the trabecular cartilage radius and their predominance within the cartilage varied with developmental stage.

A narrow intercellular space separated day 19pf prolarval trabecular cells. Cell contact was occasional (Figure 2.14A). The trabeculae were predominantly composed of round to irregularly shaped cells (Type B) that appeared progressively flatter peripherally. A second cell type that curved around the outer boundary of the condensation was also observed during day 19pf. This cell (Type A) had a sporadic distribution. In both cell types, cell surfaces were irregular to scalloped. In addition, the cytoplasm was extremely granular and electron-dense (Figure 2.14B). Nuclei of

Figure 2.14. A) Low magnification electron micrograph demonstrating intercellular spaces (I) between day 19pf condensing cells. Buccal epithelium (BE), Brain (Br). X 2,100. B) With higher magnification the lack of cell contact is more apparent. Type B cells (B) of the day 19pf condensation have a granular cytoplasm and many dilated saccules of rough endoplasmic reticulum (arrows), and possess large nuclei with prominent nucleoli (No). X 8,400. C) ECM contains a moderate electron-dense flocculent material (asterisks) similar to that found in the RER saccules and 15-40nm globules (arrowhead). Condensing cell (Cn), microtubule (Tu). X 72,000.


A
C

centrally located Type B cells were oval while the nuclei of more peripheral Type B cells were a flatter shape. Nuclei occupied most of the cell volume and possessed 1-2 prominent nucleoli in section. Mitotic figures were infrequent.

The most significant organelle within the electron-dense cytoplasm of the Type B cells was the RER. Its flattened to slightly dilated cisternae were distributed randomly throughout the cytoplasm. Stacks of parallel cisternae were rarely observed. The cisternae contained an electron-lucent, flocculent to granular material (Figure 2.14C). The RER was not extensively developed in Type A cells. Free ribosomes were abundant throughout the cytoplasm in both types A and B cells. The Golgi apparatus consisted of 1-2 sets of saccules and was similar to that described for day 18pf cells. Pinocytotic and coated vesicles occurred beneath the cell surface and were often in close contact with the cell membrane.

2.3.2.5.2. Matrix

Material within extracellular spaces of the trabecular condensations was more conspicuous than previously observed. It was composed predominately of a moderately-dense, granular and flocculent to filamentous material. This material included long 10nm fibrils and beaded strands composed of 10nm beads connected by thin, 2nm strands. Collagen fibrils (20nm in diameter) occurred randomly scattered throughout the matrix and were arranged in parallel groups where they were closely associated with the surface of cells. They were often obscured by the flocculent material. Moderately dense lamprin globules, 15-40nm in diameter (Wright

and Youson, 1983; Wright *et al.*, 1988) and scattered throughout the meshwork of matrix material, first appeared during this stage (Figure 2.14C).

2.3.2.6. Day 20pf (stage 17:burrowing)

2.3.2.6.1. Cells

An oval shaped trabecular cartilage, consisting of 18-22 cells at the widest diameter, had formed by day 20pf (Figure 2.15A). Surrounding the cartilage proper was a rudimentary perichondrium of 1-2 cell layers. Developing perichondrial cells were flattened fibroblast-like cells with extended cytoplasmic processes along their longitudinal axes. While these cells were often in close apposition to one another and cell contact in the form of desmosomes was occasionally observed, continuity of the perichondrium was incomplete. In places the peripheral cells of the developing trabeculae proper could not be identified as perichondrial or early differentiating chondroblasts. Cytoplasm of the perichondrial cells was granular and contained moderate amounts of ribosomal material. Much of the cytoplasm of these fibroblast like cells was occupied by flattened, often irregular-shaped nuclei. Small amounts of RER, occasionally in stacks of 2-3 parallel cisternae were observed especially in the ends of the cell. An occasional Golgi apparatus with associated vesicles was located in the perinuclear region. Lipid in small quantities, dense bodies and vacuoles containing heterogenous material were present.

The cartilage proper was comprised of chondroblasts in varying degrees of differentiation, isolated from one another by well-defined seams of matrix (Figure

Figure 2.15. A) Thin seams of matrix (arrow) separate cells of the trabecular cartilage proper by day 20pf. A rudimentary perichondrium (arrowhead) can be seen developing around the periphery of the cartilage nodule. Carotid artery (CA), Buccal epithelium (BE). X 2,700. B) The three basic stages of differentiating cells in the day 20pf trabecular cartilage can be defined by cytoplasmic density and extent of RER (arrows). X 12,600. Type A cell (A), Type B cell (B), Type C cell (C), Centriole (Ce), Golgi (G).

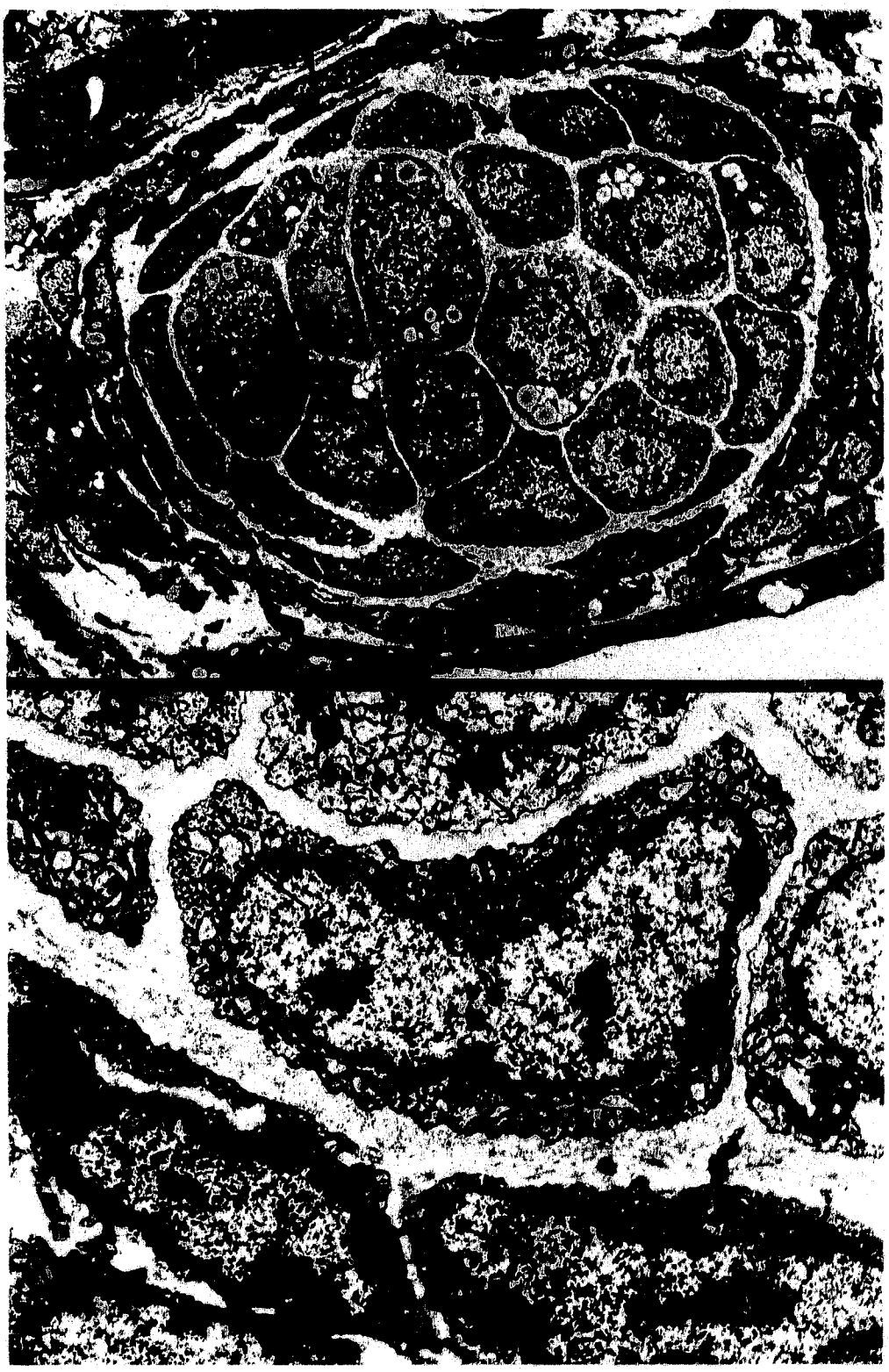

2.15A,B). The most peripherally located cells (Type A) were very electron-dense with large amounts of ribosomal material but insignificant amounts of RER. The RER occurred as flattened to slightly dilated cisternae randomly scattered throughout the cells. While Type A cells were not surrounded with cartilaginous ECM, their proximal surfaces were usually in contact with this matrix. A small Golgi apparatus with associated vesicles was found centrally located in the perinuclear region. Lipid was present in variable amounts but was less abundant than in earlier stages of differentiation. Type B cells were located adjacent to the Type A cell layer(s) and has been the predominant cell type observed in the previous stage (day 19pf). Unlike Type A cells, Type B cells were completely surrounded by cartilage matrix. Type B cells were similar to Type A cells in that they were characterized by dense cytoplasm. They differed by having moderate amounts of RER with elongated, slightly swollen to dilated saccular profiles. The Golgi apparatus was located in a perinuclear position and consisted of several stacks of lamellae and vesicles containing moderate to electron-dense material. Smooth vesicles and branching tubules of approximately 45nm in diameter were occasionally observed in contact or in close association with the cell surface. Pinocytotic and coated vesicles were also present. Other cytoplasmic inclusions frequently observed included centrioles, occasionally cilia, lipid droplets, dense bodies and multivesicular bodies. A "cap" of 3-4 cell layers composed of Type A and Type B cells was frequently observed on the lateral aspect(s) of the developing trabecular cartilage (Figure 2.16). In contrast, these cell types were

frequently absent or present in only 1-2 cells layers in the dorsal and ventral aspects of the trabeculae.

The predominant cell of the trabecular cartilage in day 20pf lampreys was Type C. These cells appeared oval to angular and were larger than the peripherally located, electron-dense Types A and B cells (Figure 2.17A). These chondroblasts possessed a large oval to round nucleus and 1-2 prominent nucleoli. The cytoplasm was less electron-dense and granular than that of peripheral cells. Elements of RER were prevalent and appeared as predominantly swollen, round to irregularly shaped, saccular cisternae filling much of the cytoplasm. These cisternae contained a light flocculent to granular substance resembling material in the ECM and were a distinguishing feature of this cell. The Golgi apparatus consisted of several stacks of saccules and many membrane bound vesicles and vacuoles. Vesicles contained light to moderately electron-dense material and were frequently observed to be in close association with the cell periphery. Mitochondria with tubular cisternae were abundant. Large membrane bound vesicles (0.17-0.24μm) containing granular electron-dense multivesicular bodies and vacuoles containing heterogenous material were more frequently observed than in cell types previously described.

2.3.2.6.2. Matrix

Extracellular matrix material had accumulated extensively by day 20pf especially within intercellular spaces (0.12-0.67 μm) surrounding the centrally located chondrocytes. Matrix in this central region showed signs of extensive organisation

Figure 2.16. The peripheral electron-dense Type A and B cells (asterisks) of the day 20pf trabeculae frequently were observed to form 3-4 cell layered "lateral caps". Buccal epithelium (BE). X 4,000.

Figure 2.17. Comparison of A) the predominant cell type (C) of day 20pf lamprey with B) the more peripheral chondroblast (B). Note the more irregular cell surface (arrowhead), denser cytoplasm and less extensively dilated RER (arrows) of cells in B compared to A. C) ECM of trabecular cartilage in day 20pf lamprey displaying the concentric organization of matrix components around the chondrocyte (Ch). D) High magnification of a similar area showing the thin strands of material extending between the beaded material (arrow). A= X 7,800; B= X 8,800;
C= X 52,000; D= X 116,000.


Ch
D

(Figure 2.17C). In the region immediately surrounding the chondrocytes, the pericellular region, the 20nm collagen fibrils were often masked by the accumulation of the granular to flocculent material and 15-40nm electron-dense lamprin globules. Around the periphery of the cell was a concentric array of moderately dense, beaded strands of material. The beads (15-30μm) occasionally appeared hollow and were regularly spaced with filamentous material (4-10nm in diameter) between them (Figure 2.17D). In some areas filamentous material extended out from the beads in a spoke-like fashion. A few dense granules (7-10nm) were found interdispersed between the beaded strands, globules and flocculent material.

At intersections of the pericellular matrices of several cells the amount of globular and flocculent material was sparse and a meshwork of collagen fibrils frequently occurred. Extracellular material surrounding the electron-dense peripheral chondrocytes was sparse and consisted of bundles of parallel 20nm collagen fibrils.

2.3.2.7. Day 22pf (stage 17:burrowing) - Day 33pf (stage 18:larval)

2.3.2.7.1. Cells

By days 22-33pf the entire cartilage proper had become surrounded by a distinct, intact perichondrium (Figure 2.18A). The perichondrial cells were thin, attenuated cells closely associated with the cartilage proper and bundles of parallel 20nm collagen fibrils (Figure 2.18B). The cartilage proper could be divided into a number of cell populations which were similar to those described for 20pf prolarvae. The subperichondrial population consisted of differentiating cells (Type A and B) each

with electron-dense cytoplasm. Similar to the peripheral A and B cell types described previously, these chondroblasts often occurred in multiple layers on lateral aspects of the trabecular bud (Figure 2.19). The centrally located electron-lucent cells of earlier stages, which possessed an abundance of extensively dilated RER (Type C cells), were observed less frequently by day 25pf. When present they were scattered among peripheral Type B cells. The predominant cell type of the trabecular cartilage in the older prolarvae was a large, oval to polygonal shaped cell (Type D) with an electron-lucent cytoplasm that contained very few free ribosomes and polysomes. In contrast to Type C cells, their RER was limited to scattered, thin, wavy profiles (Figure 2.19A,B). Golgi saccules when observed were flattened and associated with few vesicles. Other cytoplasmic constituents were scattered mitochondria and dense bodies. The round- to irregular-shaped nuclei of the cells occupied very little space within the cytoplasm and were frequently centrally located.

The principal characteristics of day 15pf-day 33pf developing trabecular cells are summarized in Table 2.1.

2.3.2.7.2. Matrix

During days 22pf-day 33pf the quantity of extracellular material increased greatly, resulting in a distinct electron-dense matrix. The most dramatic development that occurred during this stage was accumulation of 5-15nm dense matrix granules by day 22pf (Figure 2.20). By days 25-33pf, matrix material became organized into three distinct zones (Fig 2.21). In the inner aspects of the pericellular zone, the zone

Figure 2.18. A) Electron micrograph of the trabecular cartilage in cross-section in a day 31pf prolarva demonstrating the predominance of the electron-lucent Type D cell (D). Perichondrium (arrows), Type B cell (B). X 2,600. B) Higher magnification of the same cartilage bud. Collagen bundles (Co) in the perichondrium, Perichondrial cell (Pc). X 8,750.

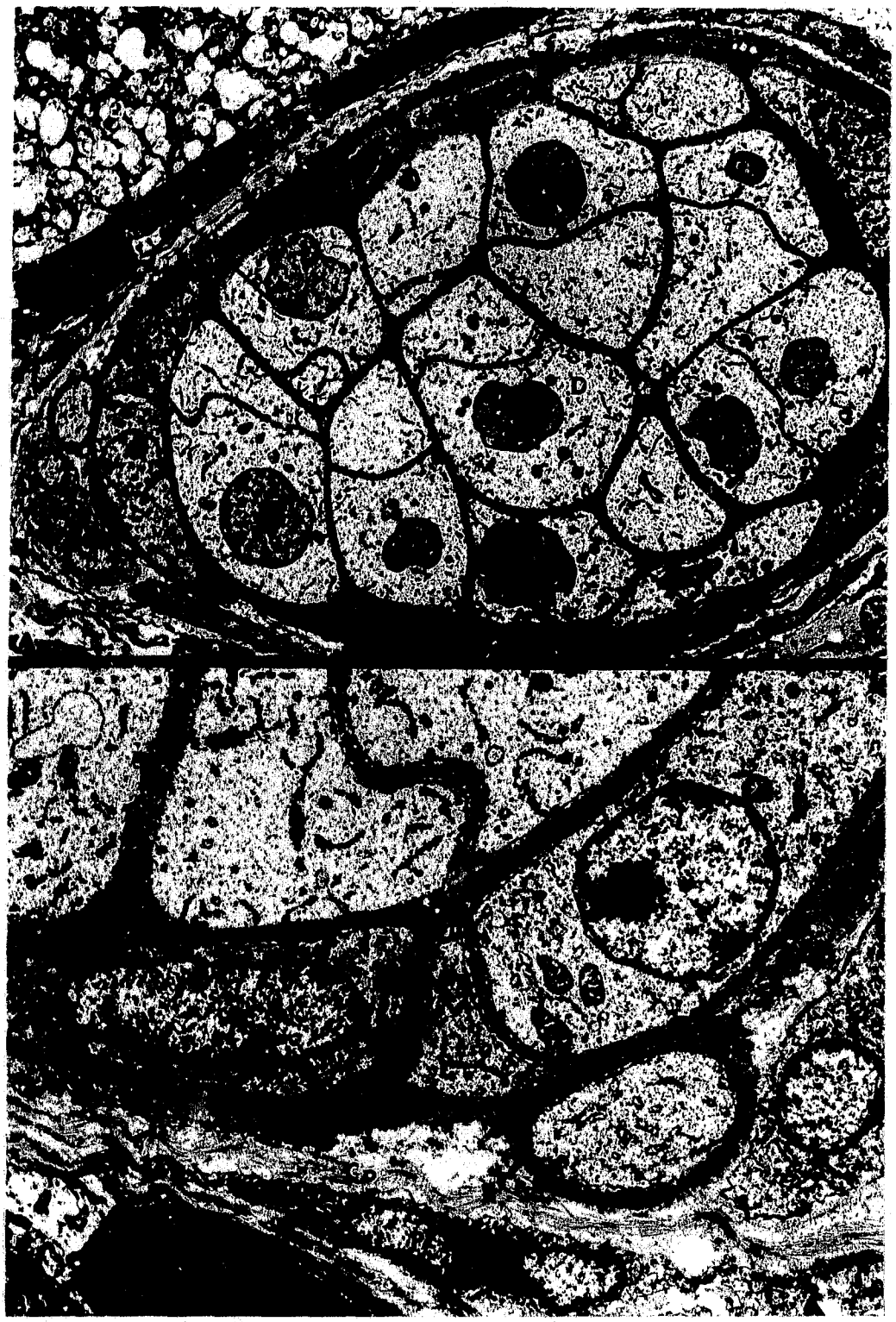

Figure 2.19. Electron-dense chondroblasts are still observed to occur in multiple layers of lateral aspects of the trabecular cartilage bud by day 31pf of the prolarval stage. Type D cell (D), Type B (B). X 6,000.

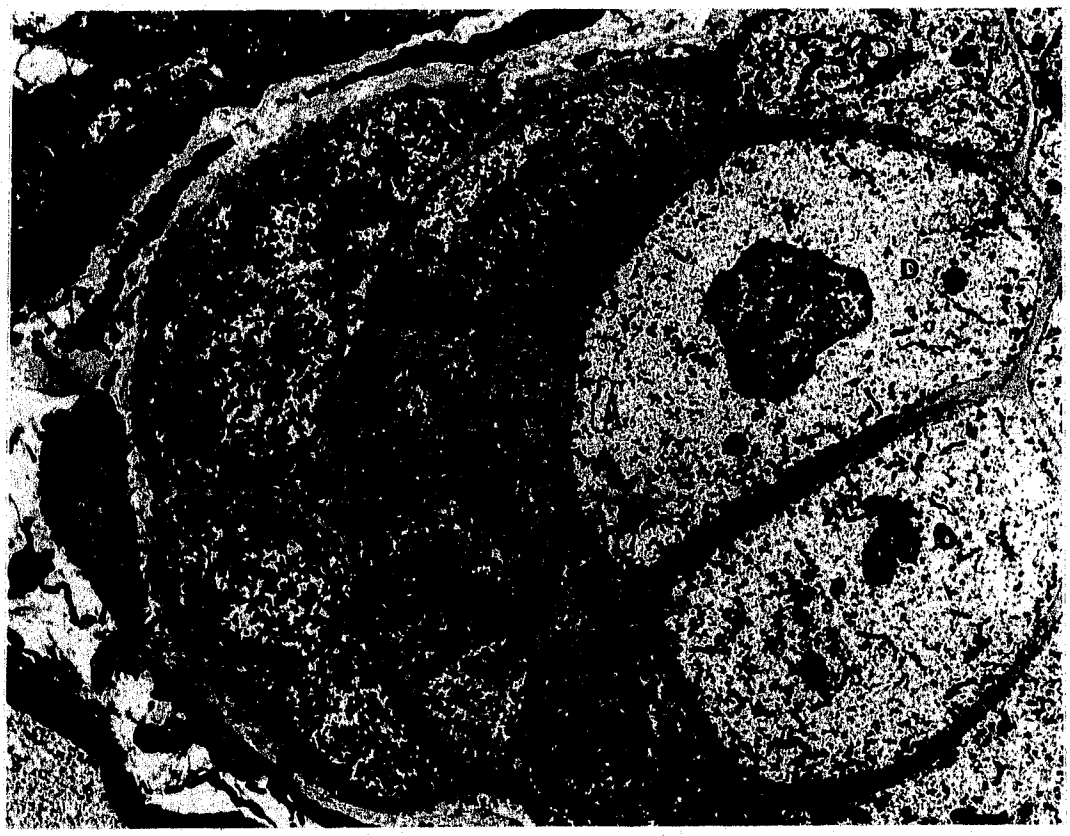
D

enveloping the cell, an electron-lucent region mostly devoid of extracellular material was observed. This inner pericellular zone was bordered by an area dominated by 5-15nm dense granules and small amounts of 15-40nm lamprin globules. Surrounding the pericellular zone was a territorial zone containing an anastomosing network of branching 15-40nm lamprin fibrils. Interdispersed between these were 5-15nm granules and granular to filamentous material. In the region bordering the territorial zones of two cells, the interterritorial zone, 15-40nm branched fibrillar material coalesced to form dense parallel bands. Groups of parallel 20nm collagen fibrils, dense matrix granules and flocculent material were also interdispersed between these bands. In extracellular spaces adjoining perichondrial and chondroblastic cells, 20nm collagen fibrils were observed interdispersed between densely packed 15-40nm globular material (Figure 2.21C).

The principal characteristics of the ECM during trabecular cartilage development are summarized in Table 2.1.

Table 2.1. Principal cellular and matrix features of developing lamprey trabeculae.

Days pf	Characteristic features
15	**Cells:** TA mesenchymal cells, large quantities of yolk, cell densities 25cells/1000μm^2, no gap junctions, no contact with other cell types, poorly developed RER and Golgi apparatus, no perichondrium. **Matrix:** 20nm collagen fibrils, no lamprin or matrix granules.
16	**Cells:** TA mesenchymal cells, moderate to large quantities of yolk, cell densities 35-46 cells/1000μm^2, no gap junctions, frequent contact with buccal epithelium and vascular endothelium, poorly developed RER, small Golgi apparatus, no perichondrium. **Matrix:** 20nm collagen fibrils, no lamprin or matrix granules.
17	**Cells:** Condensing mesenchymal cells, little or no yolk, cell densities 15-23cells/1000μm^2, occasional gap junctions, some contact with buccal epithelium and vascular endothelium, poorly developed RER, small Golgi apparatus, no perichondrium. **Matrix:** 20nm collagen fibrils, no lamprin or matrix granules.
18	**Cells:** Mesenchymal condensations, little or no yolk, cell densities 45-54cells/1000μm^2, frequent gap junctions and focal contacts, poorly developed RER, well developed Golgi apparatus, no perichondrium. **Matrix:** Greater abundance of 20nm collagen fibrils, no lamprin or matrix granules.
19	**Cells:** Differentiated chondroblasts, predominantly Type B cells surrounded by peripheral Type A cells, little to no yolk, no gap junctions, extensive RER and well developed Golgi apparatus, no perichondrium. **Matrix:** Abundant 20nm collagen fibrils, lamprin globules, proteoglycan-like material.
20	**Cells:** Predominantly Type C cells, Type A and Type B cells found on periphery, no yolk, no gap junctions, well developed RER with extensively dilated cisternae, well developed Golgi apparatus, developing perichondrium. **Matrix:** 20nm collagen fibrils, increase in lamprin, lamprin appears as individual globules and branching fibrils, first appearance of matrix granules (collapsed aggregates of aggrecan),
22-33	**Cells:** Predominantly Type D cells, Types A-C also present, no yolk, no gap junctions, fragments of RER and small Golgi apparatus in type D cells, well developed perichondrium. **Matrix:** 20nm collagen fibrils, large quantities of lamprin and matrix granules, matrix organized into three distinct zones.

Figure 2.20. Cartilage matrix granules (arrow) first appear scattered among the 10-40nm branching globules (arrowhead) during day 22pf. Cytoplasm of chondrocyte (Ch). X 76,000.

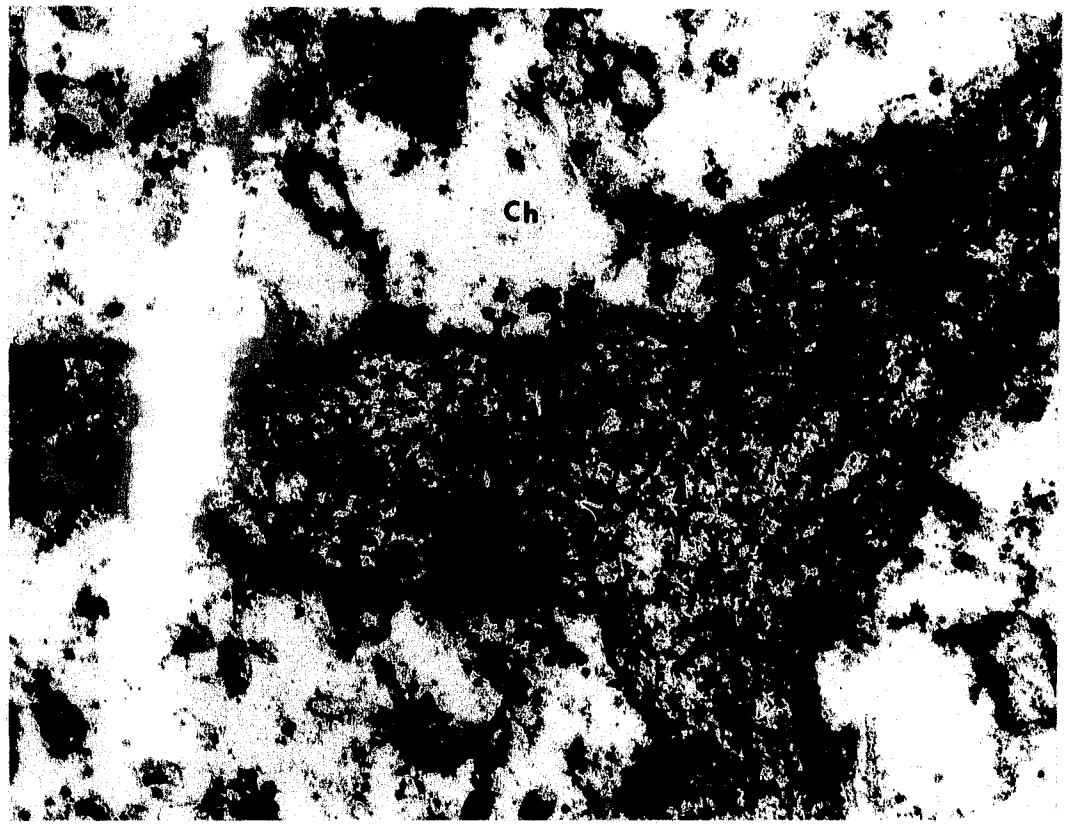
Ch

Figure 2.21. A) Day 31pf prolarva demonstrating the zonal organization of the matrix. An abundance of granular material surrounds an inner electron-lucent halo (arrow) in the pericellular region (Pe) adjacent to the chondrocyte (Ch). The 15-40nm lamprin-like globules become branched in the territorial zone (TZ) and organized in parallel arrays (asterisk) in the interterritorial zone (IZ). X 23,800. B) Higher magnification demonstrating 15-40nm lamprin fibrils (arrowheads). X 52,000. C) Bundles of collagen fibrils (Co) are interdispersed among lamprin fibrils (arrow) in the regions adjacent to the perichondrium and in the interterritorial zone of a day 31pf larva. X 28,800.

2.4. DISCUSSION

This study is the first to examine spatial and temporal patterning, and ultrastructural morphology of developing trabecular cartilage during prolarval stages of lampreys. Chondrogenesis of trabecular cartilage occurs early in the burrowing stage. Mesenchymal condensations formed by day 17pf and cartilage differentiated by day 19-20pf. The trabeculae were the first neurocranial cartilages to develop in the lamprey. Prior to their appearance the only other cartilaginous elements existing were the splanchnocranial branchial cartilages. This finding is consistent with previous descriptions of cranial ontogeny in early stages of lampreys (Sewertzoff 1916, 1917; Damas, 1944; Johnels, 1948; Newth, 1956; DeBeer, 1971) and similar to the situation in Chondrichthyes (DeBeer, 1971) and amphibians (Hanken *et al.*, 1992). The temporal pattern of development of the head cartilages is likely critical to the survival of the prolarva. The trabeculae mature concomitant with development of burrowing behaviour in which the head is used to "dig" as the lamprey enters the substrate (Piavis, 1971). This behaviour likely requires extra protection for the delicate brain.

A slight discrepancy exists between the cartilage position and extent of development described in earlier works and that observed in the present study. However, terminology used in these earlier studies is confusing, making it difficult to compare the findings. Johnels (1948), for example, does not describe the initial appearance of the condensations (referred to as "blastemas"), but indicates that they had formed from a mesenchymal "trabecular primordium" (presumably the yolk-filled

mesenchymal cells) by day 17pf. At this point the condensations were "on the verge of becoming cartilaginous" and continued to develop cranially from their juxtachordal position. In addition, early studies concerning development of lamprey trabecular cartilage described stages equivalent to day 17pf and day 25pf but did not examine intermediate stages (Damas, 1944; Johnels, 1948; Newth, 1956; DeBeer, 1971) and, therefore, left gaps in our understanding of trabecular cartilage developmental patterns in the lamprey. In contrast to these earlier reports, the findings of the present study indicate that the trabeculae did not extend as far caudally as the otic capsules until 24-48 hours after the initial appearance of the condensations. For a short period, trabeculae lengthened in both cranial and caudal directions; then growth was predominantly in a cranial direction. These slight differences in temporal and spatial patterning of trabecular development may be the result of species variation. Early studies primarily involved *Lampetra* species, and it has since been determined that while timing of the embryological stages is comparable between lamprey species, variation does exist (Smith *et al.*, 1968). Alternatively, conditions under which the lamprey were raised may have influenced developmental rates. Temperature, for example, is critical in determining developmental rates. Optimum temperature for early developmental stages of sea lamprey is 18.4^{0}C (Piavis, 1961; Langille and Hall, 1988a).

In the developing vertebrate limb, mesenchymal cells are continually recruited from tissue surrounding the distal aspects of the lengthening limb until a precartilagenous skeleton including the digits is formed (Oster *et al.*, 1988; Muller and

Alberch, 1990). This pattern results in a full compliment of differentiating cells, ranging from matrix-synthesizing chondrocytes to condensing mesenchymal cells, along the proximo-distal axis of the limb (Thorogood and Hinchcliffe, 1975). Similarly, a gradient of differentiation is observed along the craniocaudal axis in lamprey trabecular cartilage. The most developmentally advanced aspects of the nascent cartilage occur in the region ventral to the eye. Following onset of overt cartilage differentiation, lamprey trabecular cartilage continued to grow as a result of both interstitial and appositional growth, with the latter predominating. Chondroblasts were observed 1-4 cell layers thick along the perimeter of the cartilage proper during days 20-30pf, and mitotic figures, while infrequent in later stages, were always observed.

Prechondrogenic condensations of lamprey trabecular cartilage developed in an environment that was atypical to that described for other chondrogenic structures, such as avian limb. In these latter systems, environment prior to initiation of condensation formation is characteristically composed of widely spaced undifferentiated stellate mesenchymal cells that may connect via elongated filopodia (Goel, 1970; Thorogood and Hinchcliffe, 1975; Ede, 1983). In the present study, the band of cells extending in an arc between the ventral region of the eye and the notochord during day 15pf possessed filopodia and organelles common to mesenchymal cells, but ultrastructurally appeared very different due to the large quantities of yolk and lipid. This yolk-laden mesenchyme is most likely the tissue described in earlier light microscopic studies as the trabecular mesenchymal

"primordium" that appears as early as day 13pf in *Lampetra* species (Johnels, 1948). It is tempting to suggest that this visually distinct mesenchymal cell population of the TA is, at least in part, of neural crest origin. The TA region is within the cranial neural crest migrational pathway described for other species (Horstadius, 1950; Noden, 1975; Tan and Morriss-Kay, 1986; Thorogood, 1988; LeDourin *et al.*, 1993). Furthermore, it has been established by extirpation experiments that lamprey trabecular cartilage is derived from the neural crest (Langille and Hall, 1986; 1988b). The cell type composing the TA regions during day 15pf does not occur in the more caudal regions where the parachordal cartilage, a mesodermal derivative, develops (Newth, 1956; Langille and Hall, 1988b).

In avian and mammalian species, neural crest cells are indistinguishable from surrounding mesenchymal cells, through which they proceed shortly after emigration from the neural tube (Nicols, 1981; Krotoski *et al.*, 1988; Serbedzija *et al.*, 1992). A variety of markers is required to identify these cells. However, Platt (1893, 1898) was able to follow migration of neural crest derived mesenchyme (ectomesenchyme) through mesodermally derived mesenchyme in *Necturus* because of the distinctive morphology of ectomesenchymal cells. Mesodermally derived cells were reported by Platt (1893, 1898) to retain large amounts of yolk and lipid for longer periods of time than neural crest cells. This enables neural crest cells to appear visually distinctive within a mixed population. Landacre (1921) used distinctive morphological features such as cell size, staining affinity, pigment granules and yolk globules to identify neural crest cells in *Ambystoma jeffersonianum*, as they proceeded along migrational

pathways. Such morphological differences between mesenchyme originating from these two sources has been confirmed in the axolotl by Detwiler (1921) and DeBeer (1947).

Cells within the ventral medial aspect of the TA lose most of their yolk by day 16pf, prior to cells in other regions of the TA. Distinct spatial and temporal distribution pattern of comparatively yolk deficient cells in ventral medial aspects of the TA region may simply indicate that cells are metabolizing yolk as they progress ventrally. Alternatively, we may be observing metabolic changes that occur as an aspect of differentiation. It would be useful to ascertain, by antibody, lectin or vital dye analysis, whether the population of yolk-filled TA cells originate, at least in part, from the neural crest. It would also be useful to examine stages prior to day 15pf in prolarva to determine the earlier location of these distinctive cells.

In addition to the irregular appearance of mesenchymal cells in the lamprey prechondrogenic environment, variation in cell densities of the mesenchyme followed a different pattern than that described in higher vertebrates. In higher vertebrates, cellular density of mesenchymal tissue increases continually, peaking immediately prior to overt cartilage differentiation. In trabecular cartilage, however, cellular densities fluctuated, with two peaks: one at day 16pf prior to the initial appearance of condensations, and a second during day 18pf immediately before overt cartilage differentiation. Initial densities and close apposition of the cells during day 15pf probably occurred because of expansion of cell membranes as a result of excessive amounts of intracytoplasmic yolk and lipid. By day 16pf the increase in intercellular

space created the illusion of a less dense population of cells in the TA, but the actual number of cells per 1000μm^2 increased by approximately 60%. Reduction in quantities of intracellular yolk within the cells of this location by day 16pf possibly resulted in a smaller cell volume, that would account for an increase in number of cells within a defined space. Abundance of mitotic figures observed during day 16pf suggest that cell proliferation, at least in part, is responsible for this initial rise in cell density. The sharp drop in cellular density levels after this initial peak may be accounted for by differentiation of these cells into other cell types, cellular degeneration, and/or possible outward migration. Head mesenchyme is the progenitor tissue for many cell types. Neuronal, glial, and pigment cells as well as connective tissue of the head including cartilage, dermis, meninges and perivascular elements arise from the mesenchyme of the head region (LeLievre and LeDouarin, 1975; LeLievre, 1978; Noden, 1988; Thorogood, 1988). Many of these cell types appeared to be more abundant during this period.

Once the condensation phase was initiated, the pattern of chondrogenesis followed a progression of events comparable to those reported for developing cartilage in metamorphic lampreys and in other vertebrate species. The cellular density levels peaked by day 18pf, approximately 60% above that of the previous day. Increased densities occur in skeletal condensations primarily as a result of cell proliferation, inward migration or lack of outward migration (Hall and Miyake, 1992). Some mitotic activity was observed prior to overt cartilage differentiation, but mitotic figures were less prevalent in later stages. While cell proliferation is critical in the

formation of avian scleral bones (Hale, 1956; Hall, 1978, Ede, 1983; Hall and Miyake, 1992) it plays a minor role in the limb bud (Janners and Searls, 1970; Ede, 1983). An inverse relationship has been demonstrated between mitotic index and cartilage differentiation in the limb (Summerbell and Wolpert, 1972; Ede, 1983).

It is likely that increase in cellular densities in the lamprey trabecular cartilage, following initiation of condensations, resulted from cellular aggregation. Condensations in day 17pf prolarval lamprey appear to originate at a central focal point composed of a few cells which are encircled in a spiralling pattern by peripheral mesenchymal cells. Similar observations have been made in chick limb mesenchyme cultures (Ede and Flint, 1975; Holmes and Trelstad, 1980). This formation may occur as surrounding mesenchymal cells are pulled into place when the central condensing cells contract their filopodia (Ede, 1983). However, scanning electron microscopy (Ede and Wilby, 1981; Ede, 1983) and cinema-lapse photography (Ede *et al.*, 1977) suggest that active migration to the focal points plays a larger role in condensation formation.

High cell density levels have been demonstrated to be essential for cartilage differentiation since they provide cells with opportunities for cell contact and communication (for reviews see Hall, 1978; Ede, 1983; Solursh, 1983). Gap junctions were observed between core cells of the forming condensations during day 17pf and throughout the condensation by day 18pf. Similar structures have been seen in the mammalian limb (Zimmermann and Thies, 1984). Recently, an increase in gap junction formation has been demonstrated to occur in wing bud tissue cultures during

the condensation phase (Coelho and Kosher, 1991). It was postulated by these researchers that intercellular communication during this period of differentiation may regulate or be regulated by cAMP, which is a known stimulant for cartilage differentiation under certain conditions (Solursh *et al.*, 1979, Rodgers *et al.*, 1989). Actively condensing cells in the developing trabecular cartilage were also observed to be in very close contact over broad expanses of their cell membrane. This form of contact has been suggested by Shore *et al.* (1981) to be a distinct form of cell junctions, and is reported in the developing piston cartilage of metamorphic lamprey (Armstrong *et al.*, 1987) and in avian wing bud (Searls *et al.*, 1972).

In higher vertebrate systems, epitheliomesenchymal interactions are among the inductive influences that initiate differentiation of neural crest derived mesenchyme (ectomesenchyme) into cartilage (for reviews see Hall, 1978; Hall, 1983a,b; Solursh, 1983; Saunders, 1988; Hay, 1991). While it is not possible to determine purely by morphological examination, what these inductors may be in developing lamprey trabecular cartilage a number of observations allows us to speculate. First, condensations always originate ventromedial to the eye; cells located in more distal regions remained undifferentiated. In avians, development of trabecular elements within the chondrocranium follows interaction between neural crest cells and basolateral aspects of the diencephalic epithelium (Thorogood *et al.*, 1986; Thorogood, 1988; 1993a,b). While no obvious contact was observed between the TA and epithelium of the brain, their cells were in close association. It is possible that contacts occurred at an earlier point in time or were simply missed. A delay of

several days is suggested to occur between epitheliomesenchymal interactions and differentiation of cells in some systems. (Thorogood, 1993b). Temporal onset and spatial appearance of the condensation observed in this study is compatible with suggested delay between a possible interaction at the level of the brain and a response in the induced cell(s).

A second feature suggesting occurrence of epitheliomesenchymal interactions in lamprey trabecular tissue is the frequent contact observed between ventromedial mesenchymal cells of the TA and the basal lamina of the buccal epithelium, an endodermal derivative and continuation of the pharyngeal epithelium. Similar cell:matrix interactions occurred less frequently between TA cells and endothelial tissue (mesodermal derivative) of the carotid blood vessel. In amphibians (Epperlein and Lehmann, 1975; Graveson and Armstrong, 1987) and lampreys (Damas, 1944; Newth, 1956), cell contact between pharyngeal endoderm and neural crest cells is essential for formation of visceral cartilages. It is suggested that molecular substances which can diffuse through the basal lamina induce cell(s) which in turn act as inducing agents for other cells over areas as great as 300μm (Hall, 1983b). It is worth noting that dorsally located TA cells, which did not approximate the dorsal surface of the buccal cavity, remained undifferentiated and morphologically resembled the yolk-filled cells observed in earlier stages. It is possible that a combination of epitheliomesenchymal interactions may be involved in differentiation and accurate location of the lamprey trabecular cartilage.

Condensing and early chondroblastic cells of differentiating trabecular cartilage tissue had an appearance similar to those in other vertebrates. Cells entering condensation stages typically became rounder, had a high nucleo-cytoplasmic ratio, large nucleoli, abundant free ribosomes and a poorly developed RER system similar to those reported in other vertebrate systems (Gould *et al.*, 1972; Searls *et al.*, 1972; Thorogood and Hinchcliffe, 1975; Hall, 1978; Ede, 1983; Hall and Miyake, 1992). The rounded cell shape observed by day 18pf in the lamprey trabecular cartilage is similar to that described for the developing piston cartilage during stage 3 of metamorphosis (Armstrong *et al.*, 1987). Archer *et al.* (1982) has suggested that the change in cell shape is an essential step in the expression of cartilage phenotype.

Recently a number of molecules involved in regulating ultrastructural changes observed during condensation formation in higher vertebrates have been identified. Concomitant with the condensation process is an increase in collagen type I (Dessau *et al.*, 1980; Swalla *et al.*, 1988), fibronectin (Dessau *et al.*, 1980; Tomasek *et al.*, 1982) and tenascin (Mackie *et al.*, 1987). Fibronectin has collagen, glycosaminoglycan and integrin binding domains and may initiate the condensation process by assisting cell-cell and cell-matrix interactions (Dessau *et al.*, 1980; Tomasek *et al.*, 1982). Frenz *et al.* (1989) have recently demonstrated that condensation formation is markedly reduced when the heparin-binding domain of fibronectin is blocked with antibodies. This domain is the binding site for heparin-like molecules on cell surfaces. Tenascin interferes with fibronectin, disrupting the actin cell skeleton and causing cells to become round (Mackie *et al.*, 1987; Abbott *et al.*, 1991). This in turn has been shown

to stimulate expression of genes necessary for the cartilage phenotype (for discussion see Zanetti and Solursh, 1984; Kosher et al., 1986b). In contrast to our expanding knowledge of molecular chondrogenic mechanism in higher vertebrates, our understanding of similar processes in the lamprey is negligible.

As differentiation of the trabecular cartilage proceeded, cytoplasmic organelles responsible for production and secretion of matrix proteins became progressively more prevalent. Cells initially developed a granular cytoplasm with abundant ribosomal material indicating preparation for increased protein synthesis (Porter, 1964; Goel, 1970; Sheldon, 1983). Biosynthesis of cartilage matrix proteins in higher vertebrates, and presumably lampreys, involves the rough endoplasmic reticulum and Golgi apparatus (for reviews see Mayne and von der Mark, 1983; Lash and Vasan, 1983; Hascall *et al.*, 1991). Concomitant with the extensive development of these membranous networks in developing lamprey cartilage cells, was the appearance of large amounts of material in extracellular spaces. This material had an appearance similar to that observed within the ER cisternae. The temporal pattern of development of the intramembranous network corresponded with spatial developmental patterns of cartilage along the craniocaudal axis. Similar patterns of cartilage development are reported for avian and mammalian systems (Godman and Porter, 1960; Goel, 1970; Stockwell, 1979; Sheldon, 1983; Horton, 1993).

The identity of the 20nm collagen fibrils observed within the ECM prior to and during overt cartilage differentiation can only be speculated. It is not known if they are synthesized by differentiating cells of the condensation or were coincidently

trapped during cellular aggregation. Five collagens have been identified in lamprey tissues, three of which correspond to mammalian types II, V and XI (Kelley *et al.*, 1988; Brodsky *et al.*, 1994). Recent biochemical analysis of lamprey dermis has indicated possible presence of a mammalian type I collagen (Kawaguchi, 1993). While collagen fibrils observed in the region of the developing trabecular cartilage did not morphologically resemble type I, tremendous morphological variation in this collagen type is known to occur between adult stages of different species (Sheren *et al.*, 1986). The fibril diameter of collagen in embryonic animals is consistently 17-20nm between species (Bruckner and van der Rest, 1994). In higher vertebrates collagen type I is present in mesenchymal matrices prior to cartilage differentiation and is involved in the differentiation process. In addition, collagen type I is the fibril type produced by the perichondrium. Predominance of the 20nm collagen in lamprey precartilage mesenchyme and in the perichondrium suggests that it may play a role similar to collagen type I in higher vertebrates.

Alternatively, the 20nm collagen could correspond to type II, the major collagen of cartilage in higher vertebrates (van der Rest and Mayne, 1988; Bruckner and van der Rest, 1994). In lamprey, type II collagen has been found associated with the notochord (Eikenberry *et al.*, 1984; Brodsky *et al.*, 1994). Collagen type II fibrils display similar morphology between species (Sheren *et al.*, 1986) and are characteristically 20nm in diameter with indistinct banding patterns (Brodsky and Eikenberry, 1985). Armstrong *et al.* (1987) found ultrastructurally similar fibrils to those described herein, within developing matrix of piston cartilage in metamorphic

lamprey and suggested that they were type II collagen. In contrast to the present study, 20nm collagen fibrils did not occur prior to cartilage differentiation in piston cartilage and increased in quantity as differentiation progressed until they were obscured by other cartilage matrix components. Recently an alternately spliced form of collagen type II has been localized in amphibian (Seufert *et al.*, 1994), mammalian (Sandell *et al.*, 1991) and avian (Thorogood *et al.*, 1986) embryonic tissues prior to cartilage formation. Further molecular or immunocytochemical analyses are required to determine the identity and role of the 20nm collagen fibrils in developing lamprey cartilages.

In higher vertebrates the first appearance of noncollagenous matrix molecules, characteristic of the cartilage phenotype, occurs within 24-48 hours of the first appearance of collagen type II, the principal structural protein. Similarly, constituents of the matrix of lamprey trabecular cartilage are synthesized and secreted within 24-48 hours of the first appearance of 15-40nm globules which are similar in ultrastructural appearance to lamprin (Wright and Youson, 1983; Wright *et al.*, 1988), the principal structural protein in lamprey cartilage (Wright *et al.*, 1983; Robson *et al.*, 1993). At the initiation of overt cartilage differentiation in the avian, collagen type II (Kosher *et al.*, 1986b; Swalla *et al.*, 1988) and collagen type IX (Mallein-Gerin *et al.*, 1988; Castagnola *et al.*, 1988; Swiderski and Solursh, 1992a) are co-expressed and are followed within 24 hours by aggrecan and link protein (Stirpe and Goetinck, 1989; Mundlos *et al.*, 1991; Treilleux *et al.*, 1992). Cartilage matrix protein is synthesized 24-48 hours following collagen type II (Stirpe and Goetinck, 1989). The

granular to flocculent and filamentous material observed in developing lamprey cartilage appears ultrastructurally similar to higher vertebrate proteoglycans as described by Hascall *et al.* (1991). This material increased greatly by day 19pf and coincided with the first appearance of material morphologically similar to lamprin. This event was followed by a dramatic increase in matrix granules which in higher vertebrates are groups of collapsed aggrecan molecules attached to hyaluronic chains (Lash and Vasan, 1983; Hunziker and Schenk, 1984; Phillips and Pottenger, 1989). The temporal pattern of expression of matrix molecules in higher vertebrates, and presumably lampreys, is critical to the organization and interactions necessary for a functional matrix.

The nature of the beaded strands that formed a concentric pattern around the cell perimeter on day 20pf is unknown. The appearance of this material is similar to descriptions of aggrecan conglomerates with associated hyaluronic acid chains emerging from the "bead" (Phillips and Pottenger, 1989). The organized beaded strands appeared just prior to the dense matrix granules, which are known to be collapsed versions of aggrecan monomeric units (Eisenstein *et al.*, 1973; Hascall, 1980). Alternatively, the beaded strands in the present study, some of which appeared to be hollow, may be a microfibrillar component (Keene *et al.*, 1991). Microfibrils occur in the perichondrium of branchial, nasal and pericardial lamprey cartilages (Wright *et al.*, 1988) and in matrix of developing piston cartilage (Armstrong *et al.*, 1987). Further biochemical analyses of lamprey cartilage matrix is needed to identify these components.

In the present study, lamprin was initially secreted as individual amorphous globules of moderate electron density, similar to that described in developing piston cartilage in metamorphic lamprey (Armstrong *et al.*, 1987). In contrast to metamorphic lamprey, lamprin in prolarval cartilages was not preferentially deposited in association with 20nm collagen fibrils during chondrogenesis in prolarvae. One explanation for differences observed between matrix deposition during metamorphic and prolarval stages of the lamprey may be that in examination of metamorphic stages, each of which extends over a period of several weeks, initial steps in lamprin fibrillogenesis were missed. Alternatively, assembly of the lamprin fibril might differ in trabecular and piston cartilages. It has been established that lamprin displays variation in fibril morphology between adult lamprey cartilages (Wright *et al.*, 1988).

With continued development, the lamprin fibrillar component becomes organized into a pericellular zone with few individual globules, a territorial matrix zone with highly branched fibrils and an interterritorial matrix zone with highly coalescent fibrils in parallel arrays. This spatial variation in fibril organization is comparable to that observed in the adult trabecular cartilage (Wright and Youson, 1983; Wright *et al.*, 1988). Cause of the variation in fibril morphology between matrix zones is yet to be determined. Such variation may reflect stages in extracellular assembly and aggregation of lamprin molecules, effects of different density levels of lamprin, or pericellular influences preventing fibrillar assembly.

In summary, the chondrogenic process in lamprey trabecular cartilage follows a pattern similar to events described for metamorphic lampreys and higher vertebrates

as indicated by light and electron microscopy. Mesenchymal condensations develop ventromedial to the eye, and appear to form from inward migration of mesenchymal tissue around a focal point consisting of 2-4 cells. Appearance of the mesenchymal tissue prior to the condensation stages is ultrastructurally different from that described for other vertebrate systems and may represent morphologically distinct neural crest-derived mesenchyme. Cartilage differentiation occurs by days 19-20pf concomitant with the first appearance of lamprin fibrils. The initial lamprin material deposited is organized differently from that described in developing cartilage in metamorphic lamprey but soon acquires an ultrastructural appearance similar to that described for adult trabecular cartilages. To fully understand the chondrogenic process in lamprey cartilage future biochemical studies need 1) to address the identity of other components in the ECM of this non-collagenous cartilage and 2) to compare these processes to those recently determined in the collagenous-based cartilages of higher vertebrates.

3. DETECTION OF LAMPRIN mRNA IN THE ANADROMOUS SEA LAMPREY BY *IN SITU* HYBRIDIZATION

3.1. INTRODUCTION

Studies of lampreys are motivated for two principal reasons: 1) lampreys are in a unique evolutionary position, being extant representatives of the most primitive group of vertebrates, the agnathans or jawless fish, and 2) certain species such as *Petromyzon marinus* are parasites of economically important fish species. Of particular interest are various morphological and physiological transformations the skeletal tissues undergo when microphagic larvae metamorphose into parasitic adults. It has been suggested that these transformations in the skeletal system reflect functional adaptations to the varying habitat and mode of life of the developing lamprey (Hardisty, 1981). In the larva, for example, the neurocranium consists of a few simple cartilages that serve as ventral support for the brain (trabecular and parachordal cartilages) and protect the otic and nasal organs (Damas, 1944; Hardisty, 1981; Johnels, 1948). During metamorphosis new cartilages arise which support the buccal funnel, including the mouth (annular cartilage) and a rasping tongue (piston cartilage); two structures which are essential to the parasitic mode of life of adult stages (Hardisty, 1981).

Morphology of lamprey cartilage is well documented at light and electron microscope levels (Johnels, 1948; Hardisty, 1981; Wright and Youson, 1982; Wright and Youson, 1983; Armstrong *et al.*, 1987; Wright *et al.*, 1988). However, there is a

paucity of information on biochemical and molecular aspects of this primitive tissue, especially during developmental stages. Biochemical analysis has demonstrated that annular cartilage (splanchnocranium) of adult *P. marinus* is distinguished from that of higher vertebrates by the presence of a unique structural protein, lamprin (Wright *et al.*, 1983). Recently a soluble monomeric form of lamprin has been characterized as a group of highly hydrophobic, self-aggregating proteins containing tandem repeat sequences similar to those found in certain insect structural proteins, and avian and mammalian elastin (Robson *et al.*, 1993). Three cDNA fragments of the lamprin gene have been cloned and sequenced (Robson *et al.*, 1993). This new information provides us with the opportunity to expand research on lamprey cartilage in new directions.

It is of phylogenetic interest to compare morphological and molecular processes of chondrogenesis in lampreys to those of higher vertebrates. One technique that would provide us with information about these processes is *in situ* hybridization (ISH). ISH is an ideal method to study spatial and temporal distribution of lamprin while enabling conclusive identification of early chondrogenic tissue. Rudimentary cartilaginous elements in lampreys (Damas, 1944; Johnels, 1948), birds (Fell, 1925; DeBeer, 1971) and mammals (Heuser and Streeter, 1929; Leppert, 1933) have historically been distinguished from surrounding undifferentiated tissue by histological methods that relied upon routine staining of matrix and serial reconstruction. However, these staining methods are insufficiently sensitive to detect trace amounts of matrix material and, therefore, do not allow for positive identification of

chondrocytes during early differentiation. ISH analysis, however, is a technique sensitive enough to detect onset of matrix expression in differentiating cartilages in birds (Hayashi *et al.*, 1986; Swalla *et al.*, 1988) and mammals (Sandberg and Vuorio, 1987; Grover and Roughley, 1993). This investigation represents the first time ISH has been used to detect lamprin expression and thus allow for conclusive identification of chondrocytes in developing stages of lampreys.

Before a comprehensive investigation of lamprin expression was undertaken, a standardized methodology for efficient and reproducible ISH hybridization analysis of lamprey tissues had to be developed. Studies on other vertebrates have shown that optimization of variables in the ISH procedure such as probe type, length and label; tissue fixation and processing methods; pretreatment of tissue sections to block nonspecific binding and enhance signal; hybridization and wash conditions and method of signal visualization are critical to the sensitivity and specificity of ISH analysis and are dependent upon the species and tissue (Bloch *et al.*, 1986; Hayashi et al., 1986; Lewis and Baldino, 1990; McLaughlin and Margolskee, 1993; Wilcox, 1993). The purposes of the study reported here were 1) to establish an optimal protocol for detection of lamprin mRNA in developmental stages of the lamprey using ISH, and 2) to determine the spatial distribution of lamprin mRNA.

3.2. MATERIALS AND METHODS

3.2.1. Tissue preparation

Sexually mature adult lampreys were captured during their annual May upstream migration at a fish ladder (operated by the Department of Fisheries and Oceans Canada) on the LeHave River in New Germany, Nova Scotia, Canada. Eggs and sperm were extracted manually from ripe unanesthetized lamprey. Eggs were fertilized artificially and embryos were raised under laboratory conditions (as described in Chapter 2). Prolarvae, day 23-31pf, were anesthetized in 0.05% tricaine methanesulfonate (MS-222) and fixed *in toto* at room temperature in 4% paraformaldehyde in 1x PBS, pH 7.4 (4% PFA) for 5, 10, 15 or 30 minutes, or in Bouin's fluid for 15 minutes or 10 hours. Prolarva and samples of adult annular cartilage were processed for light microscopy (LM) by dehydrating through a series of graded ethanols, clearing in xylene or Americlear (Stephens Scientific, Cornwell Corporation, Riverdale, NJ) and embedding in paraffin. To prevent RNase contamination, all solutions used prior to ISH washes were either treated with 0.1% diethylpyrocarbonate (DEPC) or prepared with DEPC-treated water before autoclaving.

Metamorphic lampreys were collected from streams in southern New Brunswick, Canada, in July by electrofishing. Metamorphic lampreys were staged according to external criteria described by Youson and Potter (1979). Following anesthesia in 0.05% MS-222, animals were decapitated. Cross-sections were taken between the rostral most portion of the head and the heart region. Tissues were fixed for 30

minutes or 1 hour in 4% PFA, or 48 hours in Bouin's fluid, and processed as described above.

Female Zucker lean rats, 200g, were anesthetized with 60mg/kg sodium pentobarbital and sacrificed by pneumothoracotomy before sections of ear (elastic cartilage) and trachea (hyaline cartilage) were removed. These tissues together with samples of gill cartilage taken from sacrificed, 10-15g fingerling rainbow trout were used as negative controls. Both mammalian and teleost tissues were fixed for 30 minutes in 4% PFA and processed as per lamprey tissues.

Six micrometer sections were cut from rat, rainbow trout and lamprey prolarval, metamorphic and adult samples and mounted on acid-cleaned glass slides. The slides had been pretreated with 0.1% gelatin and 0.01% chromium potassium sulphate (Boyd, 1955). Sections were dried overnight at 42^0C and stored desiccated at -20^0C prior to use.

3.2.2. Preparation of lamprin riboprobes

A cDNA fragment of the lamprin gene, 1,798bp long, subcloned in a pGEM-4 vector (Robson *et al.*, 1993) was used to make the sense and antisense riboprobes (Figure 3.1A,B). The cDNA insert was modified by removal of the poly(A) tail through an overnight restriction digestion with the restriction enzyme *Eco*RI (New England Biolabs, Mississauga, Ontario, Canada). This endonuclease cleaves in the polycloning site of the pGEM-4 vector nearest to the SP6 promoter and at nucleotide position 1,423 of the cDNA insert (Figure 3.1A). The DNA fragments were purified

Figure 3.1. A) Diagrammatic representation of the lamprin cDNA insert in plasmid vector pGEM-4 transcribed to make ^{35}S-labelled, antisense riboprobes (L1.8-156-3). SP6 and T7 correspond to RNA polymerase promoters for SP6 RNA polymerase and T7 RNA polymerase, respectively. Horizontal arrows indicate direction of transcription. B) The nucleotide sequence of the lamprin cDNA (GenBank™/EMBL Data Bank accession number L05926) insert used in this study. Underlined boldface type indicates sequence transcribed to make the riboprobe L1.8-156-3.

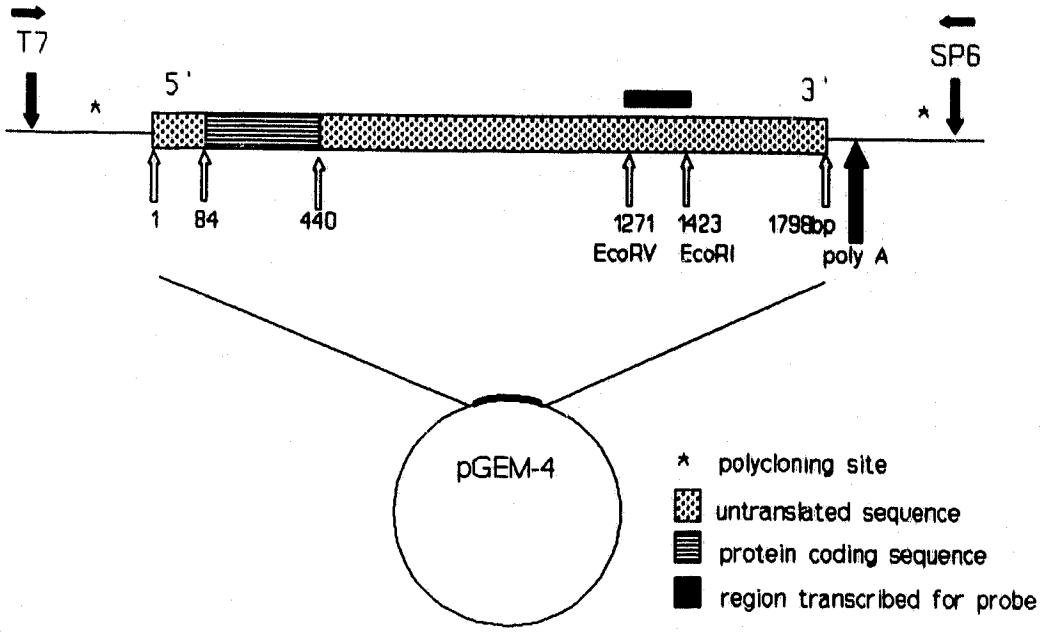

A

```
GTGAAGCTTC ATCAGCCTCA ACTCAAAGCC CTCCTCTCCT CATGGTCGAC    50
AGCGAAACGA AACAAAAAAT CCCTAAAATA AAAATGGCCG CCACCATGCA   100
AGCTCTGCTC GTGATGGCCC TCCTTCACCT CGCCACCGCG ACGCCTGTCG   150
TTACCAAGCA TAAAGTGAGC ACTTTCAGTA CGGGATTTCT GGGACACCCT   200
GTGGGAGGCC TGGGCTATGG AGGCCTTGGC TATGGAGGCC TGGGCTATGG   250
AGGTCTGGGC GTTGCTGGTC TAGGCTATGC TGGTCTAGGC TATCCCGGAG   300
CGGCTCTTGG AGGAGCATAC ACGCACCATG CAGCCCTCGG CGGACTCGGC   350
TACCCCCTGG GCATTGGCGC CGGTGTGGTG GCTCCTCACG TGGTGAACAG   400
CAAAATCGCT GCCCCGTTGG CGCCTGTTGT TGCTGCCATC TAAATCGTCA   450
CCGTGACTGG AGAATTGCTA GGCGATCGTT GACTTGCCGC ACCAGCCCTG   500
CGTCCCCTCT GCAGTCACTT CAAACAGAAG TGTTGCCTGC GGAAGTGACT   550
CAAGGCTCCG GTGAAGAAGT GACTTGATGA AGGTTATGCA CAGCCTCCGC   600
CAACTACCAC CCACCAAAGG GAGCATAGGT TCACCACCTA CTCCCCTCCC   650
ATGCCTGCCC ATTCATACCC ATCCTCCCCA AGCCCTTGAC TCTTACACAA   700
ATTCTCATCA TCATCGGCGC AATGGTATCT TTTCCCCATT TGTTAAGTTT   750
GTGACCCCTA ATCCCATGCC AATTTCCTGC AAATAACGCC ATTCGGACCC   800
TTAAGTGCGT GAGTGTGTAA TCGTGTGACA GAGTGAGTGC GTGACGAAAG   850
TGGGTGGGCC GGGTGTGCCG GCGTCTCTCC ATAACGTTTT CTGAACTTCT   900
CGGCATTAAC ACAAATGACG ATGAATGAAC ACGACCTGGA AAACAAAATC   950
TACCACGAAT AGTATAAAAT TTATATATAT ATTTTAAAAC CCTGACATTT  1000
ATCGTTAAAA AACAAAAAAA GTATGGTGGC GAGGGAAGCA CGCACACGGA  1050
TTCCGATTCT GCAATCTGGG GGAGTAAATC AATCGGGCGG GTGAAATTAG  1100
TCTGTGATGA AAGCTGTTAA CGTTAAGGAA AATATATGAA CATTTAAATC  1150
ATAATGGGAC TTAGGAATCG ACTGTTCGAC TGGACAGTAA CCAAAAATAA  1200
ATCAGCTGGA TTGGGATGAT GGGTGCTACT CCGATGGGAG TTTGGTTCAC  1250
AGGTGAATAT ATACACGAAT GATATGTGGG TTCCAAACGC CCCCTCCCCC  1300
ATATCTGTGT GTGCCCCCTT CCCCCTACAC CAAGTATACA CCTATCGTTA  1350
TTTAGCTCTT GTCAGCTCCA GAGTTTTGTT TTAACCGGTC GTGAAGTGAG  1400
GACACCTCCA AATCATCCTA CAAGAATTCG AGATCATTGT GGATCAAAGA  1450
TCTGGTTGAC TTTGGCCCCA AAACGTTTGA TAGTGGTCGG TCGAAAATTT  1500
TCGACAACGG ATTGTGTGCG TCTCGTAACG CCAAGGGTCA TTAACAGCTG  1550
TCGTGGTTTT GTCATTCGCG ATTACGATTT CATCGGCTGG AAATTCAGTT  1600
GCACCGTGGA TAACGGATGT TGAGTTACGA GCGGCTTAAC GATTGAATTA  1650
CTCGGCCGAT GAGATGGCAC AGGCGTCTGT TGGATAGTAT GATAAAGGTT  1700
GTTAAGTTCT GGATTGACTC GACGCGACTT GGGTGGGTGT GTTCTGGGAA  1750
ACGTCCTTCT TGTGTGCCGG ATTAAAATAA AAATCTGTAC TCACTGCCAA  1800
AAAAAAAAAA AA
```

B

by phenol-chloroform-isoamyl alcohol extraction (Sambrook *et al.*, 1989), then precipitated at -70^{0}C with 0.1 volume of 3M sodium acetate, pH 7.0 and 2 volumes of absolute ethanol. The recovered DNA was dried and resuspended in 20µl of TE buffer (10mM Tris-HCl, pH 7.4, 1mM EDTA). DNA fragments were size fractionated on a 1% low melting-temperature agarose gel (Figure 3.2). The band containing the linearized plasmid DNA and the 1,423bp of the cDNA (Figure 3.2, lane 4) was recovered and purified using the technique described by Favre (1992), and was then religated with T4 DNA ligase (GIBCO BRL, Burlington, Ontario, Canada). This preparation was used to transform *E. coli* strain DH5αF'IQ™ competent cells (GIBCO BRL). White colonies carrying recombinant plasmids were randomly picked from agar plates containing 50µg/ml ampicillin and 0.005% X-gal, and were analyzed by agarose gel electrophoresis. For transcription from the SP6 promoter, the selected DNA template was linearized with restriction enzyme *Eco*RV (New England Biolabs) which cuts at nucleotide position 1,271 in the lamprin cDNA (Figure 3.1A), allowing the production of 156bp "runoff" transcripts complementary to a portion of the 3' untranslated lamprin mRNA region.

Antisense riboprobes (L1.8-156-3) labelled with ^{35}S-UTP (approx. 1,330 Ci/mmol) (Du Pont Canada, Mississauga, Ontario, Canada) were made by transcribing the selected DNA template using the Riboprobe^R Gemini System II Kit (Promega, Madison, Wisconsin, USA) with SP6 RNA polymerase and the manufacturer's protocol with the following modifications. Incubation was performed for 1.5 hours and the mixture was "spiked" with 20U of SP6 polymerase after 30

Figure 3.2. Agarose gel electrophoresis of pGEM-4 vector with and without lamprin cDNA insert following enzymatic cleavage with *Eco*RI. Lane 1 contains DNA molecular weight markers, Lane 2 represents nonlinearized pGEM-4 vector, Lane 3 contains nonlinearized recombinant pGEM-4 vector, and Lane 4 contains linearized recombinant pGEM-4 vector.

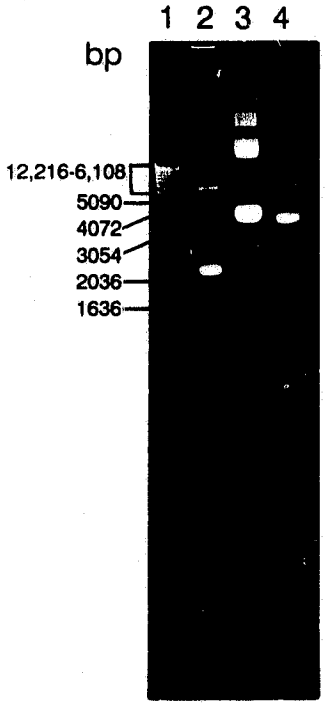
1 2 3 4
bp
12,216-6,108
5090
4072
3054
2036
1636

minutes of incubation. Following phenol-chloroform-isoamyl alcohol extraction and two ethanol precipitations, (0.1 volume of 3M sodium acetate in the first precipitation and 0.1 volume of 7.5M ammonium acetate in the second), the probe was dried under vacuum and resuspended in 5µl of 2.0M dithiothreitol (DTT). Sense riboprobes were made using the same procedure but substituting T7 polymerase for SP6 polymerase. In some experiments, "cold competitors" were made by transcribing a pGEM-4 template without a cDNA insert in the presence of four cold nucleotides, one of which was S-UTP (DuPont, Canada). Prior to hybridization the probe was boiled for 3 minutes with 2.5µl of cold competitor and immediately added to the hybridization buffer (50% deionized formamide, 0.3M NaCl, 10mM Tris-HCl pH 8.0, 1mM EDTA, 0.02% Ficoll, 0.02% polyvinylpyrrolidine, 0.02% bovine serum albumin, 0.05% yeast tRNA, 0.05% polyadenylic acid, 50mM DTT, 10% dextran sulfate) to obtain a final specific activity of 2×10^4-2.5×10^5 cpm/µl.

3.2.3. Pretreatment of tissue sections

Slides were brought to room temperature before being exposed to air. Paraffin was removed via three 5-minute changes in xylene before sections were hydrated through a series of graded ethanols and immersed in 1x PBS for 5 minutes. To determine the effect of proteolytic digestion on signal to noise ratio, tissues were 1) treated with concentrations of 1µg/ml or 10µg/ml of predigested Pronase E (Sigma Chemical Company) in 50mM Tris-HCl, pH 7.3 containing 5mM of EDTA at 37^0C or room temperature for 10, 15, or 30 minutes, 2) treated with 1 µg/ml of Proteinase

K (Sigma) in 1x PBS at 37^{0}C or room temperature for 5, 10, 15, or 30 minutes, or 3) not exposed to any proteolytic digestion. Digestion was stopped by washing for 30 seconds in 500ml of 1x PBS containing 2mg/ml glycine, tissues were post-fixed 5 minutes at room temperature in fresh 4% PFA and fixation was blocked by a 5 minute immersion in 3x PBS. All tissue sections were subsequently washed twice .

Sulfhydryl groups were blocked by first equilibrating specimens for 10 minutes at 45^{0}C in 10mM DTT in 1x PBS and then treating for 30 minutes at 45^{0}C with freshly prepared blocking solution of 10mM of iodoacetamide, 10mM N-ethylmaleimide, 10mM DTT in 1x PBS (Zeller and Rogers, 1989). Two 2-minute rinses were performed at room temperature in 1x PBS. Nonspecific binding sites caused by electrostatic interaction between the probe and basic protein groups were blocked by equilibrating specimens for 2 minutes in freshly prepared 1.9% triethanolamine (TEA) buffer, pH 8.0, and then immersing in 0.25% acetic anhydride in TEA buffer for two 5-minute changes. The acetic anhydride solution was used immediately following preparation. To determine the effectiveness of acetic anhydride and iodoacetamide/N-ethylmaleimide, these blocking agents were omitted from the protocol in some cases. Slides were washed twice in 2x saline sodium citrate (SSC) before being dehydrated through graded alcohols. Slides were air dried for 0.5 days prior to further use.

3.7.4. Hybridization

Five hundred microliters of hybridization buffer were added to 2.5µl of riboprobe competitor that had been heated 3 minutes at 100^{0}C. Twenty microliters of this prehybridization solution were applied to each tissue section. To determine the effect of prehybridization, hybridization buffer with or without a cold competitor incorporating a non-sulfated UTP was substituted for the prehybridization solution in some cases. Slides were incubated for 2 hours at 45^{0}C in a moist chamber containing a solution of 50% formamide, 0.3M NaCl, 10mM Tris-HCl and 1mM EDTA. Excess fluid was drained and blotted from around the tissue. Five to 30µl of probe L1.8-156-3 were spread on each section and tissues were covered with a piece of parafilm. Slides were incubated for 8-22 hours under the same conditions as for prehybridization.

3.2.5. Controls

Four sets of controls were used in this study: 1) hybridization with sense riboprobes; 2) hybridization with riboprobes transcribed from pGEM-4 sequences without the cDNA insert; 3) digestion of tissue sections prior to hybridization for 1 hour at 37^{0}C with 50µg/ml RNase I "A" (Pharmacia, Dorval, Quebec, Canada) in RNase buffer (5M NaCl, 0.5M EDTA, 2M Tris-HCl pH 8.0) and 4) hybridization of L1.8-156-3 with teleost and mammalian cartilage tissues.

3.2.6. Washes and RNase treatment

Washes were of high stringency and were done according to Zeller and Rogers (1989). Briefly, slides were dipped 2-3 times in Wash A (50% formamide, 2x SSC, 20mM ß-mercaptoethanol) at 55^{0}C before washing for 15 minutes with gentle agitation in two changes of this solution. Slides were further washed for two 15-minute changes in a second solution of 50% formamide, 2x SSC, 20mM ß-mercaptoethanol and 0.5% Triton X -100 (Wash B) followed by two 2-minute washes at room temperature in 2x SSC containing 20mM ß-mercaptoethanol (Wash C). Sections were rinsed in RNase buffer at 37^{0}C for 30 seconds before being incubated with 50µg/ml pancreatic RNase I "A" in RNase buffer for 30 minutes at 37^{0}C. Following a 10-minute rinse in RNase buffer the slides were washed in two 30-minute changes of Wash C at 50^{0}C, two 30-minute changes of Wash A at 50^{0}C and two 5-minute changes of 2x SSC at room temperature. Sections were then dehydrated and air dried for a minimum of 0.5 days before autoradiography.

3.2.7. Autoradiography and staining

Slides were dipped 1-2 times in Kodak NTB-2 emulsion (Eastman Kodak Company, Rochester, NY) at 42^{0}C under safelight conditions and air dried in the dark for 30 minutes. Groups of up to ten slides were placed in black, plastic boxes of 25-slide capacity containing Drierite (W.A. Hammond Co., Xenia, OH). Boxes were sealed and wrapped in light-tight bags and stored at 4^{0}C with slides in horizontal positions, tissue side up, as suggested by Rumason (1972). Exposure time ranged

from 3 days to 4 weeks. Slides were developed at room temperature in Kodak D-19 for 4 minutes, washed in distilled water for 10 seconds, fixed in Kodak rapid fix for 5 minutes, and washed twice for 5 minutes in distilled water. Slides were then air dried overnight and stained with Mayer's hematoxylin according to Baserga and Malmund (1969) before dehydrating and coverslipping. Tissues were examined and photographed using a Zeiss Photomicroscope III.

3.3. RESULTS

Strong hybridization signals, visualized as dense accumulations, often clusters, of silver grains were observed over chondrocytes in all neurocranial cartilages of adult, metamorphic (Figure 3.3A) and prolarval (Figure 3.3B) lampreys following ISH with probe L1.8-156-3. Progressively stronger signals were found from prolarval to adult stages. No hybridization signal was detected over pericardial or branchial tissues. In addition, no hybridization signal was detected over adjacent tissues within the section, sections that had been treated with RNase prior to hybridization (Figure 3.3C), sections hybridized with antisense probes containing only vector sequences or sense probes, or in teleost (Figure 3.3D) or mammalian cartilage tissues. Nonspecific background, recognized as an even dispersion of silver grains over nuclei and cytoplasm, was observed in sections hybridized with sense probe and antisense probe L1.8-156-3, and predominated over neural tissue and pigmented cells.

Good retention of morphology was achieved with fixation periods of 30 minutes in 4% PFA. In tissues fixed for periods of 15 minutes or less the preservation of

Figure 3.3. Hybridization signal visualized over A) otic capsule (O) and parachordal (Pc) cartilages in a stage 2 metamorphic lamprey and B) trabecular cartilage (arrowheads) in a day 31pf prolarva. Note absence of signal over branchial cartilage (arrow) in A. Tissues were prehybridized with cold S-UTP competitor, probe specific activity was 8 x 10^4cpm/µl and exposure time was 6 days. The absence of this signal in the following control sections demonstrates the specificity of probe L1.8-156-3. C) prolarva section pretreated with RNase and D) hyaline cartilage (H) in teleost gill. Tissues shown in C and D were prehybridized with a cold S-UTP vector sequence probes; specific activity of probe L1.8-156-3 was 2 x 10^5 cpm/µl and exposure time was 5 days. All tissues were fixed in 4% PFA for 30 minutes. Brain (Br); notochord (N); eye pigment (arrow). A= X 300; B-C= X 80; D= X 2,000.

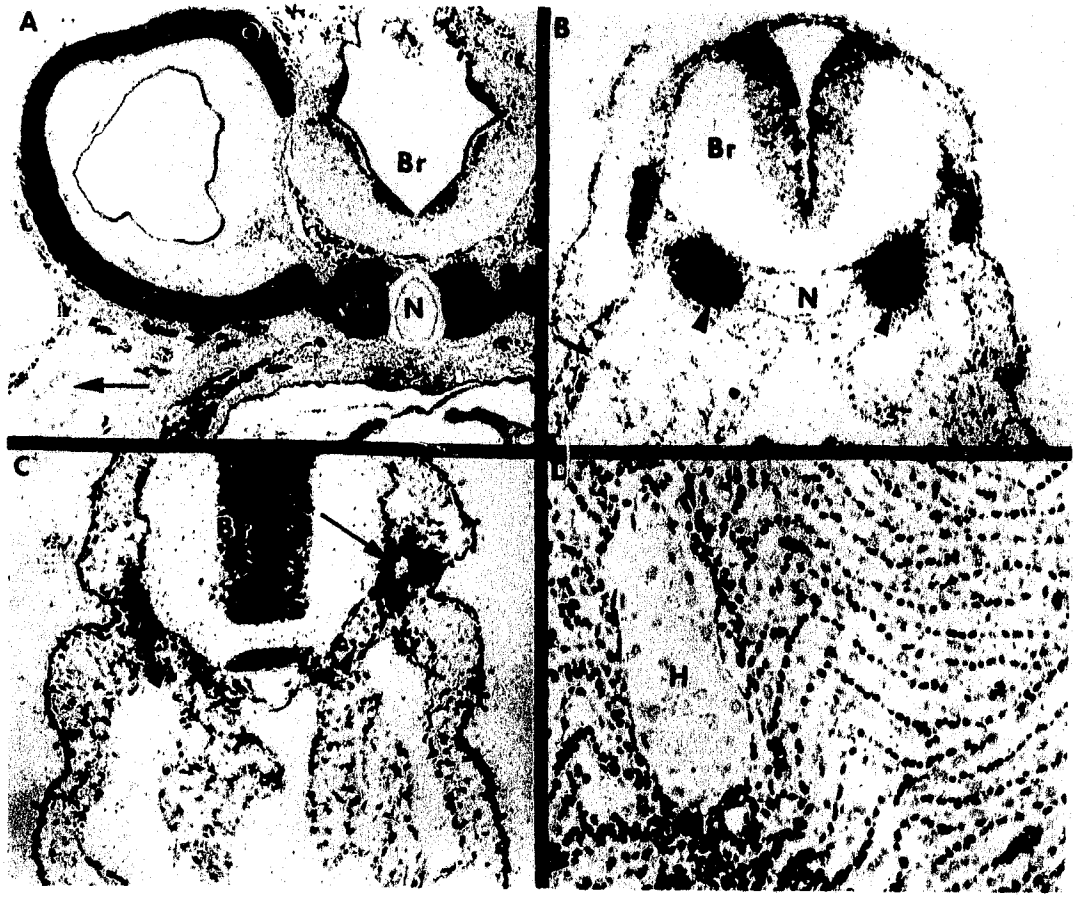
A
Br
N
B
Br
N
C
H

histological structure was poor and tissue fragments were often lost from the slide during hybridization. The autoradiographic signal was reduced in tissues exposed to fixative for more than 30 minutes and was not enhanced in tissues fixed for 15 minutes or less. An increase in nonspecific background and a decrease in signal were found in tissues fixed in Bouin's fluid for all fixation times.

The level of nonspecific background was affected by a number of variables. Proteolytic digestion of lamprey tissues with either Proteinase K or Pronase E resulted in an increase in background labelling but did not improve the signal when the fixative used was 4% PFA (compare Figure 3.4A to 3.4B). However, signal was greatly enhanced with use of proteases in Bouin's fixed tissues. Pretreatment with iodoacetamide and N-ethylmaleimide did not reduce background. Acetic anhydride treated sections demonstrated slightly less background especially over the brain. Prehybridization with a cold competitor, produced using vector sequences and cold S-UTP, resulted in a pronounced reduction of nonspecific background. However, prehybridization was less effective if proteases were used in the pretreatment or if the specific activity of probe L1.8-156-3 was greater than 9 x 10^4cpm/µl. Prehybridization with buffer with or without cold competitor incorporating non-sulfated UTP was not efficient at reducing background.

Optimal conditions for hybridization were at 45^0C for a minimum of 16-22 hours using probe L1.8-156-3 (specific activity of 6-9 x 10^4cpm/µl) and omitting dextran sulfate from the hybridization buffer. (Dextran sulfate increased the rate of hybridization, reducing the duration of hybridization to 6-8 hours of incubation, but

Figure 3.4. Comparison of proteolytic digested tissues with nondigested tissues. Note the higher levels of background particularly over neural tissues (asterisk) in A) a day 31pf prolarva pretreated with 1.0μg/ml of Proteinase K for 10 minutes at 37^0C compared to B) an adjacent section which was not digested. Arrowheads indicate hybridization signal over trabecular cartilage. Tissues were fixed in 4%PFA for 30 minutes, prehybridized with cold S-UTP vector sequence probes, probe L1.8-156-3 specific activity was 8 x 10^4 cpm/μl and exposure time was 7 days. Brain (Br), notochord (N). A= X 120; B= X 110.


Br
N
A
Br
N
B

it also produced a higher level of background.) Under these hybridization conditions a signal could be detected in prolarval stages within 5-9 days and in metamorphic or adult lamprey within 3-5 days. Exposure times greater than 9 days following hybridization with probe L1.8-156-3 with a specific activity of 9 x 10^4cpm/µl resulted in a lower signal to noise ratio due to increased background levels. Probes with a higher specific activity also resulted in an intense background prohibiting the detection of low levels of mRNA expression. Increasing the stringency of the hybridization and washes by using temperatures above 55^0C was not useful in reducing this background since higher temperatures usually destroyed tissue morphology or resulted in the loss of tissue sections from the slide.

3.4. DISCUSSION

This study demonstrates the effectiveness of probe L1.8-156-3, a 156bp ^{35}S-labelled antisense riboprobe, in detecting the expression of mRNA for lamprin, a structural protein found in the matrix of lamprey cartilage. Optimal conditions for ISH assays of mRNA for the lamprin gene were determined. The spatial distributions of lamprin mRNA in lamprey neurocranial and splanchnocranial cartilages were subsequently examined.

The specificity of probe L1.8-156-3, complementary to the 3' noncoding region of one of three known lamprin cDNAs, was confirmed by four outcomes of this study. First, hybridization of this probe was shown to be species specific. No hybridization signal was detectable in mammalian hyaline or elastic cartilage, or teleost hyaline

cartilage; three cartilages which appear morphologically similar and share some biochemical characteristics with lamprin-based cartilages (Wright *et al.*, 1988). Second, these probes were shown to be cartilage specific. ISH labelling was confined to the chondrocytes within neurocranial cartilages and did not occur in the cells of the surrounding tissues such as muscle, nerve or connective tissue. Third, pretreatment with RNase A eliminated the signal, indicating that the hybrid formed was RNA-RNA and not RNA-DNA. Fourth, noncomplementary probes such as the sense probe and the vector sequence probe did not hybridize to any of the tissue sections examined in the present study.

Fixation, proteolytic digestion and prehybridization, were found to be the three most important steps to optimize the signal to noise ratio during ISH analysis of this lamprey tissue. Our results show that cellular morphology and hybridization signal are best retained with 4% paraformaldehyde. These findings are in agreement with the results of other studies (Hoefler *et al.*, 1986; Pardue, 1990; Pechoux and Morel, 1993). Paraformaldehyde preserves cellular morphology while retaining mRNA by crosslinking proteins in the cell, but it does not inhibit penetration of nucleic acid probes (Singer *et al.*, 1986). Our observation that weaker hybridization signals occurred with Bouin's fixed tissues concur with those of Singer *et al.* (1986) who suggest that extensive crosslinking ability of Bouin's fluid reduces the accessibility of the target to the probe.

Ideal fixation times reported for ISH procedures vary depending on the tissue type and size but most studies suggest between 5 minutes to 6 hours (Hoefler *et al.*,

1986; Biroc *et al.*, 1993; Wilcox, 1993). For lamprey cartilage, the optimal fixation time of 30 minutes was at the lower end of this range. Longer fixation resulted in a decrease in signal while shorter fixation resulted in loss of morphology. Other groups report a reduction in signal intensity associated with extended exposure to fixatives (Brigati *et al.*, 1983; Wilcox, 1993).

Many ISH studies describe an improvement in hybridization signal following pretreatment with proteolytic enzymes (Hayashi *et al.*, 1986; Hoefler *et al.*, 1986; Shorrock *et al.*, 1991; Biroc *et al.*, 1993). While proteolytic digestion improved hybridization signal in lamprey cartilage that had been fixed with Bouin's fluid, we observed that protease treatment did not enhance the hybridization signal in PFA fixed tissues. In the latter, digestion increased the background, which often obscured the hybridization signal. In addition, even brief digestions of prolarval tissues with either Pronase E or Proteinase K produced an unacceptable interruption of morphology and often resulted in loss of the sections from the slide. Similar disadvantages associated with proteolytic digestion of paraformaldehyde fixed tissues have been reported by other groups (Bloch *et al.*, 1986; Singer *et al.*, 1986; Harper and Marselle, 1987).

The ability of enzymatic digestions to improve the signal to noise ratio depends on a number of variables. Jordan (1990) suggests that such treatment may be unwarranted for paraffin embedded tissues since the mechanical act of sectioning tissues increases accessibility of target to probe by effectively "slicing open" cells. The necessity of deproteinizing steps in the ISH procedure is more likely a factor of both

the type of fixative and size of probe employed (Singer *et al.*, 1986; Soghomonian, 1990). Proteolytic digestion of PFA fixed tissues removes the crosslinked proteins that loosely retain the target nucleic acids, resulting in a loss of cellular RNA and a reduction in hybridization signal. Concomitantly, such treatment might increase the availability of certain molecules which nonspecifically bind the probe. Proteolytic digestion is necessary, however, to improve accessibility of the target when a more effective fixative such as Bouin's fluid or large probes are utilized (Singer *et al.*, 1986).

Some ISH protocols include a prehybridization step (Hoefler *et al.*, 1986; Wilcox, 1993) while others omit this step (Singer *et al.*, 1986). In the present study, prehybridization was found to be imperative in reducing much of the background labelling that occurred. However, this step was only effective when a cold competitor incorporating a nonradioactive S-UTP was used. Other treatments, including prehybridization with buffer or nonsulfated probes, or using highly stringent wash and hybridization conditions did not reduce nonspecific binding. Acetylation, while decreasing the background slightly, especially in the brain region, was less effective than prehybridization with a cold competitor. These results indicate that high levels of background are associated with the ^{35}S label. This finding is consistent with other studies that have found high background to be the result of molecular interactions involving the highly active sulfur group on the nucleotide (Biroc *et al.*, 1993; McLaughlin and Margolskee, 1993). Reducing agents such as DTT and ß-mercaptoethanol are usually incorporated in hybridization solutions and washes to overcome the problem of oxidation (Lewis and Baldino, 1990; Biroc *et al.*, 1993), but

as we experienced, these reagents are not always effective. However, recent studies indicate that increasing the concentration of DTT from the standard 10mM to 200mM greatly diminishes the background (Dagerlind *et al.*, 1992; Miller *et al.*, 1993). Zeller *et al.* (1987) report success in blocking sulfhydryl groups that interact with the probe by incubating with sodium iodoacetamide and N-ethylmaleimide; this treatment did not reduce background in lamprey tissues in the present study and was subsequently omitted from the protocol.

Nonspecific binding of probe L1.8-156-3 was substantially increased when hybridization solutions included dextran sulfate, or when probe specific activities were greater than 9 x 10^4cpm/µl. Neither prehybridization nor increasing the stringency improved background levels under these circumstances. High levels of nonspecific binding associated with dextran sulfate are well documented (Coghlan *et al.*, 1984; Hoefler *et al.*, 1986). The disadvantage of loss of sensitivity was weighed against the advantage of shorter exposure times required and we subsequently omitted dextran sulfate from all hybridization solutions. While probe L1.8-156-3 of specific activity of 3-9 x 10^4cpm/µl was sensitive enough to detect lamprin mRNA in all developmental stages examined, higher specific activity may be required to detect lower levels of expression. To overcome the problem of ^{35}S-related background, several groups recommend using ^{33}P as an alternate label. Probes labelled with this isotope can be used at higher specific activities than ^{35}S-labelled probes without creating high background levels or compromising resolution (Biroc *et al.*, 1993; McLaughlin and Margolskee, 1993). While ^{35}S is more cost efficient and proved

effective as a label in the present study, further investigations into the advantages of using probes labelled with ^{33}P to study chondrogenesis in the lamprey are warranted.

Our observations that brain tissue demonstrated higher levels of background concur with the findings by Jordan (1990) who suggests that in neural tissues nonspecific labelling is the result of electrostatic interactions between the probe and the myelin (lipid). While lamprey nervous tissues lack myelin (Rovainen, 1982), the reduction in nonspecific background observed over the brain in acetylated tissues, indicates that electrostatic interactions contribute to the background. Another explanation for higher levels of background labelling in this area may be that cross-hybridizations between the probe and nucleic acids present in the brain tissue occur. Dokas (1983), and Chaudari and Hann (1983) report that the brain expresses the highest diversity of genes. Such diversity increases the potential for nucleic acids present in the brain to share homologous regions with the probe. However, the high level of stringency used in this study should have prevented formation of imperfect hybrids.

The L1.8-156-3 probe used in this study was unable to detect lamprin expression in branchial cartilage in prolarval to adult stages, or in pericardial cartilage in late metamorphic to adult stages. Ultrastructural examination has demonstrated the presence of lamprin-like fibrils in both of these cartilages (Wright *et al.*, 1988). The inability of the probe to detect lamprin mRNA in these tissues may suggest a lack of lamprin transcripts within the cell during the developmental period examined. An alternative explanation is that lamprin is the translation product of multiple messages

that are differentially expressed in lamprey cartilages. Robson *et al.* (1993) have recently identified several isoforms of the lamprin protein that differ in size (10kDa and 12kDa) and amino acid sequence, and three mRNAs (two 0.9kb and one 1.8 kb long). The probe used in the present study was transcribed from a nonhomologous region of the cDNA corresponding to the larger message and would be ineffective in detecting the presence of the 0.9kb message. Further analysis of lamprin branchial and pericardial cartilages is needed to determine matrix expression patterns in these tissues.

In summary, several aspects of the ISH procedure were optimized to achieve good signal to noise ratio when using ^{35}S-labelled lamprin riboprobes on lamprey tissues. Fixation periods of 30 minutes with 4% PFA provided adequate retention of morphology without sacrificing the intensity of the hybridization signal. Proteolytic digestion of lamprey tissues fixed with 4% PFA was avoided since it created high levels of nonspecific labelling. Pre-hybridization with a probe incorporating a nonradioactive S-UTP was found to be imperative in reducing background due to nonspecific binding of the sulfur group. Following these pretreatment steps, hybridization using a 156bp riboprobe with a specific activity of 4-9 x 10^4cpm/µl for 16-22 hours at 45^{0}C enabled detection of lamprin expression in all neurocranial cartilages following 5-11 days exposure. Under these conditions the ISH procedure applied to lamprey tissues is a specific and versatile technique. The ISH technique has a wide variety of applications for future studies which may further our

understanding of chondrogen . mechanisms such as the temporal and spatial distribution of cartilaginous components during embryogenesis.

4. SPATIAL AND TEMPORAL DISTRIBUTION OF LAMPRIN mRNA DURING CHONDROGENESIS IN THE LAMPREY: EXPRESSION IN A NONCOLLAGENOUS-BASED CARTILAGE

4.1. INTRODUCTION

Cartilage is a specialized form of connective tissue in which cells are interdispersed in a large quantity of ECM. Structural and functional properties of cartilage are determined by the molecular composition of the matrix. Tensile strength of cartilage is imparted by a predominantly collagenous, fibrillar component while resiliency results from large complexes of the cartilage proteoglycan monomer (aggrecan), link protein and hyaluronic acid (Stockwell, 1979; Hay, 1991). Elastic cartilage, in addition to the collagenous and proteoglycan component, contains elastic fibers which contribute to greater flexibility of this tissue (Bloom and Fawcett, 1994). Recent biochemical and molecular examination of cartilage matrix has demonstrated a variety of other minor components including small proteoglycans such as anchorin, decorin, fibromodulin and biglycan; glycoproteins such as fibronectin, tenascin and chondronectin; growth factors such as TGF-ß and hormones (for reviews on structure and function see Elmer, 1983; Lash and Vasan, 1983; Sandberg, 1991; Wight *et al.*, 1992; Juliano and Haskill, 1993; Yanagishita, 1993; Roughley and Lee, 1994). These molecules serve a variety of functions such as mediating attachment of chondrocytes to the matrix, modulating collagen fibrillogenesis and inducing cartilage differentiation.

In the collagenous-based cartilages of higher vertebrates the meshwork of fibers in the matrix serve as a scaffolding to which proteoglycans can attach. The characteristic collagenous fibril of most higher vertebrate cartilages is an assembly of parallel type II collagen molecules arranged around a core of type XI collagen and covalently crosslinked by surface-bound type IX collagen (van der Rest and Mayne, 1988; Bruckner and van der Rest, 1994). In many cartilages, cartilage matrix protein (CMP) bridges two individual type II collagen molecules by binding to their ends (Winterbottom *et al.*, 1992). Six other minor collagens, types I, III, V, VI, X and XIII have been identified in cartilage tissue (for reviews see Mayne and von der Mark, 1983; Sandberg, 1991; Bruckner and van der Rest, 1994). The proportion of these latter collagens present in the matrix is dependent upon the species, cartilage type, and developmental stage.

During chondrogenesis, expression of cartilage matrix components switches from molecules involved in mesenchymal differentiation to those which control assembly and organization of a matrix characteristic of the cartilage phenotype. For example, expression of collagen type I and fibronectin is downregulated (Dessau *et al.*, 1980) while collagen type II synthesis is rapidly upregulated (Kosher *et al.*, 1986b; Mallein-Gerin *et al.*, 1988; Swalla *et al.*, 1988) and co-expressed with type IX collagen (Castagnola *et al.*, 1988; Swiderski and Solursh, 1992b). In elastic cartilage, the fibrillar component of the elastic fiber is first detected concomitant with collagen type II and is followed by appearance of the amorphous component, elastin (Kostovic-Knezevic *et al.*, 1986; Lee *et al.*, 1994). As matrix synthesis continues, the cartilage

cells become more isolated from one another. In cartilage that is destined to be replaced by endochondral bone, expression of collagen type II decreases and collagen type I reappears. Collagen X is expressed in hypertrophic cartilage cells (Gibson and Flint, 1985; Schmid and Linsenmayer, 1985; Castagnola *et al.*, 1987) and is thought to form an association with preexisting type II and type IX collagen fibrils (Linsenmayer *et al.*, 1991).

In contrast to the vast amount of information available concerning the complex interaction between matrix and cells during differentiation, development, and growth in collagenous-based vertebrate cartilages, relatively little is known about these relationships in the noncollagenous-based cartilages of the lamprey, a vertebrate with an ancient evolutionary history (Janvier, 1981). Of five collagens known to occur in lamprey tissues only three, corresponding to types II, V and XI, are similar to those of mammalian tissues (Kimura and Kamimura, 1982; Eikenberry *et al.*, 1984; Sheren *et al.*, 1986; Brodsky *et al.*, 1994). Amino acid analysis indicates that collagen comprises a small portion, less than 10% dry weight, of lamprey cartilage (Wright *et al.*, 1983). Collagen type II is the major structural fibril in the lamprey notochord sheath (Eikenberry *et al.*, 1984; Brodsky *et al.*, 1994) and was suggested by Armstrong *et al.* (1987) to be the 20nm fibrils present in developing piston cartilage of metamorphic lamprey. However, type II collagen fibrils are not discernible ultrastructurally in adult lamprey cartilages (Wright and Youson, 1983; Wright *et al.*, 1988). Rather than collagen, lamprin is the principal structural protein in lamprey cartilage (Wright *et al.*, 1983; Robson *et al.*, 1993).

Armstrong *et al.* (1987), examined the transformation of mucocartilage, a loose connective tissue, into piston cartilage during metamorphosis and described ultrastructural features of the deposition of extracellular matrix. No comparable information is available for developing cartilage in lamprey embryonic or prolarval stages. Furthermore, the role that lamprin plays in chondrogenesis and chondrocyte in any developmental interval remains to be elucidated. This study reports the temporal and spatial distribution of lamprin expression in the trabecular cartilage of the anadromous sea lamprey, *Petromyzon marinus*, during early developmental stages. Comparisons are made of the expression patterns of this structural protein with those found in collagenous-based cartilages of higher vertebrates during chondrogenesis.

4.2. MATERIALS AND METHODS

The materials and protocols used in this study have been previously described in Chapters 2 and 3. In brief, 4 to 10 prolarvae per day were sampled daily between day 17pf (stage 17:early burrowing) and day 33pf (stage18:larval), with the omission of days 29 and 30pf (stage 17:late burrowing) (total of 60). Lampreys were anesthetized in 0.05% tricaine methanesulfonate (MS-222), fixed for 30 minutes in PFA and processed routinely as for LM. Pretreatment for ISH lacked proteolytic digestion and included exposure to 0.25% acetic anhydride in 1.9% triethanolamine (TEA) buffer, pH 8.0, for two 5-minute changes to block nonspecific binding sites created by electrostatic interaction between the probe and basic protein groups. Tissue sections were pre-hybridized with a cold competitor incorporating a

nonradioactive S-UTP and vector sequences (pGEM-4), for 1 hour prior to hybridization with a 156bp riboprobe (L1.8-156-3; specific activity $6x10^4$ - $2.5x10^5$ cpm/µl) for 16-22 hours at 45^0C. Tissues were then washed and treated as described previously. Visualization of the signal was by emulsion autoradiography using Kodak NTB-2 emulsion (Eastman Kodak Company, Rochester, NY). Exposure times ranged from 5-11 days. Slides were stained with Mayer's hematoxylin according to Baserga and Malmund (1969) before dehydration and coverslipping.

Three sets of controls were used in this study: 1) hybridization with sense riboprobes; 2) hybridization with riboprobes transcribed using pGEM-4 sequences without the cDNA insert and 3) digestion of tissue sections with 50µg/ml RNase I "A" (Pharmacia, Dorval, Quebec, Canada) in RNase buffer (5M NaCl, 0.5M EDTA, 2M Tris-HCl pH 8.0) for 1 hour at 37^0C prior to hybridization. Whenever possible, adjacent sections were used for control and test treatments.

4.3. RESULTS

4.3.1. General morphology

In prolarval stages of the lamprey, the paired trabeculae were oval, rod-shaped cartilages with tapered ends that lay ventrolateral to the brain and ventromedial to the eye (see Figure 1.1; Figure 2.1). By day 33pf, they extended from between the rostral limits of the otic capsules, to a point just rostral to the eye (see Figure 2.3E). In the larval stage the two trabeculae unite rostrally via the trabecular commissure (Damas, 1944, Johnels, 1948; Hardisty 1981), but this unification was not observed

to occur during prolarval stages. The thickest cross-sectional area of the prolarval trabeculae was located in the same dorsoventral plane as the central region of the eye. In this area, the precartilage condensation and later the nascent cartilage were found to be the most developmentally advanced with respect to number of cells comprising condensation, stage of cellular differentiation and quantity of cartilaginous ECM. The trabeculae were progressively less developed in more distal locations. Because of this spatial variability, comparisons between degrees of lamprin mRNA expression and morphology of the cartilage were made using cross-sections that contained the central region of the eye.

4.3.2. Light microscopy of Toluidine-blue sections

By day 17pf condensing mesenchymal cells were observed ventrolateral to the brain in regions corresponding to the future location of the paired trabecular cartilages (Figure 2.8A). One condensation formed for each cartilaginous rod. Several closely apposed cells formed a focal point or core around which more flattened mesenchymal cells became circumferentially arranged. Each condensation was closely associated with the buccal epithelium and the corresponding carotid artery. Dorsally the condensations were separated from the eye by a band of tightly packed cells whose cytoplasm was filled with lipid and oval to marquise shaped yolk globules. By day 18pf the pretrabecular cells formed distinct condensations of closely apposed oval to round cells exhibiting a high nucleo-cytoplasmic ratio. The condensations occupied the entire space between the brain and the buccal epithelium

and often created a bulge of the buccal epithelium into the buccal cavity (Figure 4.1A). Condensations of day 19pf lamprey appeared similar (Figure 4.1B). By day 20-22pf the cells were separated by thin rims of homogenous ECM material (Figure 4.1C). The now distinguishable chondrocytes displayed very light staining cytoplasm and small, central nuclei.

4.3.3. *In situ* hybridization

Weak hybridization signals, visualized as dense accumulations, often clusters, of silver grains were first detected over nuclei of cells in the trabecular region in 5 of 10 day 19pf lampreys examined (Figure 4.2B). The signal was localized in the central region of the differentiating cartilage nodule. When the probe was used at higher specific activity, nonspecific hybridization was observed as an even dispersion of silver grains over nuclei and cytoplasm especially over neural tissue and pigmented cells.

By day 20pf, mRNA expression of the lamprin gene was observed in all specimens examined (Figure 4.2C). Hybridization signals occurred in all remaining stages examined up to day 33pf (Figure 4.2D-E). Hybridization signal intensity appeared to increase parallel to matrix synthesis (Figure 4.2A-E). The most intense hybridization signal was localized over the region of the trabecular cartilage adjacent to the central region of the eye. The intensity of hybridization signal appeared to decrease over the cartilaginous tissue progressively decreased in sections taken more rostrally and caudally to this region.

Figure 4.1. T-blue sections (0.5μm) of day 18pf (A), day 19pf (B) and day 22pf (C) prolarvae. While no intracellular space is discernable between the tightly packed cells of the condensations (arrowheads) in A and B, thin seams of ECM (arrowhead) can be seen to separate the cells of the trabecular cartilage in C. Eye (Ey), Notochord (N), Brain (Br) A= X 190; B= X 170; C= X 190.


A
B
N
C
N

Figure 4.2. Positive *in situ* hybridization signals were visualized as dense grains over the nuclei of the trabeculae (arrowheads) in day 19pf (B), day 20pf (C), and day 22pf (D) and day 33pf (E) prolarvae. Note the progressive increase in hybridization signal with age. No hybridization signal was observed in day 18pf prolarvae hybridized with antisense probe (A) or day 31pf prolarvae hybridized with sense probe (F). Eye (Ey), Eye pigment (arrows), Notochord (N), Brain (Br). A= X 80; B= X 70; C, D = X 90; E= X 75; F= X 90.

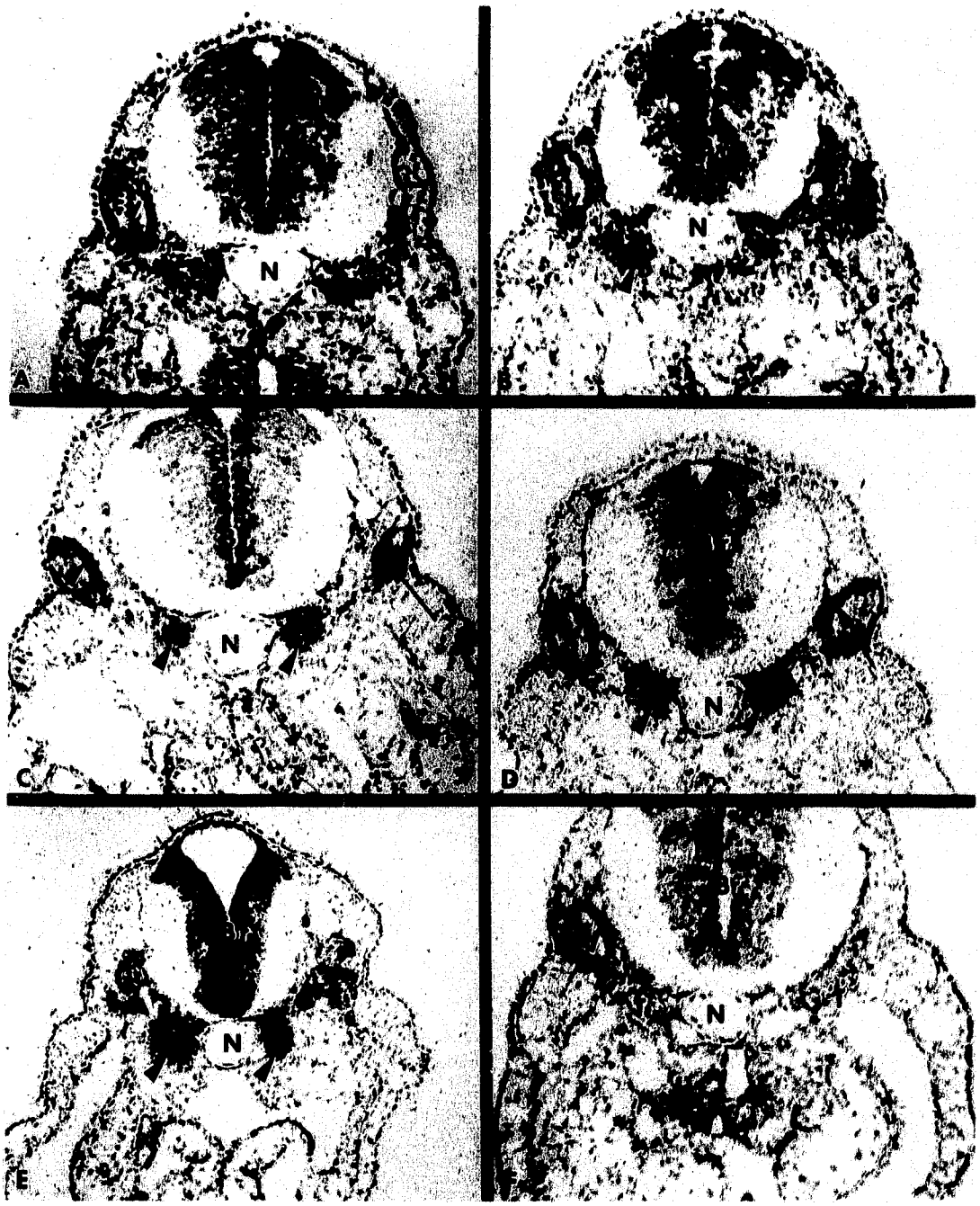
N
A
N
B
N
C
N
D
N
E
N
F

No hybridization signal was detectable in day 17pf and 18pf (Figure 4.2A), in any adjacent tissue sections that had been treated with RNase prior to hybridization, in sections hybridized with antisense probes containing only vector sequences, or in those hybridized with sense probes (Figure 4.2F).

4.4. DISCUSSION

Developing trabecular cartilage of the sea lamprey, *Petromyzon marinus*, was examined by *in situ* hybridization to define temporal and spatial localization of mRNA transcripts for lamprin, a unique matrix structural protein of lamprey cartilage. Lamprin transcripts were first detected by ISH in the trabecular cartilage by day 19pf. After day 19pf, the spatial and temporal pattern of lamprin expression paralleled that of cartilage differentiation and matrix accumulation.

The first appearance of lamprin transcripts by day 19pf correlates with ultrastructural examinations which demonstrate an increase in spaces between cells of the condensation (Chapter 2). In other vertebrates the spreading apart of these cells occurs as matrix accumulates within the extracellular space (Thorogood and Hinchcliffe, 1975; Ede, 1983). A positive association between matrix deposition and decrease in cellular density in lamprey prechondrogenic condensations is further supported by ultrastructural examinations which demonstrate the occurrence of lamprin-like fibrils in the ECM during day 19pf (see Chapter 2). Thin seams of matrix were distinguishable at the light microscopic level between chondrocytes by day 20pf.

Spatial localization of lamprin transcripts demonstrates an uneven distribution throughout developing trabecular cartilage. Intensity of hybridization signal was highest in the central core of the developing cartilage located adjacent to the eye and progressively weaker in rostral and caudal regions. In part, intensity of signal in the central core resulted from occurrence of more cells expressing transcripts. Cartilage differentiation begins at a central point and extends rostrally and caudally as differentiation progresses creating a rod shaped cartilage that is widest in diameter centrally and tapers toward each end. The spatial pattern of lamprin expression parallels the process of differentiation and matrix synthesis as described in Chapter 2. Similar distribution patterns are well documented for mRNAs of cartilage aggrecan core protein, link protein, cartilage matrix protein and collagen type II in the chick wing (Kosher *et al.*, 1986a,b; Stirpe and Goetinck, 1989; Mundlos and Zabel, 1994) and link protein and cartilage proteoglycan core protein in the human limb (Mundlos *et al.*, 1991).

Lamprin transcripts were not preferentially localized over chondrocytes within a particular region of the cross-sectional diameter of the cartilage. However, the perichondrium lacked signal. This differs from that of the limb bud in which expression is highest on the periphery where perichondrial cells are differentiating into chondrocytes. As centrally located chondrocytes of the limb bud become isolated within self-synthesized matrix they decrease matrix synthesis and rate of transcription. In the lamprey embryo such spatial patterning was not detected since few or none of the central cells had begun to hypertrophy (see Chapter 2).

The temporal pattern of lamprin expression was similar to that described for other cartilage structural proteins but there were significant differences. Once upregulation of the lamprin gene occurred, expression of transcripts appeared to increased progressively, paralleling matrix accumulation. Comparable expression patterns are reported for collagen type II mRNA in embryonic chick limb bud (Kravis and Upholt, 1985) and wing bud (Kosher *et al.*, 1986b). Progressive increase in hybridization signal intensity with age may be accounted for by an increase in transcription. This may be caused by upregulation within individual cells and/or increase in number of transcribing cells, or by stability of the lamprin message. While ISH can not ascertain which of these mechanisms is in effect, it seems likely that increase in transcription would be the major influence in early developmental stages of cartilage. In a recent examination of lamprin expression in metamorphic and adult (parasitic and upstream migrant) stages (see Chapter 3), the hybridization signal was of greatest intensity in the upstream migrant. The occurrence of stronger signals in the upstream migrant is especially intriguing since many of its systems undergo atrophy in an effort to direct all available energy towards the reproductive system (Larsen, 1980). These findings suggest that remodelling, growth and repair requirements dictate the necessity of continual "steady-state" transcription of lamprin at a high level even in the latter stages of the life cycle. However, preliminary Northern blot analyses of expression levels in larval, metamorphic and spawning stages of the lamprey seem to indicate an actual upregulation of the lamprin gene expression during spawning stages (P. Robson, personal communication). The

possibility exists that factors which influence the initiation of the upstream migrant stage may also influence the transcription of the lamprin gene. Further quantitative analyses of lamprin expression during these later developmental stages are required to fully appreciate patterns of lamprin transcription during this stage of the lamprey life cycle.

Lamprin mRNA expression is first detected during day 19pf coincident with the latter phases of the condensation stage and the commencement of lamprin synthesis. These results are similar to those reported for collagen type X (Castagnola *et al.*, 1987; Lisenmayer *et al.*, 1991), collagen type IX (Lisenmayer *et al.*, 1991; Swiderski and Solursh, 1992a,b), and cartilage proteoglycan (aggrecan) core protein (Kosher *et al.*, 1986b; Mallein-Gerin *et al.*, 1988). The expression patterns of the mRNA for these proteins and lamprin suggest a transcriptional regulatory mechanism of gene control. Similar pretranslational control mechanisms are assumed for the elastin gene (Rosenbloom *et al.*, 1991). In contrast, type I collagen synthesis is regulated at the translational level (Focht and Adams, 1984; Kosher *et al.*, 1986b; Castagnola *et al.*, 1988). The temporal pattern of expression of lamprin mRNA suggests that transcription of this gene does not play a role in inducing cartilage differentiation but rather is itself activated by chondrogenic events. While the initiator of chondrogenesis has not been elucidated, a variety of phenomena are coincident with the condensation stage and have been shown to play a role in chondrocyte differentiation in higher vertebrates. These include cell-matrix interactions (Oster *et al.*, 1985; Frenz *et al.*, 1989, Sandberg, 1991) cell-cell contact (Solursh, 1983, Coelho

and Kosher, 1991; Oberlender and Tuan, 1994), changes in cell shape (Archer *et al.*, 1982; Zanetti and Solursh, 1984), elevation in cAMP (Solursh *et al.*, 1979) and presence of hormones and growth factors (Chai *et al.*, 1994). Investigations on the regulatory region of the lamprin gene are taking place in our laboratories and will assist in furthering our knowledge of factors controlling lamprin mRNA transcription.

In contrast to the pattern of lamprin mRNA expression, low levels of collagen type II mRNA are reported to be detectable in prechondrogenic mesenchyme prior to condensation in collagenous-based cartilages of higher vertebrates. In chick wing bud, condensation occurs by stage 22 while mRNA transcripts are detectable as early as stage 18/19 (Kosher *et al.*, 1986b). In chick limb bud, collagen mRNA is detectable by stage 16 (Kravis and Upholt, 1985; Swalla *et al.*, 1988). Failure to localize lamprin transcripts prior to day 19pf may be due to the inability of the ^{35}S-probe to detect weak signals above nonspecific background associated with this isotope (Biroc *et al.*, 1993; McLaughlin and Margolskee, 1993). However, since the minimum time from transcription to translation is short, the suggestion of rapid synthesis of lamprin following upregulation of the gene is quite plausible. The regulatory mechanism for collagen type II is suggested to occur at the transcriptional level since a rapid increase in mRNA transcripts occurs coincident with the onset of chondrogenesis (Kravis and Upholt, 1985; Kosher *et al.*, 1986b; Swalla *et al.*, 1988; Stirpe and Goetinck, 1989; Swiderski and Solursh, 1992a). Detection of the protein does not coincide with appearance of the mRNA transcripts, however, suggesting occurrence of further post-transcriptional or translational regulation (Kosher *et al.*,

1986b). Widespread localization of collagen type II in prechondrogenic mesenchyme has also led to the hypothesis that collagen type II may be a causative agent in chondrogenesis (Thorogood *et al.*, 1986; Kosher and Solursh, 1989).

Recent biochemical and molecular examination of the annular cartilage of adult lamprey has revealed the existence of at least two isoforms of the lamprin protein that differ in size (10kDa and 12kDa) and amino acid sequence, and three mRNAs (two 0.9kb and one 1.8 kb) (Robson *et al.*, 1993). While Northern blots have indicated the presence of both of these messages in annular cartilage, previous ISH analyses indicate that the largest size of mRNA is not localized in branchial and pericardial cartilage (see Chapter 2). This supports the hypothesis of Robson *et al.* (1993) that production of lamprin isoforms is in part controlled by multiple genes and further demonstrates that these genes may be differentially located in specific cartilages. This aspect of lamprin regulation is similar to that for other structural proteins. Currently 15 different collagens are known (Lisenmayer, 1991). These demonstrate specific spatial distributions and are encoded by at least 25 genes (Sandberg, 1991; Lisenmayer, 1991). Elastin regulation differs however, since this structural protein is encoded by only one gene (Rosenbloom *et al.*, 1991).

The two smaller size messages for lamprin differ by one exon which suggests alternate splicing as a second means of regulation (Robson *et al.*, 1993). Alternate splicing is a common phenomenon within genes encoding ECM proteins and creates multiple forms of proteins which have different potential functions (Boyd *et al.*, 1993). It has been suggested that in chondrogenic tissues, these matrix isoforms may play

differential roles in controlling the stage of cartilage differentiation (Swiderski and Solursh, 1992a). This mechanism of gene regulation is a well defined feature of the elastin gene (Indik *et al.*, 1989; Yeh *et al.*, 1989; Rosenbloom *et al.*, 1991). An exceptionally high intron to exon ratio is reported for this gene and it is suspected that not all of the isoforms of tropoelastin are of functional significance (Boyd *et al.*, 1993). Of the two forms of type IX collagen the short form is expressed in nonchondrogenic tissue while the long form is expressed temporally and spatially with type II collagen (Swiderski and Solursh, 1992). Recently, two isoforms of collagen type II transcripts, type IIA and type IIB, also resulting from alternative spicing, have been identified (Ryan and Sandell, 1990; Nah and Upholt, 1991). Type IIA is produced only by cartilage precursor cells while the latter is produced by differentiated chondrocytes (Su *et al.*, 1991; Sandell *et al.*, 1991, 1994). It would be interesting to determine in future studies if either of the lamprey 0.9 mRNAs for lamprin are expressed in trabecular cartilage and if they are differentially expressed in prechondrogenic or chondrogenic tissues.

In summary, patterns of temporal and spatial expression of lamprin mRNA in developing trabecular cartilage exhibit similarities to those of collagen and elastin. Similar to these proteins, lamprin expression is upregulated concomitant with the mesenchymal condensation stage and is regulated at the transcriptional level. Unlike collagen type II expression, low levels of lamprin transcripts are not detected prior to upregulation. Once the lamprin gene is upregulated, the spatial and temporal pattern of transcript expression parallels that of cartilage differentiation and matrix

accumulation. The principal structural proteins of cartilage matrix play an essential role in developmental events leading to the production of a highly intricate and functional matrix. It follows that certain aspects of the patterns of expression of these molecules are critical and must be conserved throughout the vertebrates. Such overlap in molecular and biochemical characteristics also suggests the possibility of a close relationship between elastin, collagen and lamprin. Further studies are required to determine co-expression patterns of other matrix components of lamprey cartilage and regulatory mechanisms of the lamprin gene. Such information will further assist in elucidating the position of lamprin in the evolution of structural proteins in higher vertebrates.

5. GENERAL DISCUSSION

5.1. RATIONALE

The principal objective of this work was to provide an ultrastructural and molecular examination of chondrogenesis of the trabecular cartilage during prolarval stages of the sea lamprey, *Petromyzon marinus*. This work represents the first such study of chondrogenesis in the prolarval stages of the lamprey. The rationale for this study was twofold. First, information gained from such an investigation could enlighten our understanding of the evolution of skeletal tissues in among vertebrates. Lampreys are the most ancient of the vertebrates and possess a non-collagenous based cartilage. In all lamprey cartilages that have been examined biochemically to date, lamprin, rather than collagen or elastin, has been found to be the principal structural protein. While lamprin is similar to elastin and collagen in certain biochemical, morphological and functional aspects, the interrelationships between these proteins have yet to be elucidated. The second rationale for examining spatial and temporal expression patterns of lamprin is that such information will assist in the use of lamprin as a "reporter protein" in elucidating factor(s) that initiate lamprey metamorphosis. Such knowledge can be valuable in developing means for controlling the problem of lamprey parasitism.

5.2. TECHNICAL CONSIDERATIONS

As part of this investigation two technical issues had to be addressed. The first and foremost was obtaining lamprey embryos. Raising prolarval lamprey under constant, idealized laboratory conditions reduces the number of possible variables that could affect developmental rates, and enables the collection of a large number of embryos of a similar developmental stage. Several studies in the literature are concerned with utilizing a variety of techniques in obtaining the gametes from adults and subsequently raising the embryos. Piavis (1961) surgically removed gametes from adult lampreys, but this method of collection has inherent problems, including the obtaining large number of immature gametes (for discussion see Langille and Hall, 1988a). Langille and Hall (1988a) report success with rearing embryos in a closed-water system, but we have experienced a great deal of difficulty with fungal infections using these systems. The methods used in this study enabled us to collect a large number of specimens at similar stages of development and correlate the spatial and temporal development of the skeletal elements with currently accepted staging of Piavis (1961, 1971).

The second technical consideration was the optimization of current protocols for *in situ* hybridization for the detection of lamprin mRNA. Sensitivity and specificity of *in situ* hybridization analysis is tissue and species dependent and is affected by several variables including probe characteristics, fixation, treatment with proteolytic enzymes and a variety of blocking agents, and hybridization and washing conditions.

5.3. SUMMARY

1. The trabecular cartilages form during early phases of the burrowing stage of the lamprey and are likely critical for support of the brain as the prolarva assumes burrowing behaviour.

2. The trabecular cartilages originate in a population of densely packed yolk-laden mesenchymal cells that are dissimilar from prechondrogenic mesenchymal cells described for higher vertebrate systems (such as the developing limb). These cells in lampreys may be neural crest-derived mesenchymal cells of a distinctive appearance.

3. Chondrogenesis of lamprey trabecular cartilage commences with formation of mesenchymal condensations, ventromedial to the eye, by day 17pf and follows a series of events similar to that of developing piston cartilage in lamprey metamorphic stages and of all precartilaginous models in endochondral bone (with the exception of the cervical vertebral column) reported for higher vertebrates.

4. While collagen has not been previously identified as a component of adult trabecular cartilage, a 20nm distinctly banded fibril, presumably collagen, occurs within the mesenchyme prior to condensation formations and is found within the ECM of developing trabecular cartilages in the prolarva.

5. First appearance of ultrastructurally differentiated chondrocytes by day 19pf, is concomitant with first visualization of lamprin fibrils and the detection of lamprin mRNA transcripts. This temporal pattern of expression suggests a transcriptional regulatory mechanism for the lamprin gene.

6. The most developmentally advanced region of the nascent trabecular cartilage is in the same dorsoventral plane as the eye. Cartilage differentiation and lamprin expression initially progress in both rostral and caudal directions from this region. Lengthening of the trabecular cartilage is predominantly in the cranial direction and occurs by appositional growth.

7. In contrast to lamprin deposition in metamorphic piston matrix, lamprin in the trabecular cartilage initially occurs as discrete globules scattered throughout the matrix rather than being preferentially deposited over collagen fibrils. The lamprin globules subsequently aggregate into a branching format of fibrils and become organized into three matrix zones similar to those of trabecular cartilage matrix of the adult lamprey.

8. Lamprin mRNA occurs in all neurocranial cartilage in the prolarval, metamorphic and adult stages. Lamprin transcripts were not detected in pericardial and branchial cartilages and this may indicate differential expression of the two lamprin genes.

5.4 FUTURE STUDIES

To fully understand the chondrogenic mechanism in lampreys, future studies need to address a number of issues:

1) It would be interesting to determine the identity of the yolk-laden prechondrogenic mesenchymal cells. If they are neural crest cells that can be visually identified without the utilization of markers, the lamprey embryo would be a valuable model for future studies embryological studies on vertebrates.

2) It is imperative that we begin to identity the other components in lamprey cartilage matrix and determine their role in chondrogenesis and lamprin fibrillogenesis. For example, is the collagen fibril observed ultrastructurally in the matrix collagen type II? If so, is it playing a similar role as type II collagen in higher vertebrates, and how does it interact with lamprin ?

3) Cartilages, such as those of the branchial and pericardial, in which lamprin transcripts were not expressed need to be examined by *in situ* hybridization using probes complementary to the smaller mRNA to determine if lamprin mRNA is differentially expressed in various cartilages. In addition it would be useful to determine if the two alternatively spliced forms of the smaller lamprin message are differentially expressed during early developmental stages.

4) The lamprin gene needs to be examined to determine the regulatory mechanisms in place for this gene.

5) The expression patterns of lamprin mRNA in spontaneous and induced metamorphic lamprey need to be analyzed before any attempt can be made to use lamprin as a "reporter protein" in unravelling the mystery of metamorphosis.

6. REFERENCES

ABBOTT LA, LESTER SM, ERICKSON CA. Changes in mesenchymal cell-shape, matrix collagen and tenascin accompany bud formation in the early chick lung. Anat Embryol 1991; 183: 299-311.

ANDERSON DR. The ultrastructure of elastic and hyaline cartilage of the rat. Am J Anat 1964; 114: 403-434.

ARCHER CW, ROONEY P, WOLPERT L. Cell shape and cartilage differentiation of early chick limb bud cells in culture. Cell Diff 1982; 11: 245-251.

ARMSTRONG LA, WRIGHT GM, YOUSON JH. Transformation of mucocartilage to a definite cartilage during metamorphosis in the sea lamprey, *Petromyzon marinus.* J Morphol 1987; 194: 1-21.

BASERGA R, MALMUND D. Modern Methods in Experimental Pathology. Autoradiography: Techniques and Applications. New York: Harper and Row, 1969.

BEAMISH CJ. Biology of the Northe American sea lamprey, *Petromyzon marinus, Can J Fish Aquat Sci 1980; 37(11): 1924-1943.*

BENJAMIN M, EVANS EJ. Fibrocartilage. J Anat. 1990; 171: 1-15.

BERESFORD WA. Cranial skeletal tissues. In: Hanken J, Hall BK, eds. The Skull, vol 2. Patterns of Structural and Systemic Diversity. Chicago: University of Chicago Press, 1993.

BIROC SL, MURPHY-ERDOSH C, FISHER JM, PAYAN, DG. The use of ^{33}P-labelled oligonucleotides for in situ hybridization of vertebrate embryo frozen sections. Biotechniques 1993; 15(2): 250-254.

BLIECK A. At the origin of chordates. Geobios 1992; 25(1): 101-113.

BLOCH B, POPOVICI T, LE GUELLEC D, NORMAND E, CHOUHAM S, GUITTENY AF, BOHLEN P. *In situ* hybridization histochemistry for the analysis of gene expression in the endocrine and central nervous system tissues: a three year experience. J Neurosci Res 1986; 16: 183-200.

BLOOM W, FAWCETT DW. A Textbook of Histology. 12th ed. New York: Chapman and Hall, 1994.

BOYD CD, PIERCE RA, SCHWARZBAUER JE, DOEGE K, SANDELL LJ. Alternate exon usage is a commonly used mechanism for increasing coding diversity within genes coding for extracellular matrix proteins. Mat 1993; 13: 457-469.

BOYD GA. Autoradiography in Biology and Medicine. New York: Academic Press Inc., 1955.

BRIGATI DJ, MYERSON D, LEARY JJ, SPALHOLZ B, TRAVIS SZ, FONG CKY, HSIUNG GD, WARD DC. Detection of viral genomes in cultured cells and paraffin-embedded tissue sections using biotin-labelled hybridization probes. Virol 1983; 126: 32-50.

BRODSKY B, EIKENBERY EF. Supramolecular collagen assemblies. Ann NY Acad Sci 1985; 460: 73-84.

BRODSKY B, BELBRUNO KC, HARDT TA, EIKENBERRY EF. Collagen fibril structure in lamprey. J Mol Biol 1994; 242: 38-47.

BRONNER-FRASER ME. Neural crest cell formation and migration in the developing embryo. FASEB J 1994; 8(10): 699-721.

BRUCKNER P, VAN DER REST M. Structure and function of cartilage collagens. Microscopy Res Tech 1994; 28: 378-384.

CARLSON BM. Patten's Foundations of Embryology, 5th ed. Toronto: McGraw-Hill Publishing Company, 1988.

CASTAGNOLA P, TORELLA G, CANCEDDA R. Type X collagen synthesis by cultured chondrocytes derived from the permanent cartilaginous region of chick embryo sternum. Dev Biol 1987; 123: 332-337.

CASTAGNOLA P, DOZIN B, MORO G, CANCEDDA R. Changes in the expression of collagen genes show two stages in chondrocyte differentiation *in vitro*. J Cell Biol 1988; 106: 461-467.

CHAI Y, MAH A, CROHIN C, GROFF S, BRINGAS P Jr, LE T, SANTOS V, SLAVKIN HC. Specific transforming growth factor-ß subtypes regulate embryonic mouse Meckel's cartilage and tooth development. Dev Biol 1994; 162: 85-103.

CHAUDARI N, HANN WE. Genetic expression in the developing brain. SCI 1983; 220: 924-928.

COELHO CND, KOSHER RA. Gap junctional communication during limb cartilage differentiation. Dev Biol 1991; 144: 47-53.

COGHLAN JP, PENSCHOW JD, HUDSON PJ, NIALL HD. Hybridization histochemistry: use of recombinant DNA for tissue localization of specific mRNA populations. Clin Exp Hypertens 1984; A6(1&2): 63-78.

DAGERLIND A, FRIBERG K, BEAN AJ, HOKFELT T. Sensitive mRNA detection using unfixed tissue: combined radioactive and nonradioactive *in situ* hybridization histochemistry. Histochemis 1992; 98: 39.

DAMAS H. Contribution a l'etude de la metamorphose de la tete de la lamproie. Arch Biol 1935; 46: 171-227.

DAMAS H. Recherches sur le developpment de *Lampetra fluviatilis* L. Contribution a l'etudie de la cephalogenese des Vertebres. Arch Biol Paris 1944; 55: 1-284.

DE BEER GR. The differentiation of neural crest cells into visceral cartilages and odontoblasts in *Amblystoma*, and a re-examination of the germ-layer theory. Proc Roy Soc 1947; B134: 377-398.

DE BEER GR. The Development of the Vertebrate Skull. Oxford: University Press, 1971.

DESSAU W, VON DER MARK H, VON DER MARK K, FISCHER S. Changes in the patterns of collagens and fibronectin during limb-bud chondrogenesis. J Embryol Exp Morphol 1980; 57: 51-60.

DETWILER SR. Observations upon the migration of neural crest cells, and upon the development of the spinal ganglia and vertebral arches in *Amblystoma*. J Comp Neurol 1921; 33: 1-43.

DOKAS LA. Analysis of brain and pituitary RNA metabolism: A review of recent methodologies. Brain Res Rev 1983; 5: 177-218.

DYKSTRA MJ. A Manual of Applied Techniques for Biological Electron Microscopy. New York: Plenum Press, 1993.

EDE DA. Cellular condensations and chondrogenesis. In: Hall BK, ed. Cartilage, vol 2. Development, Differentiation and Growth. Toronto: Academic Press, 1983: 143-185.

EDE DA, FLINT OP. Cell movements and cell adhesion in the developing chick wing bud: studies on cultured mesenchyme cells from normal and *taipid*^{3} mutant embryos. J Cell Sci 1975; 18: 301-314.

EDE DA, WILBY OK. Golgi orientation and cell behaviour in the developing pattern of chondrogenic condensations in chick limb bud mesenchyme. Histochemis 1981; 13: 615-630.

EDE DA, FLINT OP, WILBY OK, COLQUHOUN P. The development of precartilage condensations in limb-bud mesenchyme of normal and mutant embryos *in vivo* and *in vitro*. In: Ede DA, Hinchcliffe, JR, Ball M., eds. Vertebrate Limb and Somite Morphogenesis. New York: Cambridge University Press, 1977: 161-179.

EISEN JS, WESTON JA. Development of the neural crest in the zebrafish. Dev Biol 1993; 159:50-59.

EISENSTEIN R, LARSON SE, SORGENTE N, KUETTNER KE. Collagen-proteoglycan relationships in epiphyseal cartilage. Am J Pathol 1973; 173: 443-456.

EIKENBERRY EF, CHILDS B, SHEREN SB, PARRY DAD, CRAIG AS, BRODSKY B. Crystalline fibril structure of type II collagen in lamprey notochord sheath. J Mol Biol 1984; 176: 261-277.

ELMER WA. Growth factors and cartilage. In: Hall BK, ed. Cartilage, vol 2. Development, Differentiation and Growth. Toronto: Academic Press, 1983: 369-397.

EPPERLEIN HH, LEHMANN R. Ectomesenchymal-endodermal interaction systems (EEIS) of *Triturus alpestris* is tissue culture. 2. Observations on differentiation of visceral cartilage. Differentia 1975; 4: 159-174.

ERICKSON CA, PERRIS R. The role of cell-cell and cell-matrix interactions in the morphogenesis of the neural crest. Dev Biol 1993: 159: 60-74.

EVANS HE, CHRISTENSEN GC. Anatomy of the Dog, 2nd ed. Toronto: W.B. Saunders and Company, 1979.

FAVRE D. Improved phenol-based method for the isolation of DNA fragments from low melting temperature agarose gels. Biotechnique 1992; 13(1): 24-26.

FELL HB. The histogenesis of cartilage and bone in the long bones of the embryonic fowl. J Morphol Physiol 1925; 40: 417-459.

FELL HB, CANTI RG. Experiments on the development *in vitro* of the avian knee joint. Proc R Soc London S B; 1934; 166: 316-351.

FOCHT RJ, ADAMS SL. Tissue specificity of type I collagen gene expression is determined at both the transcriptional and posttranscriptional levels. Mol Cell Biol 1984; 4: 1843-1852.

FOREY P, JANVIER P. Agnathans and the origin of jawed vertebrates. Nature Mag 1993; 361: 129-134.

FRENZ DA, JAIKARIA NS, NEWMAN SA. The mechanism of precartilage mesenchymal condensation: a major role for interaction of the cell surface with the amino-terminal heparin-binding domain of fibronectin. Dev Biol 1989; 136: 97-103.

GIBSON GJ, FLINT MH. Type X collagen synthesis by chicken sternal cartilage and its relationship to endochondral development. J Cell Biol 1985; 101: 277-284.

GODMAN GC, PORTER KR. Chondrogenesis studied with the electron microscope. J Biophys Biochem Cytol 1960; 8: 719-760.

GOEL SC. Electron microscopic studies on developing cartilage. J Embryol Exp Morphol 1970; 23(1): 169-184.

GOETINCK PF, STIRPE NS, TSONIS PA, CARLONE D. The tandomly repeated sequences of cartilage link protein contain the sites for interaction with hyaluronic acid. J Cell Biol 1987; 105: 2403-2408.

GOULD RP, DAY A, WOLPERT L. Mesenchymal condensations and cell contact in early morphogenesis of the chick limb. Exp Cell Res 1972; 72: 325-336.

GRAVESON AC, ARMSTRONG JB. Differentiation of cartilage from cranial neural crest in the axolotl (*Ambystoma mexicanum*). Differentia 1987; 35: 16-20

GROVER J, ROUGHLEY PJ. Versican gene expression in human articular cartilage and comparison of mRNA splicing variation with aggrecan. Biochem J 1993; 291: 361-367.

HALE LJ. Mitotic activity during the early skeletal differentiation of the scleral bones in the chick. Quart J Microsc Sci 1956; 97: 355-368.

HALL BK. Chondrogenesis of the Somatic Mesoderm. New York: Springer-Verlag Berlin Heidelberg, 1977.

HALL BK. Developmental and Cellular Skeletal Biology. New York: Academic Press, 1978.

HALL BK. Tissue interactions and chondrogenesis. In: Hall BK, ed. Cartilage. vol 2. Development, Differentiation and Growth. Toronto: Academic Press, 1983a: 187-222.

HALL BK. Epithelial-mesenchymal interactions in cartilage and bone development. In: Sawyer RH, Fallon JF, eds. Epithelial-Mesenchymal Interactions in Development. New York: Praeger 1983b: 189-214.

HALL BK, HORSTADIUS S. The Neural Crest. Oxford: Oxford University Press, 1988.

HALL BK, MIYAKE T. The membranous skeleton: the role of cell condensations in vertebrate skeletogenesis. Anat Embryol (Berlin) 1992; 186: 107-124.

HANKEN J, KLYMKOWSKY MW, SUMMERS CH, SEUFERT DW, INGEBRIGTSEN N. Cranial ontogeny in the direct-developing frog, *Eleutherodactylus coqui* (Anura: Leptodactylidae), analyzed using whole-mount immunohistochemistry. J Morphol 1992; 211: 95-118.

HARDINGHAM, FUSANG AJ, DUDHIA J. The structure, function and turnover of aggrecan, the large aggregating proteoglycan from cartilage. Eur J Clin Chem Clin Biochem 1994; 32: 249-257.

HARDISTY MW. Biology of the Cyclostomes. London: Chapman and Hall, 1979.

HARDISTY MW. The skeleton. In: Hardisty MW, Potter, IC, eds. The Biology of Lampreys, vol 3. London: Academic Press, 1981: 333-376.

HARDISTY MW, POTTER IC. The behaviour, ecology and growth of larval lampreys. In: Hardisty MW, Potter IC, eds. The Biology of Lampreys, vol 1. London: Academic Press, 1971: 85-125.

HARPER ME, MARSELLE LM. RNA detection and localization in cells and tissue sections by *in situ* hybridization of ^{35}S-labelled RNA. Methods Enzymol 1987; 151: 539-551.

HASCALL GK. Ultrastructure of the chondrocytes and extracellular matrix of the rat chondrosarcoma. Anat Rec 1980; 198: 135-146.

HASCALL VC, HEINEGARD DK, WIGHT TN. Proteoglycans: metabolism and pathology. In: Hay ED, ed. Cell Biology of Extracellular Matrix, 2nd ed. New York: Plenum Press, 1991: 149-176.

HAY ED. Collagen and other matrix glycoproteins in embryogenesis. In: Hay ED, ed. Cell Biology of Extracellular Matrix, 2nd. ed. New York: Plenum Press, 1991: 419-462.

HAYASHI M, NINOMIYA Y, PARSONS J, HAYASHI K, OLSEN BR, TRELSTAD RL. Differential localization of mRNAs of collagen types I and II in chick fibroblasts, chondrocytes, and corneal cells by *in situ* hybridization using cDNA probes. J Cell Biol 1986; 102: 2302-2309.

HEUSER CH, STREETER GL. Early stages in the development of the pig embryos, from the period of initial cleavage to the time of the appearance of limb buds. Carnegie Cont to Emb. 1929; 20: 1-29.

HILDEBRAND M. Analysis of Vertebrate Structure. Toronto: John Wiley and Sons, 1974.

HOEFLER H, CHILDERS H, MONTMINY MR, LECHAN RM, GOODMAN RH, WOLFE HJ. *In situ* hybridization methods for the detection of somatostatin mRNA in tissue sections using antisense RNA probes. Histochem J 1986; 18: 597-604.

HOLMES LB, TRELSTAD RL. Cell polarity in precartilage mouse limb mesenchyme cells. Dev Biol 1980; 78: 511-520.

HORSTADIUS S. The Neural Crest. Its Properties and Derivatives in the Light of Experimental Research. Toronto: Oxford University Press, 1950.

HORTON WA. Morphology of connective tissue: cartilage. In: Horton WA, ed. Connective Tissue and its Heritable Disorders. Chicago:Wiley-Liss, Inc. 1993: 73-84.

HORTON WA, MACHADO MA, ELLARD J, CAMPBELL D, PUTNAM EA, AULTHOUSE AL, SUN X, SANDELL LJ. An experimental model of human chondrocyte differentiation. Limb Dev Regeneration 1993; 553-540.

HUMASON GL. Animal Tissue Techniques, 4th ed. San Francisco: W.H. Freeman and Company, 1972.

HUNT P, WILKINSON D, KRUMLAUF R. Patterning the vertebrate head: murine Hox 2 genes mark distinct subpopulations of premigratory and migratory cranial neural crest. Development 1991; 112: 43-50.

HUNTER SJ, CAPLAN AI. Control of cartilage differentiation. In: Hall BK, ed., Cartilage, vol 2. Development, Differentiation, and Growth. Toronto, Academic Press, 1983: 87-119.

HUNZIKER EB, HERRMANN W. Ultrastructure of cartilage. In: Bonucci E, Motta PM, eds. Ultrastructure of Skeletal Tissues. Boston: Kluwer Academic Publishers, 1984: 79-109.

HUNZIKER EB, SCHENK RK. Cartilage ultrastructure after high pressure freezing, freeze substitution, and low temperature embedding. II. Intercellular spaces matrix structure-preservation of proteoglycans in their native state. J Cell Biol 1984; 98: 277-282.

INDIK Z, YEH H, ORNSTEIN-GOLDSTEIN N, KUCICH U, ABRAMS W. ROSENBLOOM JC, ROSENBLOOM J. Structure of the elastin gene and alternative splicing of elastin mRNA: Implications for human disease. Am J Med Genetics 1989; 34: 81-90.

JANNERS MY, SEARLS RL. Changes in rate of cell proliferation during the differentiation of cartilage and muscle in the mesenchyme of the embryonic chick wing. Dev Biol 1970; 23: 136-165.

JANVIER P. The phylogeny of the Craniata, with particular reference to the significance of fossil "agnathans". J Vert Paleontology 1981; 1(2): 121-159.

JANVIER P. Patterns of diversity in the skull of jawless fishes. In: Hanken J, Hall BK., eds. The Skull, vol 2, Patterns of Structural and Systemic Diversity. Chicago: University of Chicago Press, 1993: 131-151.

JOHNELS AG. On the development and morphology of the skeleton of the head of *Petromyzon*. Acta Zool (Stockh.) 1948; 29: 140-279.

JORDAN, CA. *In situ* hybridization in cells and tissue sections: A study of myelin gene expression during CNS myelination and remyelination. In: Chesselet MF, ed. *In situ* Hybridization Histochemistry. Boston: CRC Press, 1990.

JULIANO RL, HASKILL S. Signal transduction from the extracellular matrix. J Cell Biol 1993; 120(3): 577-585.

JUNQUEIRA LC, CARNEIRO J, LONG EJ. Basic Histology. California: Lange Medical Pub., 1986.

KAWAGUCHI T. Chemical nature of collagen in the dermis of the lamprey, *Entosphenus japonicus*. Comp Biochem Physiol 1993; 104B: 559-566.

KEENE DR, MADDOX BK, HUEY-JU K, SAKAI LY, GLANVILLE RW. Extraction of extendable beaded structures and their indentification as fibrillin-containing extracellular matrix microfibrils. J Histochem Cytochem 1991; 39: 441-449.

KENT Jr GC. Comparative Anatomy of the Vertebrates, 2nd ed. Saint Louis: C.V. Mosby, 1969.

KELLEY J, TANAKA S, HARDT T, EIKENBERRY EF, BRODSKY B. Fibril forming collagen in lamprey. J Biol Chem 1988; 263: 980-987.

KIMURA S, KAMIMURA T. The characterization of lamprey notochord collagen with special reference to its skin collagen. Comp Biochem Physiol 1982; 73B(2): 335-339.

KOSHER, RA. Chondroblast and Chondrocyte. In: Hall BK, ed. Cartilage, vol 1. Structure, Function and Biochemistry, Toronto: Academic Press, 1983: 59-85.

KOSHER RA, SOLURSH M. Widespread distribution of type II collagen during embryonic chick development. Dev Biol 1989; 131: 558-566.

KOSHER RA, GAY SW, KAMANITZ JR, KULYK WM, RODGERS BJ, SAI S, TANAKA T, TANZER ML. Cartilage proteoglycan core protein gene expression during limb cartilage differentiation. Dev Dynam 1986a; 118: 112-117.

KOSHER RA, KULYK WM, GAY SW. Collagen gene expression during limb cartilage differentiation. J Cell Biol 1986b; 102: 1151-1156.

KOSTOVIC-KNEZEVIC LJ, BRADAMANTE Z, SVAJGER A. On the ultrastructure of the developing elastic cartilage in the rat external ear. Anat Embryol 1986; 173: 385-391.

KRAVIS D, UPHOLT WB. Quantification of type II procollagen mRNA levels during chick limb cartilage differentiation. Dev Biol 1985; 108: 164-172.

KROTOSKI DM, FRASER SE, BRONNER-FRASER M. Mapping of neural crest pathways in *Xenopus laevis* using inter- and intra-specific cell markers. Dev Biol 1988; 127: 119-132.

LANDACRE FL. The fate of the neural crest in the head of the urodeles. J Comp Neurol 1921; 33: 1-43.

LANGILLE RM, HALL BK. Evidence of cranial neural crest contribution to the skeleton of the sea lamprey, *Petromyzon marinus*. In: Slavkin HC, ed. Progress in Developmental Biology, Part B. New York: Alan R Liss Inc., 1986: 77-111.

LANGILLE RM, HALL BK. Artificial fertilization, rearing, and timing of stages of embryonic development of the anadromous sea lamprey, *Petromyzon marinus* L. Can J Zool 1988a; 66: 549-554.

LANGILLE RM, HALL BK. Role of the neural crest in development of the trabeculae and branchial arches in the embryonic sea lamprey, *Petromyzon marinus L.* Development 1988b; 102: 301-310.

LARSEN LO. Physiology of adult lampreys, with special regard to natural starvation, reproduction, and death after spawning. Can J Fish Aquat Sci 1980; 37(11): 1762-1779.

LASH JW, VASAN NS. Glycosaminoglycans of cartilage. In: Hall BK, ed. Cartilage, vol 1. Structure, Function and Biochemistry. Toronto: Academic Press, 1983: 215-251.

LE DOUARIN NM, TEILLET MA. Experimental analysis of the migration and differentiation of neuroblasts of the autonomic nervous system and of neuroectodermal mesenchymal derivatives, using a biological cell marking technique. Dev Biol 1974; 41: 162-184.

LE DOUARIN NM, ZILLER C, COULEY GF. Patterning of neural crest derivatives in the avian embryo: *in vivo* and *in vitro* studies. Dev Biol 1993; 159: 24-49.

LEE KA, PIERCE RA, DAVIS EC, MECHAM RP, PARKS WC. Conversion to an elastogenic phenotype by fetal hyaline chondrocytes is accompanied by altered expression of elastin-related macromolecules. Dev Biol 1994; 163: 241-252.

LE LIEVRE CS. Participation of neural crest-derived cells in the genesis of the skull in birds. J Embryol Exp Morphol 1978; 47: 17-37.

LE LIEVRE CS, LE DOUARIN NM. Mesenchymal derivatives of the neural crest: Analysis of chimeric quail and chick embryos. J Embryol Exp Morphol 1975; 34: 125-154.

LEPPERT F. Untersuchungen uber die funktionelle struktur des schuller-blattknorpels des pferdes. Gegenb Morphol Jahrb 1933; 72: 309.

LEWIS ME, BALDINO, F Jr. Probes for *in situ* hybridization histochemistry. In: Chesselet MF, ed. *In Situ* Hybridization Histochemistry. Boston: CRC Press, 1990: 2-38.

LINSENMAYER TF. In: Hay ED, ed. Cell Biology of Extracellular Matrix, 2nd ed. New York: Plenum Press, 1991: 7-44.

LINSENMAYER TF, CHEN Q, GIBNEY E, GORDON MK, MARCHANT JK, MAYNE R, SCHMID TM. Collagen types IX and X in the developing chick tibiotarsus: analyses of mRNAs and proteins. Development 1991; 111: 191-196.

LUNA LG. Manual of Histologic Staining Methods of the Armed Forces Institute of Pathology, 3rd ed. Toronto: McGraw-Hill Book Company, 1960.

MACKIE EJ, THESLEFF I, CHIQUET-EHRISMANN R. Tenascin is associated with chondrogenesis and osteogenic differentiation in vivo and promotes chondrogenesis in vitro. J Cell Biol 1987; 105(6 Pt 1): 2569-2579.

MAISEY JG. Phylogeny of early vertebrate skeletal induction and ossification patterns. Evol Biol 1988; 22: 1-36.

MALLEIN-GERIN F, KOSHER RA, UPHOLT WB, TANZER ML. Temporal and spatial analysis of cartilage proteoglycan core protein gene expression during limb development by *in situ* hybridization. Dev Biol 1988; 126: 337-345.

MAYNE R, VON DER MARK K. Collagens of cartilage. In: Hall BK, ed. Cartilage, vol 1. Structure, Function and Biochemistry. Toronto: Academic Press, 1983: 181-214.

MCLAUGHLIN SK, MARGOLSKEE RF. ^{33}P is preferable to ^{35}S for labelling probes used in *in situ* hybridization. Biotechniques 1993; 15(3): 506-511.

MILLER MA, KOLB PE, RASKIND MA. A method for simultaneous detection of multiple mRNAs using digoxigenin and radioisotopic cRNA probes. J Histochem Cytochem 1993; 41(12): 1741-1750.

MOSS ML, MOSS-SALENTIJIN L. Vertebrate cartilages. In: Hall BK, ed. Cartilage, vol 1. Structure, Function and Biochemistry. New York: Academic Press, 1983: 1-30.

MULLER GB, ALBERCH P. Ontogeny of the limb skeleton in *Alligator mississippiensis*: developmental invariance and change in the evolution of archosaur limbs. J Morphol 1990; 203: 151-164.

MUNDLOS S, ZABEL B. Developmental expression of human cartilage matrix protein. Dev Dynam 1994; 199: 241-252.

MUNDLOS S, MEYER R, YAMADA Y, ZABEL B. Distribution of cartilage proteoglycan (aggrecan) core protein and link protein gene expression during human skeletal development. Mat 1991; 11: 339-346.

NAH HD, UPHOLT WB. Type II collagen mRNA containing an alternately spliced exon predominates in the chick limb prior to chondrogenesis. J Biol Chem 1991; 266: 23446-23452.

NEWTH DR. On the neural crest of the lamprey embryo. J Embryol Exp Morphol 1956; 4: 358-375.

NICHOLS DH. Neural crest cell formation in the head of the mouse embryo as observed using a new histological technique. J Embryol Exp Morphol 1981; 64: 105-120.

NODEN DM. An analysis of the migratory behaviour of avian cephalic neural crest cells. Dev Biol 1975; 42: 106-130.

NODEN DM. Interactions and fates of avian craniofacial mesenchyme. Development 1988; 103: 121-140.

OBERLENDER SA, TUAN RS. Expression and functional involvement of N-cadherin in embryonic limb chondrogenesis. Development 1994; 120: 177-187.

OLSON MD, LOW FN. The fine structure of developing cartilage in the chick embryo. Am J Anat 1971; 131: 197-216.

OSTER GF, MURRAY JD, MAINI PK. A model for chondrogenic condensations in the developing limb: the role of extracellular matrix and cell tractions. J Embryol Exp Morphol 1985; 89: 93-112.

OSTER GF, SHUBIN N, MURRAY JD, ALBERCH P. Evolution and morphogenetic rules: The shape of the vertebrate limb in ontogeny and phylogeny. Evolution 1988; 42(5): 862-884.

OSUMI-YAMASHITA N, ETO K. Mammalian cranial neural crest cells and facial development. Dev Growth Differ 1990; 32(5): 451-459.

PARDUE ML. *In situ* hybridization. In: Hames BD, Higgins SJ. eds. Nucleic Acid Hybridization, a Practical Approach. Oxford: IRL Press, 1990: 179-202.

PECHOUX C, MOREL G. *In situ* hybridization in semithin sections. In: Morel G, ed. Hybridization Techniques for Electron Microscopy. Boca Raton: CRC Press, 1993.

PHILLIPS FM, POTTENGER LA. *In vitro* reconstruction of a cartilage matrix granule network. Anat Rec 1989; 225: 26-34.

PIAVIS GW. Embryological stages in the sea lamprey and effects of temperature on development. U.S. Fish Wildl Serv Fish Bull 1961; 61: 111-143.

PIAVIS GW. Embryology. In: Hardisty MW, Potter IC, eds. The Biology of Lampreys, vol 1. New York: Academic Press, 1971: 361-399.

PLATT JB. Ectodermic origin of the cartilages of the head. Anat An 1893; 8: 506-9.

PLATT JB. The development of the cartilaginous skull and of the branchial and hypoglossal musculature in Necturus. Morph J 1898; 25: 377-464.

PORTER KR. Cell fine structure and biosynthesis of intercellular macromolecules. Biophys J 1964; 4(Suppl.): 167-196.

POTTER IC, WRIGHT GM, YOUSON JH. Metamorphosis in the anadromous sea lamprey, *Petromyzon marinus* L. Can J Zool 1978; 56(4, part 1): 561-570.

RIEPPEL O. Patterns of diversity in the reptilian skull. In: Hanken J, Hall BK., eds. The Skull, vol 2, Patterns of Structural and Systemic Diversity. Chicago: University of Chicago Press, 1993: 345-351.

ROBSON P, WRIGHT GM, SITARZ E, MAITI A, RAWAT M, YOUSON JH, KEELEY FW. Characterization of lamprin, an unusual matrix protein from lamprey cartilage. J Biol Chem 1993; 268(2): 1440-1447.

RODGERS BJ, KULYK WM, KOSHER RA. Stimulation of limb cartilage differentiation by cyclic AMP is dependent on cell density. Cell Diff Devel 1989; 28: 179-188.

ROMER AS, PARSONS TS. The Vertebrate Body, 5th ed. Toronto: W.B. Saunders Company, 1977.

ROSENBLOOM J, BASHIR M, YEH H, ROSENBLOOM J, ORNSTEIN-GLODSTEIN N, FAZIO M, KAHARI VM, UITTO J. Regulation of elastin gene expression. Ann NY Acad Sci 1991; 624; 116-36.

ROUGHLEY PJ, LEE ER. Cartilage proteoglycans: structure and potential functions. Microscopy Res Tech 1994; 28: 385-397.

ROVAINEN CM. Neurophysiology. In: Hardisty MW, Potter IC, eds. The Biology of Lampreys, vol 4A. Toronto: Academic Press, 1982: 1-136.

RYAN MC, SANDELL LJ. Differential expression of a cysteine-rich domain in the amino-terminal propeptide of type II (cartilage) procollagen by alternative splicing of mRNA. J Cell Biol 1990; 265(18): 10334-10339.

SAMBROOK J, FRITSCH EF, MANIATIS T. Molecular cloning: a laboratory manual, vol 3, 2nd ed. New York: Cold Spring Harbor Laboratory Press, 1989.

SANDBERG M. Matrix in cartilage and bone development: current views on the function and regulation of major organic components. Ann Med 1991; 23: 207-217.

SANDBERG M, VUORIO E. Localization of types I, II and III collagen mRNAs in developing human skeletal tissues by *in situ* hybridization. J Cell Biol 1987; 104: 1077-1084.

SANDELL LJ, MORRIS N, ROBBINS JR, GOLDRING MB. Alternatively spliced type II procollagen mRNAs define distinct populations of cells during vertebral development: differential expression of the amino-propeptide. J Cell Biol 1991; 144: 1307-1319.

SANDELL LJ, SUGAI JV, TRIPPEL SB. Expression of collagens I, II, X, and XI and aggrecan mRNAs by bovine growth plate chondrocytes in situ. J Orthop Res 1994; 12: 1-14.

SATO TA. A modified method for lead staining thin sections. J Elect Micro 1968; 17: 158-159.

SAUNDERS EJ. The roles of epithelial-mesenchymal cell interactions in developmental processes. Biochem Cell Biol 1988; 66: 530-540.

SCHAFFER J. Die strutzgewebe. In: Mollendorff WV, ed. Handbuch der Mikroskopischen Anatomie des Menschen, vol 2. Berlin: Springer, 1930: 1-390.

SCHMID TM, LINSENMAYER TF. Immunohistochemical localization of short chain cartilage collagen (type X) in avian tissues. J Cell Biol 1985; 100: 598-605.

SEARLS RL, HILFER SR, MIROW SM. An ultrastructural study of early chondrogenesis in the chick wing bud. Dev Biol 1972; 28: 123-137.

SERAFINI-FRACASSINI A, SMITH JW. The Structure and Biochemistry of Cartilage. London: Churchill Livingstone, 1974.

SERBEDZIJA GN, FRASER SE, BRONNER-FRASER M. Pathways of trunk neural crest migration in the mouse embryo as revealed by vital dye labelling. Development 1992; 108: 605-612.

SEUFERT DW, HANKIN J, KLYMKOWSKY MW. Type II collagen distribution during cranial development in *Xenopus laevis*. Anat Embryol (Berl) 1994; 189(1):81-9.

SEWERTZOFF AN. Etudes sur l'evolution des Vertebrates inferieurs. I. Arch Russ Anat Histol Embryol I 1916.

SEWERTZOFF AN. Etudes sur l'evolution des Vertebrates inferieurs. II. Arch Russ Anat Histol et Embryol I 1917.

SHELDON H. Transmission electron microscopy of cartilage. In: Hall BK, ed. Cartilage, vol 1. Structure, Function and Biochemistry. Toronto, Academic Press, 1983: 87-104.

SHEREN SB, EIKENBERRY EF, BROEK DL, VAN DER REST M, DOERING T, KELLY J, HARDT T, BRODSKY B. Type II collagen of lamprey. Comp Biochem Physiol 1986; 85B(1): 5-14.

SHORE RC, BERKOVITZ BKB, MOXHAM BJ. Intercellular contacts between fibroblasts in the peridontal connective tissue of the rat. J Anat 1981; 133: 67-76.

SHORROCK K, ROBERTS P, PRINGLE JH, LAUDER I. Demonstration of insulin and glucagon mRNA in routinely fixed and processed pancreatic tissue by in situ hybridization. J Pathol 1991; 165: 105-110.

SINGER RH, BENTLEY J, LAWRENCE, VILLNAVE C. Optimization of *in situ* hybridization using isotopic and non-isotopic detection methods. Biotechniques 1986; 4(3): 230-250.

SMITH BR. Sea Lamprey in the Great Lakes of North America. In: Hardisty MW, Potter IC, eds. The Biology of Lampreys, vol 1. London: Academic Press, 1971.

SMITH AJ, HOWELL JH, PIAVIS GW. Comparative embryology of five species of lampreys of the upper Great Lakes. Copia 1968; 3: 461-4469.

SOGHOMONIAN JJ, *In situ* hybridization histochemistry at the electron microscopic level. In: Chesselet MF, ed. *In Situ* Hybridization Histochemistry. Boston: CRC Press, 1990: 165-174.

SOLURSH M. Cell-cell interactions and chondrogenesis. In: Hall BK, ed., Cartilage, vol 2. Development, Differentiation and Growth. Toronto: Academic Press, 1983: 121-141.

SOLURSH M, REITER RS, AHRENS PB, PRATT RM. Increase in levels of cyclic AMP during avian limb chondrogenesis in vitro. Different 1979; 15: 183-186.

STEMPLE DL, ANDERSON DJ. Lineage diversification of the neural crest: *in vitro* investigations. Dev Biol 1993; 159: 12-23.

STIRPE NS, GOETINCK PF. Gene expression during cartilage differentiation: temporal and spatial expression of link protein and cartilage matrix protein in the developing limb. Development 1989; 107: 23-33.

STOCKWELL RA. Biology of Cartilage Cells. New York: Cambridge University Press, 1979.

SU MW, SUZUKI HR, BIEKER JJ, SOLURSH M, RAMIREZ F. Expression of two nonallelic type II procollagen genes during *Xenopus laevis* embryogenesis is characterized by stage-specific production of alternatively spliced transcripts. J Cell Biol 1991; 115(2): 565-575.

SUMMERBELL D, WOLPERT L. Cell density and cell division in the early morphogenesis of the chick wing bud. Nature New Biol 1972; 239: 24-26.

SWALLA BJ, UPHOLT WB, SOLURSH M. Analysis of type II collagen RNA localization in chick wing buds by *in situ* hybridization. Dev Biol 1988; 125: 51-58.

SWIDERSKI RE, SOLURSH M. Localization of type II collagen, long form α1(IX) collagen, and short form α1(IX) collagen transcripts in the developing chick notochord and axial skeleton. Dev Dynam 1992a; 194: 118-127.

SWIDERSKI RE, SOLURSH M. Differential co-expression of long and short form type IX collagen transcripts during avian limb chondrogenesis in ovo. Development 1992b; 115: 169-179.

TAKAGI M. Ultrastructural cytochemistry of cartilage proteoglycans and their relation to the calcification process. In: Bonucci E, Motta PM, eds. Ultrastructure of Skeletal Tissues. Boston: Kluwer Academic Publishers, 1990: 111-127.

TAN SS, MORRISS-KAY GM. Analysis of cranial neural crest cell migration and early fates in postimplantation rat chimeras. J Embryol Exp Morphol 1986; 98: 21-58.

THOROGOOD P. The developmental specification of the vertebrate skull. Development 1988; 103: 141-153.

THOROGOOD P. The problems of building a head. Current Biol 1993a; 3(10): 705-708.

THOROGOOD P. Differentiation and Morphogenesis. *In:* Hanken J, Hall BK, eds. The Skull: vol 1 Development. Chicago: University of Chicago Press, 1993b: 112-152.

THOROGOOD PV, HINCHLIFFE JR. An analysis of the condensation process during chondrogenesis in the embryonic chick hind limb. J Embryol Exp Morphol 1975; 33(3): 581-606.

THOROGOOD PV, BEE J, VON DER MARK K. Transient expression of collagen type II at epitheliomesenchymal interfaces during morphogenesis of the cartilaginous neurocranium. Dev Biol 1986; 116: 497-509.

TOMASEK JJ, MAZURKIEWICZ JE, NEWMAN SA. Nonuniform distribution of fibronectin during avian limb development. Dev Biol 1982; 90: 118-126.

TOSNEY KW. The segregation and early migration of cranial neural crest cells in the avian embryo. Dev Biol 1982; 89: 13-24.

TREILLEUX I, MALLEIN-GERIN F, LE GUELLEC D, HERBAGE D. Localization of the expression of type I, II, III collagen, and aggrecan core protein genes in developing human articular cartilage. Matrix 1992; 12: 221-232.

UPHOLT WB, OLSEN BR. The active genes of cartilage. In: Hall BK, Newman SA, eds. Cartilage: Molecular Aspects. Boca Raton: CRC Press, 1991.

URIST, MR. The origins of cartilage: Investigations in quest of chondrogenic DNA. In: Hall BK, ed. Cartilage, vol 2. Development, Differentiation and Growth. Toronto: Academic Press, 1983: 1-85.

VAN DER REST M, MAYNE R. Type IX collagen proteoglycan from cartilage is covalently cross-linked to type II collagen. J Biol Chem 1988; 263(4): 1615-1618.

WEBSTER D, WEBSTER M. Comparative Vertebrate Morphology. New York: Academic Press, 1974.

WIGHT TN, KINSELLA MG, QWARNSTROM EE. The role of proteoglycans in cell adhesion, migration and proliferation. Curr Opinion Cell Biol 1992; 4: 793-801.

WILCOX JN. Fundamental principles of in situ hybridization. J Histochem Cytochem 1993; 41(12): 1725-1733.

WINTERBOTTOM N, TONDRAVI MM, HARRINGTON TL, KLIER FG, VERTEL BM, GOETINCK PF. Cartilage matrix protein is a component of the collagen fibril of cartilage. Dev Dynam 1992; 193: 266-276.

WRIGHT GM, YOUSON JH. Ultrastructural of mucocartilage in the larval anadromous sea lamprey, *Petromyzon marinus* L. Am J Anat 1982; 165: 39-51.

WRIGHT GM, YOUSON JH. Ultrastructure of cartilage from young adult sea lamprey, *Petromyzon marinus* L: A new type of vertebrate cartilage. Am J Anat 1983; 167: 59-70.

WRIGHT GM, KEELEY FW, YOUSON JH. Lamprin: A new vertebrate protein comprising the major structural protein of adult lamprey cartilage. Exper 1983; 39: 495-497.

WRIGHT GM, ARMSTRONG LA, JACQUES AM, YOUSON JH. Trabecular, nasal, branchial and pericardial cartilages in the sea lamprey, *Petromyzon marinus*: Fine structure and immunohistochemical detection of elastin. Am J Anat 1988; 182: 1-15.

YANAGISHITA M. Function of proteoglycans in the extracellular matrix. Acta Pathol Jpn 1993; 43: 283-293.

YEH H, ANDERSON N, ORNSTEIN-GOLDSTEIN N, BASHIR MM, ROSENBLOOM JC, ABRAMS W, INDIK Z, YOON K, PARKS W, MECHAM R, ROSENBLOOM J. Structure of the bovine elastin gene and S1 nuclease analysis of alternative splicing of elastin mRNA in the bovine nuchal ligament. Biochem 1989; 28: 2365-2370.

YOUSON JH, POTTER IC. A description of the stages in the metamorphosis of the anadromous sea lamprey, *Petromyzon marinus* L. Can J Zool 1979; 57(9): 1808-1817.

YOUSON JH. Morphology and physiology of lamprey metamorphosis. Can J Fish Aquat Sci 1980; 37: 1687-1710.

ZANETTI NC, SOLURSH M. Induction of chondrogenesis in limb mesenchymal cultures by disruption of the actin cytoskeleton. J Cell Biol 1984; 99: 115-123.

ZELLER R, BLOCH KD, WILLIAMS BS, ARCECI RJ, SEIDMAN CE. Localized expression of the atrial natriuretic factor gene during cardiac embryogenesis. Genes Devel 1987; 1: 693-698.

ZELLER R, ROGERS M. *In situ* hybridization to cellular RNA. In: Ausubel FM, Brent R, Kingston RE, Moore DD, Seidman JG, Smith JA, Struhl K, eds. Current Protocols in Molecular Biology, vol 2. New York: Green Publishing Associates, Inc. and John Wiley and Sons Inc., 1989: 14.3.1-14.3.4.

ZIMMERMANN B, THIES M. Alterations of lectin binding during chondrogenesis of mouse limb buds. Histochem 1984; 81: 353-361.

7. APPENDIX A

PIAVIS STAGING CHARACTERISTICS FOR *PETROMYZON MARINUS*

PROLARVAL STAGE	DAYS (PF)*	CHARACTERISTIC FEATURE
15:Pigmentation	13-16	first appearance of dorsal melanophores bilateral to midbrain; previous tail flexion disappears
16:Gill-cleft	15-17	appearance of functional gill-slits; melanophores migrate ventrally
17:Burrowing	17-33	first appearance of bilateral eye spots; head and tail used to burrow
18:Larval	33-40	lumen of yolk-filled gut opens

* days post-fertilization

Note: The characteristic features listed are only a partial list of criteria used by Piavis (1961, 1971) and reflect those emphasized in the present study. The first characteristic listed is the initial point of that stage.